CLINICAL MEASUREMENT OF CORNEAL BIOMECHANICAL PROPERTIES: TANGENT ELASTIC MODULUS

HON YING

Ph.D

The Hong Kong Polytechnic University

2017

The Hong Kong Polytechnic University

School of Optometry

Clinical Measurement of Corneal Biomechanical Properties: Tangent Elastic Modulus

Hon Ying

A thesis submitted in partial fulfillment of the requirements for the degree of Doctor of Philosophy

Aug 2016

CERTIFICATE OF ORIGINALITY

I hereby declare that this thesis is my own work and that, to the best of my knowledge and belief, it reproduces no material previously published or written, nor material that has been accepted for the award of any other degree or diploma, except where due acknowledgement has been made in the text.

_____ (Signed)

Hon Yiha (Name of student)

Abstract

Thesis Title: **Clinical measurement of corneal biomechanical properties: tangent elastic modulus**

Chief supervisor: Dr. Andrew K.C. LAM

In vivo corneal biomechanical measurement is challenging to perform. Corneal Visualization Scheimpflug Technology (Corvis ST) is a recently launched non-contact tonometer, which was used to measure corneal deformation and its recovery during tonometry in the initial stage of the current study. Two of eight corneal biomechanical parameters (deformation amplitude and time to first applanation) showed favourable repeatability. The usefulness of the Corvis ST is limited because it is restricted to measuring parameters only at the central cornea.

A novel corneal indentation device (CID) was developed which was able to precisely measure corneal stiffness, as the force required to indent the cornea to a unit depth. The tangent elastic modulus of the human cornea, or corneal tangent modulus in short, can be calculated from corneal stiffness, thickness, and radius of curvature measured at the central cornea. Using standard mechanical terminology, such as tangent modulus and stiffness, can better describe intrinsic properties of the cornea. Repeatability of the corneal stiffness and corneal tangent modulus measurements, as well as their diurnal variation was evaluated in human subjects before the CID was applied in other clinical studies. Corneal stiffness had an intraclass correlation coefficient (ICC) of 0.75 and a coefficient of variation (CV) of 7.32 %, whereas corneal tangent modulus had an ICC of 0.84 and a CV of 7.34 %. Neither parameter exhibited significant diurnal variation.

The prevalence of myopia is high in Asian countries. It is not known whether axial elongation affects corneal tangent modulus in myopic eyes. The CID was used in two age- and central corneal thickness-matched low (n = 32) and high (n =32) myopic subjects. Corneal stiffness (approximately 0.063 Nmm^{-1}) and corneal tangent modulus (approximately 0.48 MPa) were determined to be similar in the two groups. However, the intraocular pressure (IOP) was significantly higher in the high myopia group. Any

difference in corneal tangent moduli could be masked by the difference in IOP between the two groups. In view of a linear dependency on IOP, the corneal tangent modulus in individual eyes was normalized to 15.5 mmHg, the mean IOP for normal eyes. The corneas of high myopes revealed a significantly lower tangent modulus (0.47 ± 0.087 MPa) than that of low myopes (0.57 ± 0.099 MPa). The corneas of the high myopes could be considered as less stiff. Due to the inherent continuity between cornea and sclera, corneal tangent modulus measurement may be useful as an index of the scleral coat of the eye.

Orthokeratology has become one of the effective myopia intervention. A pilot study was conducted to monitor changes in corneal stiffness and tangent modulus in subjects receiving orthokeratology treatment for one month. Eighteen young myopes were recruited. Corneal stiffness was determined to be stable throughout the treatment period, and was approximately 0.063 to 0.065 Nmm^{-1}. The mean corneal tangent modulus measurement increased from a baseline of 0.47 MPa to 0.52 MPa at one month, returning to 0.48 MPa after cessation of lens wear for three months. The predictive role of pre-treatment corneal tangent modulus on orthokeratology response deserves further research.

Regional mechanical alteration might be expected in diseased or postoperative corneas, but clinical devices cannot measure corneal biomechanics away from the central cornea. The feasibility of the CID to measure corneal stiffness at the peripheral cornea was examined in 25 young adults. Peripheral corneal measurements were performed twice at 3 mm from the temporal limbus, once with subjects looking straight ahead and then with subjects looking nasally. The mean central corneal stiffness was 0.070 Nmm^{-1}, while that of temporal corneal stiffness was 0.074 Nmm^{-1} when the subjects were looking straight ahead, and 0.080 Nmm^{-1} when the subjects were looking nasally. The increased temporal corneal stiffness at nasal gaze may be attributable to corneal thickening and pulling of extraocular muscles. More work is needed to deduce the corneal tangent modulus at the peripheral cornea.

Publications arising from the thesis

Paper published:

Hon, Y., Chen, G. Z., Lu, S. H., Lam, D. C. & Lam, A. K. 2017. High myopes have lower normalised corneal tangent modulus (less 'stiff' corneas) than low myopes. *Ophthalmic Physiol Opt*, 37, 42-50.

Hon, Y., Wan, K., Chen, G. Z., Lu, S. H., Lam, D. C. & Lam, A. K. 2016. Diurnal variation of corneal tangent modulus in normal Chinese. *Cornea*, 35, 1600-1604.

Lam, A. K., Hon, Y., Leung, L. K. & Lam, D. C. 2015. Repeatability of a novel corneal indentation device for corneal biomechanical measurement. *Ophthalmic Physiol Opt*, 35, 455-61.

Hon, Y. & Lam, A. K. 2013. Corneal deformation measurement using Scheimpflug noncontact tonometry. *Optom Vis Sci*, 90, e1-8.

Conference presentations:

Lam, A. K., Hon, Y., Wong, C. K., Tse, S. H., Chen, G. Z., Lu, S. H., Lam, D. C. Short-term orthokeratology on corneal tangent elastic modulus – a pilot study. ARVO Annual Meeting 2016, Seattle, USA. Poster presentation.

Hon, Y., Lam, A. K., Chen, G. Z., Lu, S. H., Lam, D. C. Corneal stiffness and tangent modulus in low and high myopes. The 10th Asia Cornea & Contact Lens Conference 2016, Hong Kong. Poster presentation.

Hon, Y., Lam, A. K., Lam, D. C. Corneal stiffness and tangent elastic modulus in low and high myopes. The 11th Joint Eye Research Day 2015, Hong Kong. Oral presentation.

Acknowledgements

TO MY CHIEF SUPERVISOR I would like to say a very sincere thank you to Dr. Andrew Lam, for his persistent guidance and advice provided throughout my time as his research student. Under his supervision, I learnt to be a diligent researcher and a person who is consistent and responsible at work. Without his continuous support and encouragement, I could not survive through the tough years of my PhD life.

TO OUR COLLABORATORS I would like to thank Prof. Yong-ping Zheng, Prof. David C. C. Lam, Dr. Match Ko, Dr. Leo Leung and Dr. Rick Chen who enriched me with new knowledge about biomechanical engineering. My gratitude is also extended to Li-Ke, Yanping and Luke for their technical support in my experimental work.

TO MY RESEARCH COMPANION Throughout this time we have shared the ups and downs of tough research life. I did not feel alone when we fought hard to complete data taking and paper writing together. I cherish the friendship we have built and the continuous support given to each other.

TO MY SUBJECTS Thank you all very much for spending your valuable time for the experiments. The data taking would not be smooth without your help and participation.

TO MY FAMILY AND FRIENDS I would like to express my deepest gratitude to my parents and Eric, for their love and understanding. I feel sorry for the limited time I have spent with them in these years. Thank you very much for the support and freedom that allowed me to focus fully on my work.

Table of Contents

List of Abbreviations

AL	Axial length
ANOVA	Analyses of variance
Appl 1	First applanation
Appl 2	Second applanation
AS-OCT	Anterior segment optical coherence tomography
CCT	Central corneal thickness
CH	Corneal hysteresis
CID	Corneal indentation device
Corvis ST	Corneal Visualization Scheimpflug Technology
CRF	Corneal resistance factor
CRT	Corneal Reshaping Therapy
CXL	Collagen cross-linking
CV	Coefficient of variation
D	Diopter
DA	Deformation amplitude
DCT	Dynamic contour tonometry
Dk	Oxygen permeability
ETDRS	Early Treatment Diabetic Retinopathy study
GAT	Goldmann applanation tonometry
HC-time	Time from start until highest concavity
Hi Con	Highest concavity
ICC	Intraclass correlation coefficient
IOP	Intraocular pressure
IR	Infrared
IOPcc	Corneal-compensated intraocular pressure
IOPg	Goldmann-correlated intraocular pressure
KC	Keratoconus
K_p	Peripheral corneal radius at 3 mm from the temporal limbus
LASIK	Laser in situ keratomileusis
LASEK	Laser-assisted subepithelial keratectomy
LogMAR	Logarithm of the minimum angle of resolution

meanK	Mean corneal radius of curvature
mm	Millimeter
mmHg	Millimeter of mercury
ms	Millisecond
MPa	Megapascal
n/a	Not available
NCT	Noncontact tonometer
NTG	Normal tension glaucoma
OHT	Ocular hypertension
ORA	Ocular Response Analyzer
ortho-k	Orthokeratology
P1	First applanation pressure
P2	Second applanation pressure
PCT	Peripheral corneal thickness at 3 mm from the temporal limbus
POAG	Primary open-angle glaucoma
Q	Quality score
QS	Quality Specification
RMANOVAs	Repeated measures analyses of variance
SCL	Soft contact lens
SD	Standard deviation
SER	Spherical equivalent refraction
$SimK_1$	Simulated flattest keratometry reading
$SimK_2$	Simulated steepest keratometry reading
SMILE	Small incision lenticule extraction
$Stiff_{cent}$	Corneal stiffness measured at central cornea
$Stiff_{prim}$	Corneal stiffness measured at 3 mm from temporal limbus (central fixation)
$Stiff_{nasal}$	Corneal stiffness measured at 3 mm from temporal limbus (nasal fixation)
Sw	Within-subject standard deviation
UCVA	Uncorrected visual acuity
UTM	Universal testing machine
UVA	Ultraviolet A

V_{in}	Velocity of first applanation
V_{out}	Velocity of second applanation
WS	Waveform score
µm	Micrometer
1st A-time	Time from start until the first applanation
1st A-length	Length of the flattened cornea in the first applanation
2nd A-time	Time from start until the second applanation
2nd A-length	Length of the flattened cornea in the second applanation

Chapter 1
Introduction

1.1 Corneal structures and corneal biomechanics

The cornea is an avascular and transparent tissue that forms about 15 % of the outer tunic of the eye. Corneal dimensions vary greatly between individuals. In general, the anterior cornea is steepest centrally and flattens toward the periphery providing an asphericity between -1 and 0, where its shape is commonly described as a prolate ellipsoid (Kiely et al., 1982). The population means for the anterior and posterior corneal radii at the central cornea, are 7.8 and 6.5 mm, respectively. The rate of corneal flattening from the center towards the periphery can be different along the horizontal and vertical meridians. The average horizontal corneal diameter is about 11 to 12 mm, which is usually 1 mm larger than its vertical diameter. The cornea is the major refractive interface of the eye with a total power of at least 40 D and a refractive index of 1.376. In order to provide an even and smooth refractive surface for vision, the cornea is covered superficially by a thin layer of tear film (Dawson et al., 2011).

The corneal tissue is traditionally considered to be composed of five parallel layers (Oyster, 1999). The epithelium is the outermost layer of the cornea, and consists of 6 to 8 layers of cells stacked on top of one another to a thickness of around 50 µm. Below the epithelium lies an acellular layer about 10 µm thick, known as Bowman's layer and consists of randomly arranged collagen fibrils which serve as an anchoring point for the anterior stroma. The corneal stroma accounts for 90 % of corneal thickness. Most of the collagen content of the cornea is concentrated in the stroma. Layers of collagen fibrils assemble into lamellae, where at least 200 laminae are superimposed on one another and are interposed with layers of fibroblasts. Stromal collagen fibrils are all approximately the same diameter and are spaced at regular intervals. The space between fibrils is filled with proteoglycans and water forming a gel-like matrix.

Descemet's membrane acts as a modified basement membrane of the corneal endothelium. In adults, it is around 10 to 15 μm thick. Several types of collagen fibrils are present in Descemet's membrane, forming a regular and springy lattice. The corneal endothelium is a single cellular layer that lines the entire posterior surface of the cornea. It is separated from the stroma by Descemet's membrane and is about 5μm thick. The endothelial cells are usually uniform-in-size with a predominantly hexagonal shape. The irregularity could increase due to age, surgical injury or corneal edema due to contact lens wear (Dawson et al., 2011).

In 2013, a new corneal layer, Dua's layer, was discovered between the corneal stroma and Descemet's membrane (Dua et al., 2013). The Dua's layer is acellular and thin (mean thickness: 10 μm). Its toughness is attributable to multiple lamellae of collagen bundles that run in different directions. More research is needed to confirm the significance of Dua's layer, including its impact on corneal biomechanical properties.

As the main refracting component and outer tunic of the eye, the cornea requires good mechanical strength to withstand both internal and external forces to ensure the corneal shape can be maintained for stable vision and protect the internal structure of the eye. The study of deformation and equilibrium of corneal tissue under different forces refers to corneal biomechanics (Garcia-Porta et al., 2014). Knowledge of corneal biomechanics can help distinguish normal and diseased corneas, explore treatment through biomechanical intervention, and improve surgical outcomes (Fung, 1993).

The biomechanical properties of the cornea are dominated by the stroma, which is highly collagenous and comprises most of the corneal thickness. X-ray diffraction studies have shown that the stromal collagen fibrils exhibit different preferential orientations. They vary from central to peripheral and from anterior to posterior cornea (Kotecha, 2007, Ruberti et al., 2011) (Figure 1.1). A greater force is needed to stretch the human cornea parallel with the direction of fibrils than perpendicular to them, which gives rise to anisotropy of tissue. The predominant collagen fibrils contribute to the elasticity of the cornea because they transmit forces and resist deformation. Clinically, corneal elasticity

may also be referred to as corneal stiffness (Elsheikh et al., 2007b). Recently, there has been increasing awareness of the presence of elastic fibers mainly in the deeper layers of the peripheral stroma (Kamma-Lorger et al., 2010, Lewis et al., 2015). They appear to be arranged parallel to the circumferentially oriented collagen lamellae and are believed to provide additional corneal resistance to deformation along with collagen. The proteoglycan matrix in the stroma contributes to viscosity of the cornea as the fluid allows energy dissipation due to sliding of interfibrillar collagen fibrils and lamellae (Dawson et al., 2011). Therefore, the cornea behaves as a viscoelastic material, having both elasticity and viscosity properties.

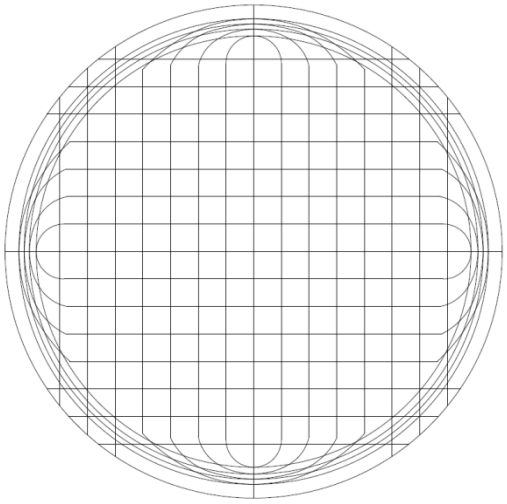

Figure 1.1 Simplified illustration showing the orientation of stromal collagen fibrils in the cornea. Fibrils run preferentially in the vertical and horizontal directions in the central cornea, but in a circumferential direction in the peripheral cornea near the limbus. (Reproduced from (Elsheikh et al., 2008c))

As the corneal tissue is a layered structure, distinctive biomechanical characteristics are present in its individual layers. Both the cellular epithelium and endothelium do not have collagen fibrils. Elsheikh et al. (2008a) found that the presence of epithelium only increased overall corneal stiffness by 1-3 %, hence it could be ignored in numerical

simulations. Similarly, the biomechanical contribution of the single-layered endothelium to the overall corneal biomechanics may also be minimal (Dawson et al., 2011). Although Seiler et al. (1992) did not find any significant difference in corneal stiffness when Bowman's layer was removed using an excimer laser, Last et al. (2012) observed a high stiffness value for Bowman's layer, when individual layers were tested using atomic force microscopy. The mechanical properties of the stroma depend on its thickness. It has been reported that the anterior third of the stroma appears as a lamellar interwoven fabric, which is much stiffer than its non-woven posterior portion (Simon & Ren, 1994, Kohlhaas et al., 2006). It is inferred that Descemet's membrane possesses considerable stiffness due to its hexagonal network of collagen fibrils. However, different results have been reported when measured by various methods (Randleman et al., 2008, Last et al., 2012). Information about the biomechanical properties in each layer is far from complete. In general, Bowman's layer, stroma and Descemet's membrane can be regarded as the key composite structures that characterize overall corneal biomechanical properties (Dawson et al., 2011).

1.2 Common terminologies used in corneal biomechanics

The gold standard for inspecting mechanical behavior of materials involves stress and strain measurements. These common engineering terms are explained with help of diagrams (Fratzl, 2008). As shown in Figure 1.2, when a piece of material is subjected to a compressive force, stress (units Pascal or Nm^{-2}) is defined as the normal force (F) divided by the surface area (A). The deformation due to stress is referred to as strain ε, which represents a change of length over initial length ($\Delta L/L$). The ratio of stress and strain is called elastic (or Young's) modulus (unit in Pascal or Nm^{-2}). During compression, a material expands in the direction perpendicular to the applied stress. The Poisson's ratio is defined as the ratio of the expansion in the horizontal axis (ε_2) relative to the contraction in the vertical axis (ε_1) and is denoted as v (Figure 1.2). Most materials have a Poisson's ratio ranging between 0 and 0.5, depending on its compressibility. Because the cornea is mainly composed of water, it is regarded as an incompressible material. Hence the Poisson's ratio of the cornea is close to 0.5 (Uchio et al., 1999).

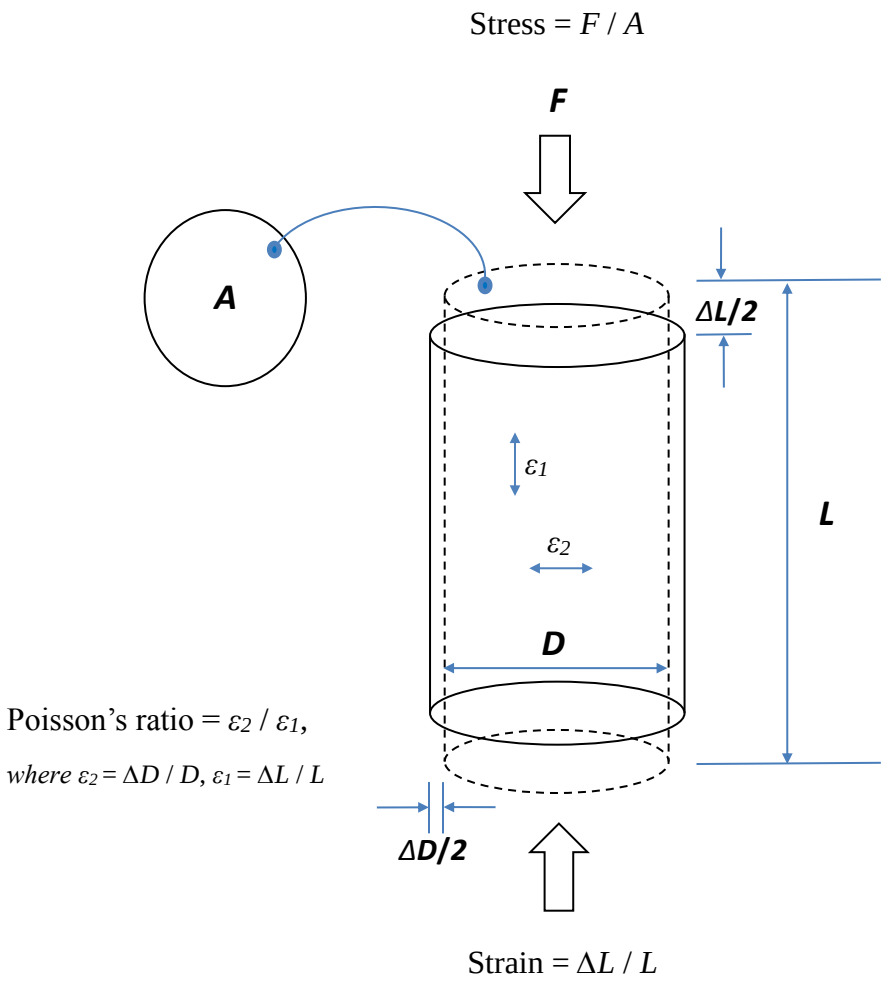

Figure 1.2 Simplified illustration of stress and strain measurements. A compressive force *F* is exerted onto a material with surface area *A*. Its length *L* is decreased by Δ*L* while its width *D* is increased by Δ*D*. Stress is defined as *F* divided by *A* while strain in the direction of applied *F* represents Δ*L* over *L*. The Poisson's ratio *v* is calculated as the ratio of the expansion in the horizontal axis (ε_2) relative to the contraction in the vertical axis (ε_1).

The amount of strain under the same stress can vary in different materials. A typical curve of stress-strain relationship can be drawn to represent the mechanical behavior of materials. A material is defined as elastic when it returns to its original form when stress is removed. A material is called linear elastic when the stress-strain curve is linear (Figure 1.3a). Materials can also be assumed linear elastic under small deformation. Most biological materials, including the cornea, are viscoelastic and exhibit a nonlinear stress-

strain relationship (Figure 1.3b). In contrast, on unloading, viscoelastic material returns to its original form in a time-dependent manner following a different pathway. The area between loading and unloading is called hysteresis and it represents the energy lost during the stress-strain cycle (Buzard, 1992, Kotecha, 2007, Fratzl, 2008).

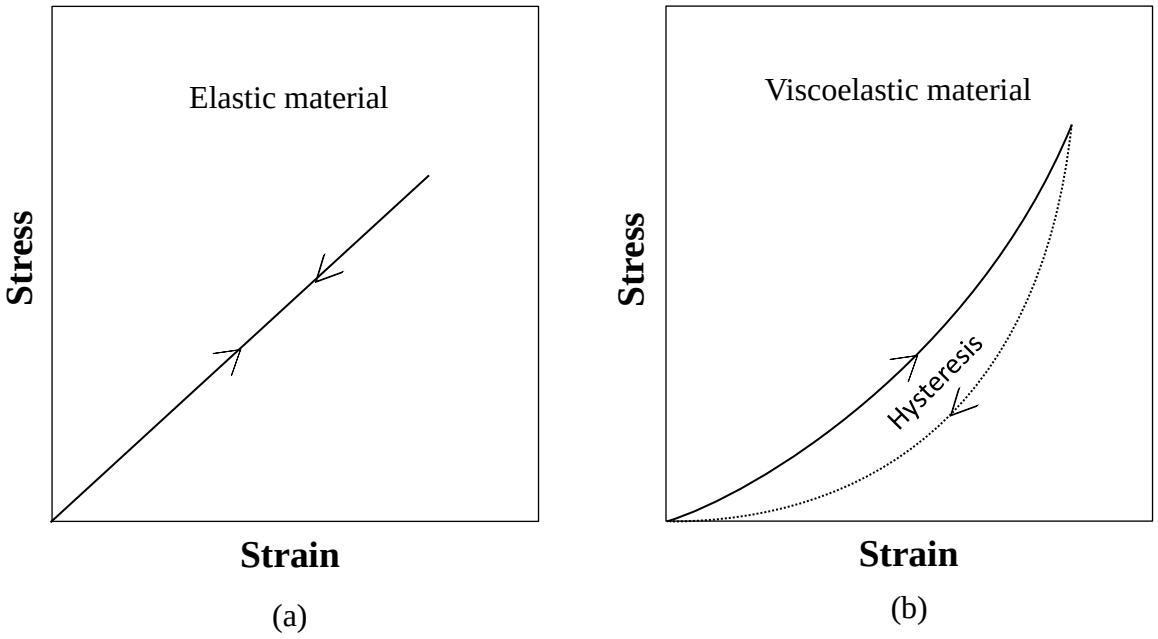

Figure 1.3 (a) A linear stress-strain relationship of an elastic material, with the same pathway between loading (*arrow pointing upwards*) and unloading (*arrow pointing downwards*). **(b)** A nonlinear stress-strain relationship of a viscoelastic material, with different pathway between loading (*solid line, arrow pointing upwards*) and unloading (*dotted line, arrow pointing downwards*). The area between the two curves is called hysteresis.

Elastic modulus is the slope of the stress-strain curve. In metals such as steel, elastic modulus is a constant value under certain limits of stress and strain (Buzard, 1992). In contrast, elastic modulus of corneal tissue increases with increasing stress (Hoeltzel et al., 1992, Hjortdal, 1996, Elsheikh & Anderson, 2005). Elastic modulus describes the stiffness of a material. A higher modulus indicates a stiffer material, which requires a larger force to deform (Fratzl, 2008).

1.3 Measurements of corneal biomechanics

1.3.1 *Ex vivo/in vitro*

Early corneal biomechanical investigations were performed on *ex vivo/in vitro* animal or human corneas (Nyquist, 1968, Woo et al., 1972, Nash et al., 1982, Jue & Maurice, 1986, Hoeltzel et al., 1992). The most frequently used conventional techniques include strip extensiometry and inflation testing. The former involves cutting and extending corneal strips, while the latter entails inflating corneal buttons on artificial pressure chambers (Buzard, 1992). These methods are advantageous because a complete tissue behavior can be investigated under a wide range of stress and strain measurements. Data obtained by using these techniques serves as the basis of corneal modeling. However, both techniques are destructive and are unable to mimic *in vivo* cornea conditions, such as preservation of corneal shape and hydration, and support from surrounding ocular tissue (Ruberti et al., 2011).

Nevertheless, destructive methods were able to identify altered corneal biomechanics in diseased and treated corneas. Strip extensiometry showed that corneas from keratoconus patients were more extensible than normal corneas (Andreassen et al., 1980, Nash et al., 1982). When corneal strips were treated with collagen cross-linking (CXL), elastic moduli were significantly increased, which indicated stiffened corneas (Wollensak et al., 2003, Kohlhaas et al., 2006). Inflation technique also demonstrated increased corneal stiffness after CXL (Matteoli et al., 2016). These findings aroused interest for clinical corneal biomechanical investigations.

1.3.2 *In vivo*

Nondestructive methods for corneal biomechanical measurement were explored before clinical implementation. Several approaches have been introduced. Ultrasonic imaging technique was applied onto the cornea of the porcine globe to measure its elasticity (Dupps et al., 2007, Tanter et al., 2009). Due to the relationship between shear wave propagation speed and the mechanical properties of corneal tissue, the shear elastic modulus could be deduced when a shear wave was transmitted across the tissue and the propagation speed was recorded (Kling, 2014). Scarcelli et al. (2012) developed

Brillouin optical microscopy, which applied a light scattering method and measured the shift in photon energy (Brillouin shift) in the corneal tissue. However, Brillouin shift could be used to indicate collagen density rather than tissue stiffness. Alternatively, corneal indentation was applied whilst corneal deformation was monitored in terms of curvature change, strain, or local displacement using videotopography (Grabner et al., 2005), ultrasound elasticity microscopy (Hollman et al., 2002) or optical coherence elastography (Ford et al., 2009), respectively. Jaycock et al. (2005) used noncontact electronic speckle pattern interferometry to trace corneal displacement during hydrostatic loading. Further investigation utilized high-speed optical coherence tomography to observe corneal deformation by air puff indentation (Alonso-Caneiro et al., 2011, Dorronsoro et al., 2012). It was observed that stiff corneas showed reduced deformation responses.

Of these investigations, only those of Grabner et al. (2005) attempted *in vivo* measurement on human subjects and all other nondestructive techniques were restricted to laboratory testing.

Currently, the only commercially available clinical devices for *in vivo* corneal biomechanical measurements are the Ocular Response Analyzer (ORA; Reichert Inc., USA) (Luce, 2005) and the Corneal Visualization Scheimpflug Technology (Corvis ST; Oculus, Germany) (Ambrósio Jr et al., 2013). Both devices act like ordinary noncontact tonometers (NCT) which indent the cornea using a precisely metered air puff. The ORA uses an infrared electro-optical detector system to track the changes in anterior corneal curvature and records two applanation (flattening) pressures. It claims to measure the viscoelastic properties of the cornea. A high-speed Scheimpflug camera in the Corvis ST is able to capture corneal deformation along a horizontal cross-section under a constant air puff pressure. However, the deformation parameters are raw, and so cannot directly delineate the true mechanical properties of the tissue (Roberts et al., 2011, Girard et al., 2015).

The growth and increased scope of clinical research related to corneal biomechanics have been attributed to the commercialization of the ORA over the last 10 years. A clear understanding of its working principles and factors affecting its corneal biomechanical parameters are essential for interpretation of current clinical findings. At the commencement of this study in 2011, the ORA was the only commercially available device in the market. Hence, a review on the ORA measurements is presented in the next section.

1.4 The Ocular Response Analyzer (ORA)

1.4.1 Principle

The ORA, which is a modified NCT, has 4 key components for monitoring applanation pressures (Luce, 2005): a solenoid-driven air pump, a pressure transducer, an infrared (IR) light emitter, and detector. The IR light emitter directs a beam of light onto the cornea at the start of measurement (Figure 1.4). The convex shape of the cornea causes the reflected light to be dispersed to a wide angle. Upon auto-alignment to the corneal apex, the air pump delivers a collimated stream of air directly onto the eye. As the cornea starts to move inward, the reflected light beam begins to converge and directs an increasing amount of light to the detector. When the cornea reaches the first applanation state, which represents a central corneal flattening of approximately 3 mm in diameter, the reflected light is collimated and the detector registers a signal peak, causing the pressure transducer to record the first applanation pressure (P1). Following the first applanation, air puff pressure continues to impinge the cornea to a reversed concave shape. Once again, the reflected IR becomes dispersed and the signal amplitude from the detector decreases, causing a decline of air puff pressure. Gradually, the cornea rebounds and passes through a second applanation state. The transducer records the applanation pressure a second time (P2) when the reflected light reaches a maximum intensity. Eventually, the cornea returns to its normal configuration at the end of the measurement. The entire process takes approximately 20 milliseconds.

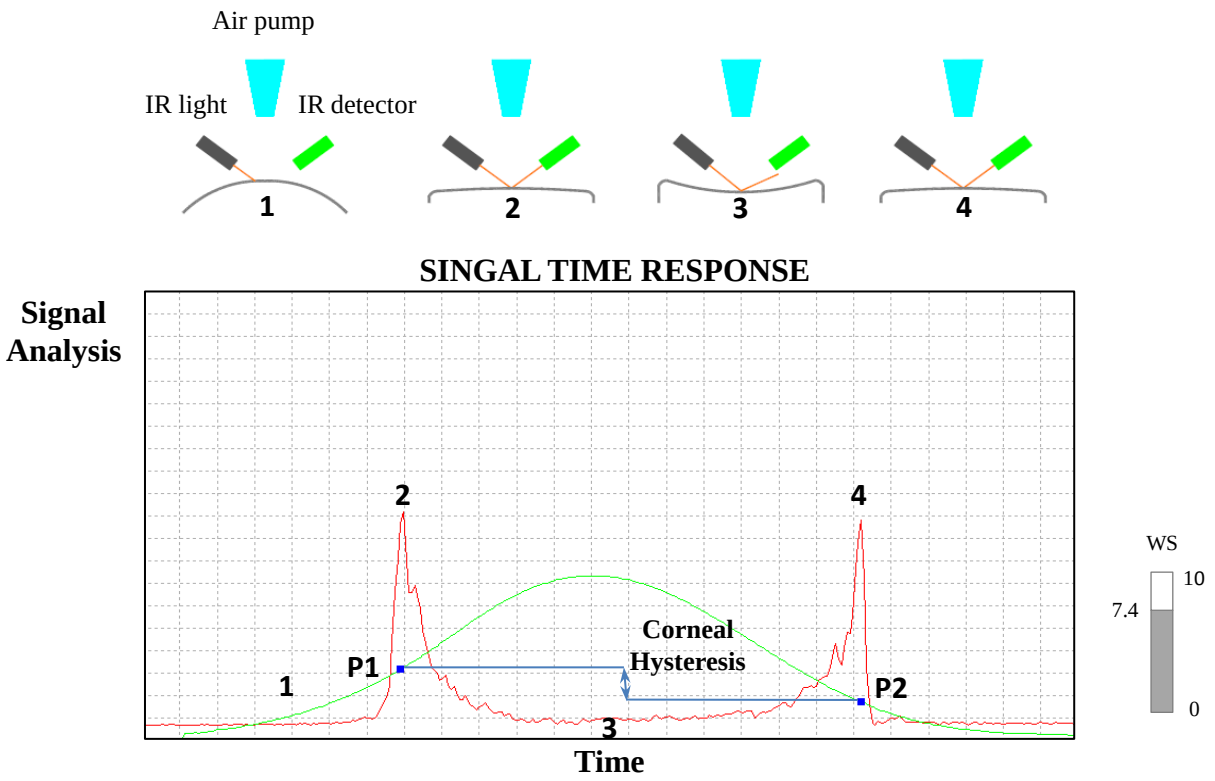

Figure 1.4 Measurement mechanism of the Ocular Response Analyzer (ORA). (1) The air pump delivers an air puff to the eye. The infrared (IR) detector continuously records light intensity of IR (*red signal waveform*). (2) When the air puff pressure increases (*green signal curve*), the cornea moves inward and passes through a first applanation state (P1) with a first signal peak. (3) Maximum corneal concavity is reached following maximum air puff pressure. (4) The air puff pressure decreases as the the cornea passes through a second applanation state (P2) with a second signal peak. The difference between P1 and P2 is called corneal hysteresis. A waveform score (WS) is shown in a grey bar.

A combined plot regarding the signal intensity from air puff pressure (in green) and IR detector (in red) versus time can be visualized after each ORA measurement (Figure 1.4). The two applanation pressures (P1 & P2) are indicated as blue squares, in which P2 is always lower than P1. The ORA reports two tonometric readings, which are the Goldmann-correlated intraocular pressure (IOPg) and the corneal-compensated intraocular pressure (IOPcc). It is claimed that IOPg ([P1+P2]/2) is analogous to intraocular pressure (IOP) measurements using the Goldmann applanation tonometry (GAT). The IOPcc (P2 – 0.43 x P1) is empirically derived from a set of pre- and post-laser in situ keratomileusis (LASIK) data (Medeiros & Weinreb, 2006). Correction constants are found to minimize the difference in applanation pressures between pre and post LASIK patients. Thus, the IOPcc gives an IOP reading which is less affected by corneal properties (Luce, 2006).

Due to the viscoelastic properties of the cornea, energy absorption during rapid corneal deformation causes a discrepancy between the applanation pressures, P1 and P2. The difference between P1 and P2 (P1-P2) is called corneal hysteresis (CH) (Figure 1.4). The ORA also provides another corneal biomechanical parameter, corneal resistance factor (CRF, P1 – 0.7 x P2). The CRF is empirically derived to maximize its correlation with central corneal thickness (CCT) and minimize its correlation with IOPcc (Luce, 2006). It is suggested that CRF represents the overall resistance of the cornea, while it is strongly influenced by corneal geometry.

The process of corneal deformation during an ORA measurement is reflected as a waveform (Figure 1.4). According to the manufacturer, a reliable measurement can be identified by two applanation signal peaks with approximately symmetrical height and a waveform with a fairly smooth signal curve. A waveform score (WS) on a scale of 0 to 10 is provided as a quality indicator for the ORA measurement but there is no guideline for the use of WS. It is generally considered that the quality of measurement is better with a higher WS. Various studies have suggested their own WS recommendations to increase measurement reliability. These have included using a WS of at least 3.5 to 7.6 or more, and selecting the best score value or averaging 2 to 4 repeated measurements (Lam et al., 2010, Ayala & Chen, 2012, Goebels et al., 2012, Mandalos et al., 2013, Vantomme et al., 2013).

1.4.2 Factors affecting Corneal Hysteresis (CH) and Corneal Resistance Factor (CRF)

Since the release of the ORA for use in clinical practice, extensive studies have been conducted to investigate various factors affecting CH and CRF, as well as the usefulness of CH and CRF in clinical diagnosis and management.

1.4.2.1 Age

Ex vivo studies confirmed the corneal stiffening effect with increasing age (Elsheikh et al., 2010). Stiffness of donor corneas was doubled from age 20 to age 100 (Knox Cartwright et al., 2011). This phenomenon could be explained by the growth of corneal collagen fibrils in non-enzymatic cross-linking with age (Malik et al., 1992, Daxer et al., 1998). The influence of age on CH and CRF is not as prominent as in experimental studies. Kotecha et al. (2006) was the first group to report a reduction of CH by approximately 0.28 mmHg per decade. However, their results could have been confounded by the inclusion of patients with ocular hypertension, pigment dispersion syndrome, and glaucoma. The population-based study of Foster et al. (2011) was the largest in scale, consisting of over four thousands subjects. They found a decline of CH and CRF of 0.34 mmHg and 0.31 mmHg per decade, respectively. Mild and negative association between CH or CRF and age was shown in extreme age ranges (Fontes et al., 2008, Kida et al., 2008, Kamiya et al., 2009b, Kotecha et al., 2014, Strobbe et al., 2014, Rosa et al., 2015). Ortiz et al. (2007) and Kida et al. (2006, 2008) found significant difference in CH between two different age groups, with a lower CH in the older age group. In general, CH and CRF do not vary significantly with age in younger subjects (Kirwan et al., 2006, Lim et al., 2008a, Song et al., 2008, Chang et al., 2010, Huang et al., 2013, Bueno-Gimeno et al., 2014a). Other studies failed to find any significant association between CH or CRF and age in the general population (Touboul et al., 2008, Narayanaswamy et al., 2011, Radhakrishnan et al., 2012). However, some studies were limited by a narrow age range and uneven age distribution. Conversely, Franco & Lira (2009) demonstrated a mild increasing trend of CRF with age, but the results were clinically insignificant. In view of great inter-subject variability, the aging effect on corneal biomechanics could be

difficult to detect *in vivo* using the ORA (Plakitsi et al., 2011).

1.4.2.2 Gender

A few studies found that women had slightly higher CH and CRF than men (Fontes et al., 2008, Song et al., 2008, Foster et al., 2011, Narayanaswamy et al., 2011, Radhakrishnan et al., 2012). Interestingly, Strobbe et al. (2014) reported the opposite findings. However, any gender difference in CH and CRF was within 5 %. Other studies disclosed no gender difference in CH and CRF (Kamiya et al., 2008, Lim et al., 2008a, Chang et al., 2010, Huang et al., 2013). Though there might be small or insignificant fluctuation of corneal properties from hormonal changes during monthly menstrual cycle (Goldich et al., 2011, Seymenoglu et al., 2011), study on gender difference on these parameters appears to have little clinical value.

1.4.2.3 Circadian rhythm

Most studies confirmed that CH and CRF were stable in normal subjects during waking hours (Laiquzzaman et al., 2006, Gonzalez-Meijome et al., 2008a, Kotecha et al., 2009, Oncel et al., 2009, Villas-Boas et al., 2009). Notably, Villas-Boas et al. (2009) also found CH to be stable in glaucoma patients.. In contrast, the manufacturer reported a circadian rhythm in raw ORA data , but this was only from a single subject (Luce, 2005). In an investigation of younger and older groups of subjects, Kida and associates (2006, 2008) revealed stable CH values for both groups when it was measured at a two-hourly intervals in a 24-hour cycle. The circadian rhythm of CRF was only studied in the older group and its stability was also demonstrated. On the other hand, Shen et al. (2008b) reported a significant increase in CRF immediately after awakening compared with that before sleep. This result was replicated by another study which demonstrated an overnight increase of CRF (by 1.5 mmHg) occurred during sleep (Lau & Pye, 2012). Significant corneal swelling could be a contributing factor because ORA measurements were taken within 10 minutes upon awakening in these two studies. Nevertheless, Kida et al. (2008) performed ORA measurements 30 minutes after the subjects were awakened, by which time., corneal swelling had subsided as shown in their graph of CCT changes over 24 hours.

1.4.2.4 Central corneal thickness

There have been numerous reports showing moderate and positive association between CH and CCT, and between CRF and CCT in different diagnostic groups including normal, diseased, and treated eyes (Shah et al., 2006, Lam et al., 2007, Kida et al., 2008, Touboul et al., 2008, Franco & Lira, 2009, Oncel et al., 2009, Sullivan-Mee et al., 2012, Kotecha et al., 2014, Strobbe et al., 2014, Rosa et al., 2015). Strobbe and colleagues (2014) stated that CH and CRF increased by 0.01 mmHg and 0.03 mmHg respectively for each 1 μm increase in CCT. Leite et al. (2010) reported black subjects showed lower CH and CRF, as well as thinner CCT compared to white subjects, but both CH and CRF did not demonstrate significant between-group difference after CCT adjustment. However Haseltine et al. (2012) found significant difference in CH between races when CCT was considered as a covariate. Regardless of the disparity in statistical results from the two studies, individual CCT variation could potentially confound clinical interpretation on corneal biomechanics.

Lau & Pye (2012) found that diurnal changes in CH and CRF varied directly with that in CCT over 24 hours. However, other investigators did not demonstrate time-dependent variations between CH or CRF and CCT (Kida et al., 2006, Kida et al., 2008, Shen et al., 2008b). Kida et al. (2008) concluded that an increase of corneal hydration during eye closure did not alter collagen fibers and ground substance of the same cornea, thus corneal biomechanical properties were not affected. Nevertheless, different results could be observed at different measurement times.

1.4.2.5 Other corneal parameters

As CH and CRF are measured via corneal applanation, measurement could be sensitive to corneal factors other than corneal thickness, such as corneal radius and corneal astigmatism, similar to their influence on GAT (Mark & Mark, 2003, Rask & Behndig, 2006). However, several studies found there was minimal influence of corneal radius on CH and CRF in normal eyes (Fontes et al., 2008, Kamiya et al., 2008, Franco & Lira, 2009, Chang et al., 2010). It could be difficult to demonstrate any significant univariate correlations between CH or CRF and corneal radius because ORA parameters are also associated with age, CCT, IOP,

and other factors (Rosa et al., 2015). Studies with large sample sizes demonstrated that flatter corneas were associated with lower CH and CRF (Broman et al., 2007, Lim et al., 2008a, Liu et al., 2008, Narayanaswamy et al., 2011). A population-based study involving Chinese subjects reported that CH and CRF decreased by 0.96 mmHg and 0.80 mmHg respectively for each millimeter increase in corneal radius (Narayanaswamy et al., 2011).

Broman et al. (2007) found no association between corneal astigmatism and CH, although a weak correlation was shown between corneal astigmatism and CRF (Pearson's correction = 0.2), Wong and Lam (2011) concluded that corneal astigmatism did not appear to have a clinical effect on ORA measurements.

An increase of corneal thickness would result in an increase of corneal volume. Recently studies found that CH and CRF were positively associated with corneal volume (Sedaghat et al., 2012, Rosa et al., 2015), similar to the influence associated with CCT.

1.4.2.6 Intraocular pressure

The human eye can be regarded as a pressurized vessel enclosed by an outer wall consisting of the cornea and sclera. According to Laplace's law, wall tension increases when the internal pressure increases (Roberts, 2014). Therefore, cornea may behave stiffer" at a higher IOP. Corneal biomechanical measurement is inherently influenced by IOP. This phenomenon has been verified by inflation testing of postmortem human eyes (Elsheikh et al., 2007b).

The association between IOP and CH or CRF has been explored clinically. Luce (2005) found that CH remained stable within individual eyes when their IOP was elevated by a custom ophthalmodynamometer and measured by GAT. Kotecha et al. (2006) applied hypotensive eye drops in either normal or ocular hypertensive eyes and illustrated a weak and reverse relationship between CH change and GAT IOP change (Figure 1.5). Lau & Pye (2012) reported a positive association between diurnal changes of GAT IOP and CRF alterations, but such association was not found with CH alterations. Other studies also showed positive association

between GAT IOP and CRF (Medeiros & Weinreb, 2006, Bayoumi et al., 2010, Lau & Pye, 2011b, Narayanaswamy et al., 2011). The lack of association between GAT IOP and CH was reported in some subject groups (Touboul et al., 2008, Bayoumi et al., 2010, Rosa et al., 2015), but others revealed lower CH in higher GAT IOP (Kamiya et al., 2008, Narayanaswamy et al., 2011).

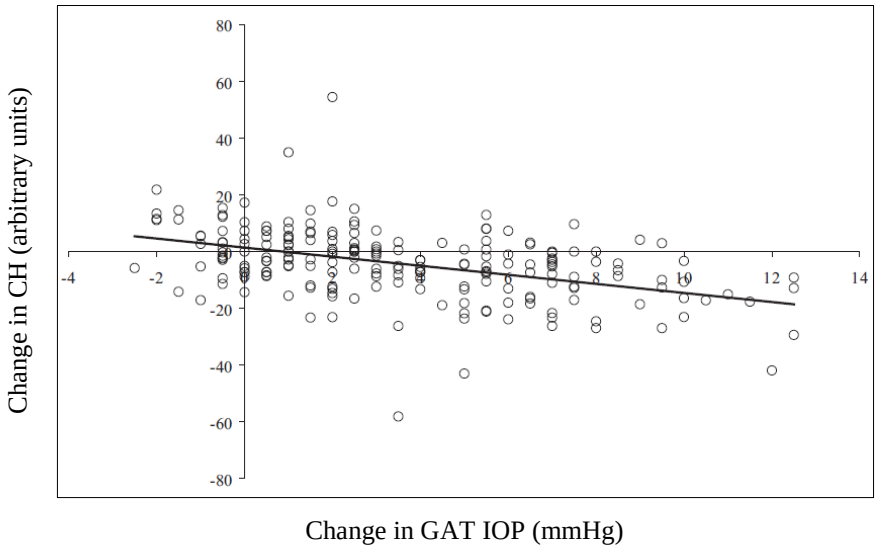

Figure 1.5 Increase in CH with reduction in GAT IOP in both normal and ocular hypertensive eyes (Kotecha et al., 2006).

The IOP dependence of CH and CRF could be influenced by the tonometry techniques employed (Kotecha et al., 2006). Liu & Roberts (2005) in their theoretical mathematical model found that the accuracy of GAT was heavily influenced by mechanical properties of the cornea. Kotecha et al. (2014), using dynamic contour tonometry (DCT), found that DCT IOP was a significant predictor for CRF. On the other hand, CH could not be predicted from DCT IOP. Apart from GAT, IOPcc is an intraocular pressure less influenced by corneal geometry. Several studies reported lower CH when IOPcc was high (Franco & Lira, 2009, Alhamad & Meek, 2011, Roberts et al., 2014). However, IOPcc, CH and CRF are all derived from the same raw ORA data. This IOP dependence might partly reflect an artifact of the ORA measurement.

1.4.2.7 Refractive error & axial length

Axial length (AL) is the primary determinant of refractive error. The scleral stiffness and thickness are reduced in eyes developing myopia (McBrien et al., 2009). On the other hand, myopic eyes tended to have flatter corneal curvature and thinner corneal thickness (Goss et al., 1997, Chang et al., 2001). Hence, it is speculated that the biomechanical properties of cornea and sclera might be linked, suggesting less stiff corneas in myopes.

Many researchers have investigated the effect of refractive error or axial length on CH and CRF. A significant negative correlation between CH and myopia was observed in both Chinese children and adults (Shen et al., 2008a, Song et al., 2008, Chang et al., 2010, Huang et al., 2011, Jiang et al., 2011, Narayanaswamy et al., 2011, Wong & Lam, 2015). Consistent findings were also found in subjects from other ethnicities (Plakitsi et al., 2011, Altan et al., 2012, Bueno-Gimeno et al., 2014a, Del Buey et al., 2014). Notably, subjects with high myopic anisometropia had significantly lower CH in the high myopic eye compared with the fellow emmetropic eye (Xu et al., 2010). On the other hand, CRF was independent of refractive status (Shen et al., 2008a, Jiang et al., 2011, Narayanaswamy et al., 2011, Plakitsi et al., 2011, Wong & Lam, 2015) or its association with refractive status was less significant than CH (Chang et al., 2010, Bueno-Gimeno et al., 2014a, Del Buey et al., 2014). The refractive error showed no association with CH and CRF in Brazilian subjects (Fontes et al., 2008). Lim et al. (2008a) also did not find any association between corneal biomechanical parameters and refractive error or AL in Singaporean children. Moreover, they speculated there were limitations of ability of ORA to detect corneal biomechanical difference in their subjects. In contrast, Radhakrishnan et al. (2012) found a weak but significant correlation between CRF and refractive error, with higher CRF in myopic eyes compared with normal eyes.

Despite the majority of the studies indicating reduced CH in high myopic eyes, this finding is limited by a considerable degree of variability in CH among different refractive groups.

1.4.3 Clinical application of CH and CRF in different ocular conditions

1.4.3.1 Keratoconus

Keratoconus (KC) is a common corneal dystrophy characterized by a localized reduction in corneal radius and thickness, and progressive topographic irregularity (Pinero et al., 2012). These structural alterations of the cornea could be explained by a displacement of stromal lamellae and slippage between collagen fibrils (Meek et al., 2005). The disruption of the normal collagen fibril network in KC corneas might lead to changes in corneal biomechanics. Strip extensiometry has revealed that keratoconus corneas were less stiff than normal corneas (Andreassen et al., 1980, Nash et al., 1982). Clinical studies showed reduced CH (from 0.5 – 3.2 mmHg) and CRF (from 1.2 – 4.7 mmHg) in KC patients compared with healthy controls (Ortiz et al., 2007, Shah & Laiquzzaman, 2009, Saad et al., 2010, Yenerel et al., 2010, Touboul et al., 2011, Kara et al., 2013). The differences were smaller but statistically significant after controlling for confounding factors including age, gender, and CCT (Schweitzer et al., 2010, Fontes et al., 2011a, Fontes et al., 2011b, Johnson et al., 2011, Galletti et al., 2012, Ruisenor Vazquez et al., 2013). Increase in KC severity was also associated with greater CH and CRF reduction (Shah et al., 2007, Cohen, 2009, Shah & Laiquzzaman, 2009, Pinero et al., 2010, Johnson et al., 2011, Mikielewicz et al., 2011, Gkika et al., 2012, Wolffsohn et al., 2012). However, the stand-alone CH or CRF showed low sensitivity and specificity in differentiating subclinical or manifest KC (Fontes et al., 2010, Schweitzer et al., 2010, Galletti et al., 2012) and a large overlap seems to exist between normal and keartoconus corneas (Shah et al., 2007, Kirwan et al., 2008, Fontes et al., 2011b, Johnson et al., 2011).

1.4.3.2 Corneal collagen cross-linking

Corneal collagen cross-linking (CXL) is a widely-used treatment option to halt the progression of KC. The procedure promotes the formation of covalent bonds within the corneal collagen fibrils and lamellae using riboflavin and ultraviolet A (UVA) radiation that strengthens the corneal tissue (Tan & Mehta, 2011). In laboratory experiments, a significant corneal stiffening effect by CXL has been demonstrated using *in vitro* human corneas (Wollensak et al., 2003, Knox Cartwright et al., 2012). The increase in biomechanical stiffness was also

maintained for 8 months in treated rabbit eyes (Wollensak & Iomdina, 2009). In view of the results from stress-strain measurements, the biomechanical changes involved in the process were also explored. During intraoperative measurements, Vinciguerra et al. (2010) observed an increase of CH and CRF after riboflavin impregnation and UVA radiation. They suggested that the corneas were more resistant and stiffer due to the dehydrating effect of riboflavin solution. Two studies showed CH and CRF to be significantly higher one month after CXL than their preoperative values (Vinciguerra et al., 2010, Greenstein et al., 2012). However, one study reported a lower CH and CRF in children at 1 month follow-up after transepithelial CXL (without removal of corneal epithelium) (Salman, 2016). Most recent studies reported no significant changes of CH and CRF induced by CXL at different time points of follow-up (Sedaghat et al., 2010, Mikielewicz et al., 2011, Spoerl et al., 2011, Gkika et al., 2012, Goldich et al., 2012, Goldich et al., 2014, Hallahan et al., 2014, Sedaghat et al., 2015). CH and CRF might not be useful to detect corneal biomechanical response to CXL.

1.4.3.3 Corneal refractive surgery

Corneal refractive surgery is a popular surgical treatment for correction of myopia. Permanent removal of certain corneal tissue causes disruption of stromal lamellae and thus leads to alternation of corneal biomechanics (Guirao, 2005, Dupps & Wilson, 2006). Studies have shown statistically significant reduction of CH (from 1.1 – 2.3 mmHg) and CRF (from 1.9 – 3.5 mmHg) after different refractive treatments (Ortiz et al., 2007, Pepose et al., 2007, Chen et al., 2008, Hamilton & Pye, 2008, Kirwan & O'Keefe, 2008, Kamiya et al., 2009a, Qazi et al., 2009, Shah & Laiquzzaman, 2009, Chen et al., 2010b, Ryan et al., 2011, Wang et al., 2014, Chen et al., 2016). A slight postoperative recovery was noticed after 1 to 12 months, but the two parameters remained lower than their preoperative values (Kamiya et al., 2009a, Chen et al., 2010b, Ryan et al., 2011, Wang et al., 2014).

Upon comparison of different surgical techniques, laser *in situ* keratomileusis (LASIK) showed greater CH and CRF changes than photorefractive keratectomy (PRK), which could be due to flap creation and ablation of deeper stromal layers in the former technique (Kamiya et al., 2009a). Thus these investigators suggested

that PRK might be a safer surgical option for myopia correction. Two studies showed similar reduction in CH and CRF between LASIK and laser-assisted subepithelial keratectomy (LASEK) (Kirwan & O'Keefe, 2008, Qazi et al., 2009). Indeed, when evaluating the raw ORA data, greater corneal biomechanical impact was delineated after LASIK (Qazi et al., 2009). Changes in CH or CRF were more pronounced in LASIK or LASEK than other new surgical procedure such as small incision lenticule extraction (SMILE) (Wang et al., 2014, Chen et al., 2016). All these observed differences might be attributable to the creation of stromal flap during LASIK. Gatinel et al. (2007) monitored the changes in CH and CRF from one eye of a patient after flap creation, while photoablation procedure was not performed. CH and CRF significantly reduced by 1.8 mmHg and 2.2 mmHg, respectively, in a course of 25 days. However, Uzbek et al. (2011) reported no significant changes in CH and CRF following flap creation and reposition using larger patient pool. In porcine eyes, corneal flaps as thick as 300 μm demonstrated significant reduction in CH and CRF compared with thin flaps of 100 μm (Medeiros et al., 2011). Nevertheless, more tissue ablation could induce more biomechanical changes. A higher myopic correction or a deeper ablation was associated with greater changes of CH and CRF (Ortiz et al., 2007, Chen et al., 2008, Kirwan & O'Keefe, 2008, Kamiya et al., 2009a, Qazi et al., 2009). Hyperopic LASIK caused less reduction in CH and CRF than myopic LASIK. Hence, a different ablation profile might also contribute to different postoperative corneal biomechanics changes (de Medeiros et al., 2010).

Iatrogenic corneal ectasia is a serious but uncommon complication of refractive surgery (Rad et al., 2004). Weakened corneal biomechanics may be an important risk factor for postoperative ectasia (Roberts & Dupps, 2014). The predictive value of CH and CRF on screening postoperative ectasia prior to refractive surgery was investigated, but the study was not completed due to difficulties in subject recruitment and the rare occurrence of the condition (Ambrosio & Randleman, 2013). In a case report, CH or CRF lower than 8.8 mmHg were suggested as a cutoff for high risk ectatic development following LASIK (Ambrosio et al., 2010). Kerautret et al. (2008) also reported unilateral corneal ectasia after bilateral LASIK treatment. Although similar CH and CRF were found between the two

eyes, a significant inter-ocular difference was revealed from the raw ORA data. This indicates the importance of studying the morphology of the waveform signals.

1.4.3.4 Soft contact lens wear

Cankaya and associates (2012) found that myopic soft contact lens (SCL) wearers had higher CRF than those who never wore contact lenses (10.4 ± 1.9 mmHg vs. 9.6 ± 1.9 mmHg). Such changes were independent of duration of lens wear which ranged from 1 to 14.5 years. However, the contact lens materials were not specified in their study. Corneal edema can be effectively induced by short-term eye closure during low-oxygen transmissible SCL wear (O'Neal & Polse, 1986, Hutchings et al., 2010). Its effect on ORA parameters was also investigated. Lu et al. (2007) reported a 0.6 mmHg increase of CRF, accompanied by 13.1 % of central corneal swelling, immediately after three-hour lens wear under eye closure. The correlation between changes of CCT and CRF was weak but significant. Lau and Pye (2011a) found 7.8 % central corneal swelling after a two-hour patching with SCL wear. Considering normal fluctuations of ORA parameters in the control eyes, corrected CRF was elevated by a maximum of 0.6 mmHg while corrected CH was reduced by 0.6 mmHg after lens removal. It was suggested that changes in ORA parameters during contact lens-induced corneal edema might be explained by unknown factors other than changes in CCT (Lu et al., 2007, Lau & Pye, 2011a). The response of ORA parameters reported in their studies may not be applicable to actual pathological cases involving corneal edema (Garcia-Porta et al., 2014).

1.4.3.5 Orthokeratology

Orthokeratology (ortho-k), or corneal reshaping therapy, is a clinical technique that uses a special rigid gas permeable contact lens to reshape the cornea to reduce myopia (Caroline, 2001). The cornea becomes flatter and thinner at the central treatment zone (Alharbi & Swarbrick, 2003, Villa-Collar et al., 2009). The changes in corneal biomechanical properties in ortho-k treatment are not fully understood. In a one month of short-term ortho-k treatment, Yeh et al. (2013) reported a reduction in CH and CRF, but they concluded the changes were clinically insignificant. Nieto-Bona et al. (2012) found significant decreases in CH but not in CRF. These two studies involved young adult subjects with different ethnicities.

Throughout a 6-month study period, Chen (2011) observed a decreasing trend of CRF with longer duration of lens wear but CH remained stable . In contrast, an initial transient reduction of CH and CRF reversed and returned to original values after 3- and 6-month of lens wear in Mao et al.'s (2010) study. Although both studies recruited Chinese subjects, the latter consisted of younger children. Either CH or CRF showed a tendency to return to its baseline level after lens cessation (Chen, 2011, Nieto-Bona et al., 2012). According to the literature, the changes of CH and CRF during ortho-k treatment were too subtle to be detected clinically. Other investigators have attempted using CH and CRF to predict response of ortho-k. A pilot study involving 8 subjects demonstrated that a higher baseline CH was associated with slower response (3 hours of lens wear) and recovery (3 hours after lens removal), by monitoring the changes in steep keratometry and CCT (Gonzalez-Meijome et al., 2008b). However, Glavine (2009) did not find significant association between CH or CRF and ortho-k response over a 3-month treatment period in 41 subjects.

Older corneas showed a slower response to short-term ortho-k (Jayakumar & Swarbrick, 2005). Regarding the age-related changes in corneal microstructure (Malik et al., 1992, Daxer et al., 1998) and mechanical properties (Elsheikh et al., 2010, Knox Cartwright et al., 2011), it is worthwhile to explore the predictive role of ortho-k effect using other corneal biomechanical measurement techniques.

1.4.3.6 Glaucoma & ocular hypertension

A thin cornea is widely accepted as a risk factor for glaucoma development and progression. Despite its effect on IOP measurement error, the possibility that other corneal properties are related to glaucoma susceptibility cannot be excluded (Gordon et al., 2002, Medeiros et al., 2003, Pakravan et al., 2007). CH or CRF could be associated with some changes in optic nerve head morphology. For example, lower CH was significantly associated with greater cup depth (r = -0.34) and cup-to-disc ratio (r = -0.41) in newly diagnosed glaucoma patients (Prata et al., 2012). In a study consisting of 602 healthy adults, lower CH and CRF were associated with smaller rim area and larger linear cup-to-disc ratio measured by confocal scanning laser ophthalmoscopy in multivariable analyses (Khawaja et al.,

2014). Comparing glaucomatous eyes with and without acquired pit in the optic disc, Bochmann et al. (2008) found significantly lower CH in the former group and suggested that corneal biomechanics might play a pressure-independent role in optic nerve damage. In contrast, Wells et al. (2008) reported positive association between CH and optic nerve head deformability in glaucoma patients during an artificial acute IOP elevation. Other studies did not find any association between CH and optic disc parameters either in healthy or glaucoma subjects (Lim et al., 2008b, Insull et al., 2010, Carbonaro et al., 2014). In addition, CH and CRF had no association with retinal nerve fiber layer thickness measurements (Lim et al., 2008b, Mansouri et al., 2012, Vu et al., 2013).

Many studies have reported lower CH in eyes with primary open-angle glaucoma (POAG) than in normal eyes (Sullivan-Mee et al., 2008, Mangouritsas et al., 2009, Detry-Morel et al., 2011, Detry-Morel et al., 2012, Kaushik et al., 2012, Pillunat et al., 2016). There was a mean CH difference of 0.7 mmHg between the worse and better eyes in POAG patients presenting asymmetric visual field defects, with a significantly lower CH in the worse eye (Anand et al., 2010). Hirneiss et al. (2011) also found lower CH in the glaucomatous eye compared with the fellow eye in unilateral glaucoma. However, the CH difference disappeared when CH was corrected for IOP. Lower CH and CRF were found in eyes with normal tension glaucoma (NTG) compared with normal eyes (Grise-Dulac et al., 2012, Kaushik et al., 2012, Morita et al., 2012, Shin et al., 2015b). Several studies revealed minimal CH difference between POAG and NTG (Ang et al., 2008, Shah et al., 2008, Detry-Morel et al., 2011). Perhaps POAG and NTG share similar etiology relating to ocular biomechanics. Higher CH and CRF were shown in eyes with ocular hypertension (OHT) compared with glaucomatous and normal eyes. Nevertheless, OHT patients also had greater CCT and IOP readings (Shah et al., 2008, Sullivan-Mee et al., 2008, Detry-Morel et al., 2011, Kaushik et al., 2012, Pensyl et al., 2012).

Eyes with lower CH were associated with a faster rate of visual field loss in glaucomatous eyes (Congdon et al., 2006, De Moraes et al., 2012, Park et al., 2015, Helmy et al., 2016). In particular, Medeiros et al. (2013) suggested that 1 mmHg

decrease in CH was associated with 0.25% per year decline in the visual field index as determined by the Humphrey visual field analyzer. Chee et al. (2013) showed that lower CH was associated with structural glaucomatous optic nerve progression detected by flicker chronoscopy. It is interesting to note increases in CH (from 0.4 to 2.3 mmHg) after surgical (Sun et al., 2009, Pakravan et al., 2014) or medical treatment (Tsikripis et al., 2013) of glaucoma. In contrast, association between CH or CRF and severity of primary angle closure glaucoma could not be demonstrated (Nongpiur et al., 2015).

1.4.4 Problems of the ORA

Since the introduction of the ORA in 2005, corneal biomechanics have become an important area in the field of ophthalmology and optometry. However, interpretation of CH and CRF can be difficult because they are not expressed as standard mechanical terms like stiffness or elasticity. Roberts (2014) stated that CH and CRF are viscoelastic parameters including both elastic and viscous properties of the cornea. Since different combinations of elasticity and viscosity could give the same CH value (Glass et al., 2008), it might explain the lack of sensitivity of ORA in detecting collagen crosslinked corneas (Vinciguerra et al., 2010). Dupps (2007) suggested CH as a measure of viscous damping of corneal tissue. Less attention has been given to the biomechanical meaning of CRF. The manufacturer stated that CRF is empirically derived to maximize its association with CCT (Luce, 2006).

The ORA parameters are uniquely defined under specific measurement conditions. McMonnies (2012) has criticized the technique stating that the loading and unloading sequence using air puff applanation is unusual and it deviates from the classical method of determining hysteresis. Specifically, corneal recovery from maximum indentation is not only caused by the potential energy stored in the indented cornea. Other assisting and opposing forces could be present, which include the distending force of elevated IOP from inward applanation and residual air pressure beyond maximum indentation. Moreover, the loading rate of air pressure varies when measuring different corneas. All these factors could contribute to unpredicted variations in CH values. Whether CH represents an intrinsic corneal property is therefore questioned.

Despite the criticism on the methodology of the device, most investigators have been pursuing the clinical relevance of CH and CRF in disease diagnosis and management. Nevertheless, the major obstacle is the large overlapping of these values between normal and diseased groups. As discussed in Section 1.4.2, various factors could also confound CH and CRF measurements unless they are carefully controlled.

The ORA detects and records inward and outward applanation pressures at the central cornea using a reflection of IR light. The smoothness of the reflective surface can affect ORA measurement. Tear film instability due to ocular diseases (Leung et al., 2008, Dienes et al., 2015) or refractive surgeries (Ang et al., 2001) may result in poor quality of the applanation signals (Dupps, 2007, Terai et al., 2012). A waveform score is applied to evaluate the quality of measurement. However, it could be difficult to obtain good quality scores in compromised corneas. Besides, the ORA measurement is restricted to the central cornea. It cannot be used to assess other corneal regions, such as the presence of peripheral cones in some keratoconus cases (Wilson et al., 1991, Ertan et al., 2009). CH or CRF measured at the central cornea far away from the keratoconus cone may produce similar corneal biomechanics results to those of normal corneas (Dupps, 2007). Although it has been shown that the raw waveform signals provided by the ORA could improve its sensitivity over CH and CRF alone (Kerautret et al., 2008, Wolffsohn et al., 2012, Roberts et al., 2014), the aforementioned limitations of ORA still exist, and also its unique measurement conditions (McMonnies, 2012) should not be overlooked.

1.5 Knowledge gap

The ORA is the first clinical device that has attempted to measure corneal biomechanical properties in terms of CH and CRF. The impact of various influencing factors and the clinical applicability on CH and CRF has been discussed, but global conclusions on its usefulness have not been reached. The interpretation of CH and CRF is difficult because the parameters are derived empirically and do not directly indicate standard mechanical properties (such as elastic modulus) (Roberts, 2014). Currently, the ORA allows advanced analysis of its signal waveform in the hope of improving its diagnostic capability (Spoerl et al., 2011, Landoulsi et al., 2013).

Nevertheless, a new clinical device for corneal biomechanics assessment is warranted to overcome current limitations in the ORA.

1.6 Goals of this PhD study

A new clinical device, the Corneal Visualization Scheimpflug Technology (Corvis ST) was recently launched, coinciding with the initial stage of this PhD study. Working as a modified NCT, it measures corneal deformation and recovery using images captured by a Scheimpflug camera. On the other hand, a group of mechanical engineers developed a novel corneal indentation device (CID). The CID precisely measures corneal stiffness as the force required to indent the cornea to a unit depth. The tangent elastic modulus of cornea, or corneal tangent modulus in short, could be calculated. However, the CID had not been applied to human corneas. Both devices are new instruments for *in vivo* corneal biomechanical measurements.

A series of clinical studies were conducted in this PhD study and the goals were to:

- evaluate intraexaminer repeatability and intersession reproducibility of the Corvis-generated corneal biomechanical parameters in normal subjects
- examine repeatability and diurnal variation of the CID-derived corneal stiffness and corneal tangent modulus in normal subjects
- compare corneal tangent modulus in low and high myopes
- investigate the effect of short-term orthokeratology on corneal stiffness and corneal tangent modulus
- explore the feasibility of the CID to conduct corneal biomechanical measurement at different corneal locations

The ultimate goal was to establish effective and reliable method for clinical corneal biomechanical assessment.

1.7 Hypotheses

Understanding current limitations in measuring corneal biomechanics and developing new techniques for measurement it will allow better estimates of the corneal biomechanical properties *in vivo*. It is anticipated that:

- Any new clinical devices developed for corneal biomechanical measurements would show good repeatability and reproducibility, and demonstrate

acceptable diurnal variation in normal subjects

- Corneal biomechanical properties are weakened in high myopes compared with low myopes
- Orthokeratology alters corneal biomechanical properties but the effect would be reversible
- Corneal biomechanical properties can be measured at different corneal locations using newer techniques

Chapter 2

Repeatability of a Scheimpflug-based noncontact tonometry for corneal biomechanical measurement

2.1 Introduction

A recent technological breakthrough has made dynamic measurement of corneal deformation possible with the use of Corneal Visualization Scheimpflug Technology (Corvis ST; Oculus, Germany) (Ambrósio Jr et al., 2013). A noncontact tonometer (NCT), the Corvis ST emits a consistent air puff maximal pressure in each measurement. At the same time, a built-in high-speed Scheimpflug camera captures complete corneal movement along an 8 mm horizontal cross-section at a rate of 4330 image frames per second. Practically, a complete corneal deformation process due to air puff indentation lasts approximately 32 ms. In this time, 140 image frames of the cornea are collected and a video clip is generated for visualization (Figure 2.1). The Corvis ST works by tracing the anterior and posterior surface from the image frames and establishes numerous corneal deformation parameters, in addition to ordinary tonometry and pachymetry readings (Figure 2.2). Basically, data acquisitions for corneal deformation parameters are performed under three distinct phases, namely, the first applanation (App 1), the highest concavity (Hi Con.) and the second applanation (App 2), respectively. The cornea is initially flattened (App 1) by an emission of air puff and continues to deform to its maximum concave shape (Hi Con.). Air puff pressure declines when it reaches the peak value, allowing the cornea to rebound to a second flattening stage (App 2) and eventually returns to its original shape. Detailed description of 10 Corvis output parameters is shown in Table 2.1.

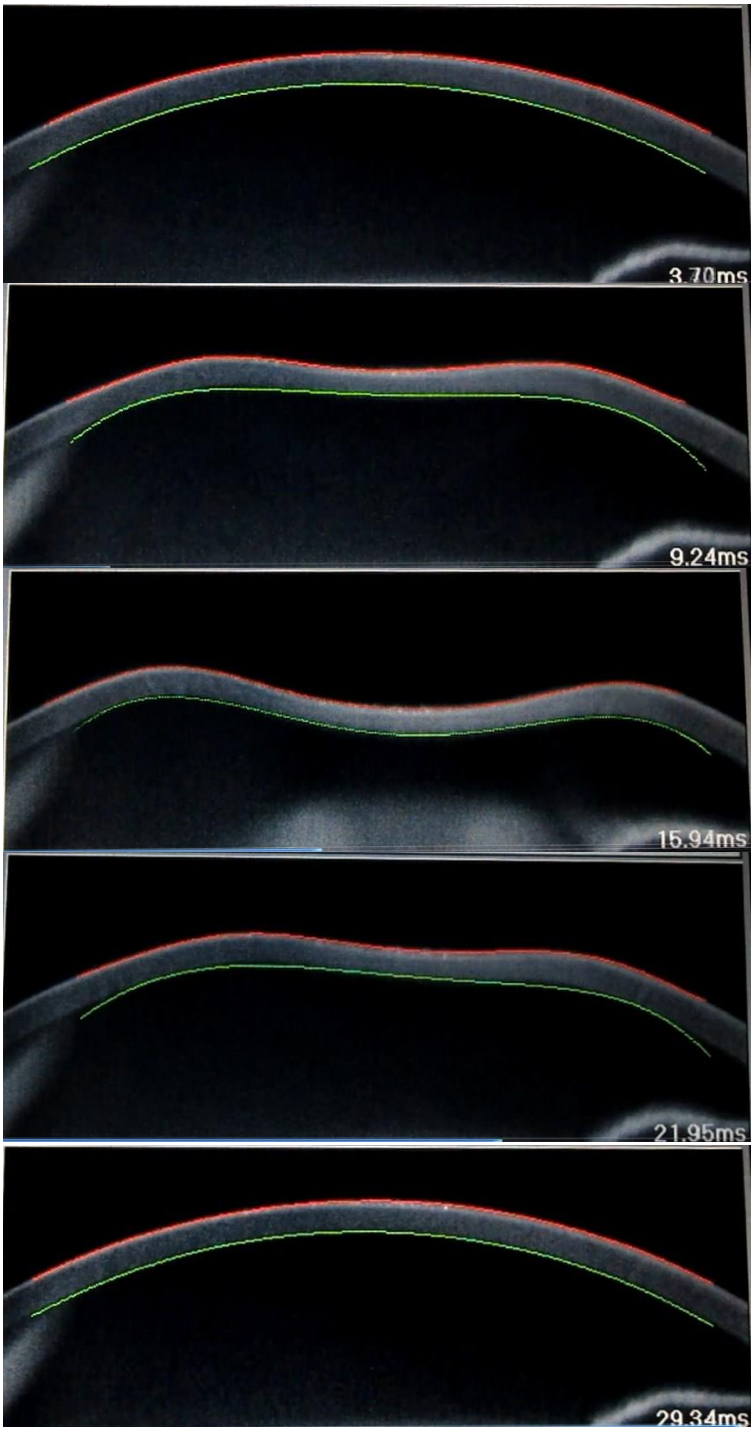

Figure 2.1 Timed snapshots of the video output from the Corvis ST. The anterior and posterior corneal surfaces are outlined using red and green respectively.

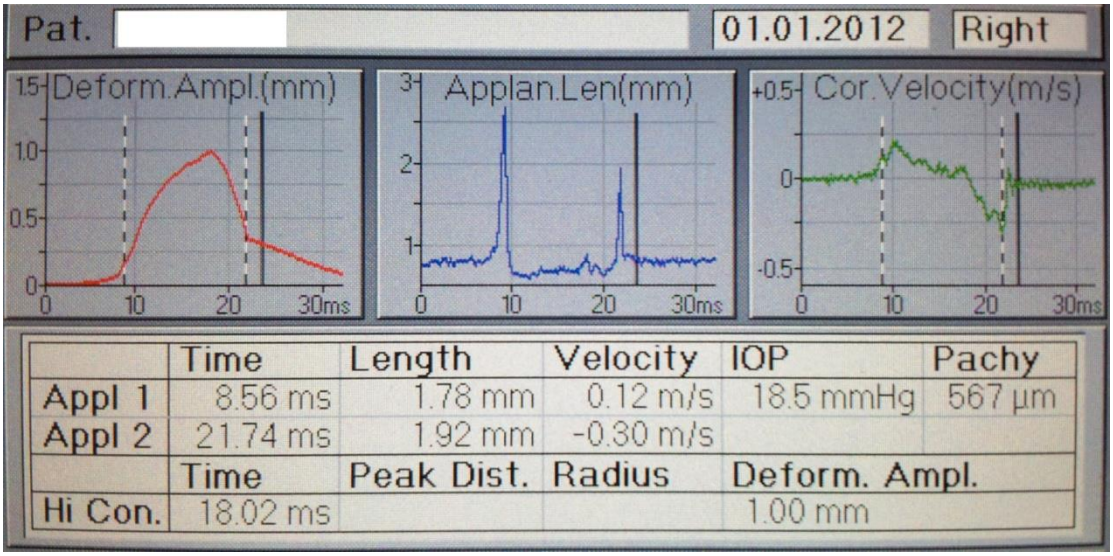

Figure 2.2 Ten Corvis ST parameters are displayed after each measurement. Values of peak distance (Peak Dist.) and corneal radius at highest concavity (Radius) were not shown in an early version of the software.

Table 2.1 Description of the Corvis ST output parameters.

Parameter	Abbreviation	Description
Intraocular pressure	IOP	An ordinary NCT measurement which is based on the first applanation
Pachymetry	CCT	Measurement of central corneal thickness (CCT) with optical pachymetry
Time of Appl 1	1st A-time	Time from start until the first applanation
Length of Appl 1	1st A-length	Length of the flattened cornea in the first applanation
Velocity of Appl 1	V_{in}	Corneal velocity during the first applanation moment
Time of Appl 2	2nd A-time	Time from start until the second applanation
Length of Appl 2	2nd A-length	Length of the flattened cornea in the second applanation
Velocity of Appl 2	V_{out}	Corneal velocity during the second applanation moment
Time of Hi Con	HC-time	Time from start until the highest concavity of cornea is reached
Deformation amplitude	DA	Maximum deformation amplitude (from start to the highest concavity) at the corneal apex

Appl 1 = first applanation; Appl 2 = second applanation; Hi Con = highest concavity

For Corvis ST to be of clinical value, it is important that measurements made are repeatable and reproducible. "Repeatability" is defined as the variability in repeated measures by one examiner without changing all other factors. "Reproducibility" refers to the variability in repeated measures when factors are varied, for example, in different visits (McAlinden et al., 2011).

The purpose of this study was to evaluate the intraexaminer repeatability and intersession reproducibility of Corvis-generated parameters in normal subjects.

2.2 Methodology

2.2.1 Subjects

Thirty-seven normal subjects (20 male and 17 female) with a mean ± standard deviation (SD) age of 27.1 ± 8.5 years (range from 20 to 53 years) were enrolled in this study. All subjects had unremarkable general and ocular health. Exclusion criteria included Corvis-generated intraocular pressure (IOP) ≥ 21 mmHg, rigid lens wear, current pregnancy, history of refractive surgery, corneal disease or trauma. Soft lens wearers were required to cease contact lens wear for at least 24 hours before the data collection. All procedures followed the Declaration of Helsinki and the protocol was reviewed and approved by the ethics review board of The Hong Kong Polytechnic University. Informed consent was obtained from each subject before the commencement of the study. Only their right eyes were measured.

2.2.2 Procedures

Data taking was conducted between 9 to 11 am (first session) and 3 to 5 pm (second session) within a day by the same practitioner. In each session, corneal topography and noncontact tonometry were measured using Pentacam (Oculus, Germany) and Corvis ST respectively. Subjects were asked to fixate on the internal target while image positioning was adjusted by the examiner using a joystick. Upon perfect alignment, auto acquisition was achieved. Three valid readings were obtained from each instrument in each session. The Pentacam system with 25-image mode was used. An "OK" in Quality Specification (QS) was required for successful acquisition. The simulated keratometry

readings ($SimK_1$, flattest keratometry reading; $SimK_2$, steepest keratometry reading) were exported for analysis. In Corvis ST, default settings were used. A sequence of data was displayed on screen following successful measurement (Figure 2.2). A video of instant corneal deformation during air puff indentation was shown and the numerical data were exported for further analysis.

2.3 Statistical analysis

Statistical analyses and graphics were performed using SPSS (version 18.0, SPSS, Inc., USA) and Microsoft (Excel 2013, Microsoft Corp., USA) softwares, respectively. All the data were tested for normality using Shapiro-Wilk tests. Appropriate parametric or nonparametric statistical tests were used for further analyses. The level of significance chosen was 5 %.

To determine intra-examiner repeatability of the Corvis ST parameters, the within-subject standard deviation (S_w) of three consecutive measurements in the first session was first calculated (Bland & Altman, 1996). Analytical results were presented in different ways. Precision (coefficients of repeatability) was calculated by multiplying S_w x 1.96, in which the difference between any single measurement and the true value would be expected to be less than the precision for 95 % of observations. Repeatability was calculated by multiplying S_w x 2.77 and it reflects the greatest expected difference between any pair of measurements for 95 % of observations. Additionally, coefficient of variation (CV) was computed by dividing S_w by the mean of each Corvis ST parameter and then multiplying by 100. Intraclass correlation coefficient (ICC) was also assessed to evaluate intraexaminer reliability.

To determine intersession reproducibility, averaged results of the Corvis ST parameters from each session were used. Intersession differences were first evaluated by paired sample t-tests or Wilcoxon signed-rank tests. Subsequently, Bland-Altman analyses (Bland & Altman, 1986) were performed on the corneal deformation parameters with good intraexaminer repeatability and no significant intersession differences. When no significant association was found between the mean difference and the mean (by Pearson

or Spearman's correlation) in two sessions, the 95 % limits of agreement (LA) plot was drawn for each selected parameter.

Because corneal deformation can be affected by corneal geometry such as corneal thickness and corneal radius, association between corneal deformation amplitude (DA) and central corneal thickness (CCT) by Corvis ST and between simulated keratometry readings ($SimK_1$ and $SimK_2$) by Pentacam were evaluated respectively, using the measurements obtained in the first session.

2.4 Results

The mean spherical equivalent refractive error of the study population was -3.56 ± 2.91 D (range from -12.25 to +1.25 D). The mean values of Corvis ST parameters and corneal curvature are described in Table 2.2. The CCT and SimKs were normally distributed. For the Corvis deformation parameters, only lengths of the 2 applanation states (1^{st} A-length & 2^{nd} A-length), time of highest concavity (HC-time) and DA followed a normal distribution.

Intraexaminer repeatability results are presented in Table 2.3. The recommended ICC value for health research is 0.75 or above (Streiner DL, 2003). Based on ICC values, the most repeatable corneal parameter from Corvis ST was CCT, followed by DA, time of first applanation (1^{st} A-time) and IOP. Though time of second applanation (2^{nd} A-time) had small intrasession variability, the ICC value was only fair. Poor repeatability was shown in the remaining parameters due to large CVs and low ICCs. No significant intersession differences were shown in all parameters (IOP, 1^{st} A-time, 2^{nd} A-time, velocity of first applanation (V_{in}), velocity of second applanation (V_{out}), 2^{nd} A-length, HC-time, DA and SimKs) except in CCT and 1^{st} A-length (Table 2.4).

Table 2.2 Measurements of Corvis ST parameters and simulated corneal curvatures of the study population.

Parameter	Mean ± SD	Range
IOP (mmHg)	14.26 ± 1.28	11.33 to 16.67
CCT (μm)	550.6 ± 27.3	501.0 to 610.0
1st A-time (ms)	7.89 ± 0.21	7.40 to 8.27
1st A-length (mm)	1.76 ± 0.16	1.47 to 2.18
V_{in} (ms^{-1})	0.12 ± 0.016	0.09 to 0.15
2nd A-time (ms)	22.54 ± 0.30	22.05 to 23.13
2nd A-length (mm)	1.80 ± 0.35	1.17 to 2.63
V_{out} (ms^{-1})	-0.35 ± -0.05	-0.44 to -0.25
HC-time (ms)	17.55 ± 0.36	17.02 to 18.33
DA (mm)	1.08 ± 0.10	0.92 to 1.36
$SimK_1$ (D)	42.59 ± 1.48	38.83 to 45.63
$SimK_2$ (D)	43.76 ± 1.65	39.70 to 47.00

IOP = intraocular pressure; CCT = central corneal thickness; 1st A-time = time from start until the first applanation; 1st A-length = cord length of the cornea in the first applanation; V_{in} = corneal velocity during the first applanation moment; 2nd A-time = time from start until the second applanation; 2nd A-length = cord length of the cornea in the second applanation; V_{out} = corneal velocity during the second applanation moment; HC-time = time from start until the highest concavity of cornea is reached; DA = maximum deformation amplitude at the corneal apex; $SimK_1$ = simulated flattest corneal curvature; $SimK_2$ = simulated steepest corneal curvature; SD = standard deviation

Table 2.3 Intra-examiner repeatability† of Corvis ST parameters.

Parameter	Precision	Repeatability	CV (%)	ICC (95 % CI)
IOP (mmHg)	1.39	1.97	4.98	0.75 (0.61 to 0.85)
CCT (μm)	10.85	15.34	1.01	0.96 (0.93 to 0.98)
1st A-time (ms)	0.22	0.31	1.42	0.77 (0.64 to 0.86)
1st A-length (mm)	0.56	0.79	16.28	-0.05 (-0.20 to 0.17)
V_{in} (ms^{-1})	0.05	0.08	22.81	0.02 (-0.15 to 0.23)
2nd A-time (ms)	0.44	0.62	0.99	0.59 (0.41 to 0.74)
2nd A-length (mm)	0.99	1.40	27.91	0.12 (-0.07 to 0.34)
V_{out} (ms^{-1})	0.10	0.14	14.88	0.40 (0.20 to 0.60)
HC-time (ms)	1.28	1.8	3.71	-0.04 (-0.20 to 0.17)
DA (mm)	0.08	0.13	4.33	0.80 (0.68 to 0.88)

†Precision (1.96 S_w), repeatability (2.77 S_w), within-subject coefficient of variation (CV) and intraclass correlation coefficient (ICC).

IOP = intraocular pressure; CCT = central corneal thickness; 1st A-time = time from start until the first applanation; 1st A-length = cord length of the cornea in the first applanation; V_{in} = corneal velocity during the first applanation moment; 2nd A-time = time from start until the second applanation; 2nd A-length = cord length of the cornea in the second applanation; V_{out} = corneal velocity during the second applanation moment; HC-time = time from start until the highest concavity of cornea is reached; DA = maximum deformation amplitude at the corneal apex.

Table 2.4 Intersession differences and significances of Corvis ST parameters.

Parameter	Mean difference ± SD	P-value
IOP (mmHg)	0.25 ± 1.02	0.26[a]
CCT (μm)	2.6 ± 7.5	< 0.05[b]
1st A-time (ms)	0.027 ± 0.15	0.34[a]
1st A-length (mm)	-0.065 ± 0.18	< 0.05[b]
V_{in} (ms^{-1})	-0.0031 ± 0.027	0.35[a]
2nd A-time (ms)	-0.082 ± 0.29	0.14[a]
2nd A-length (mm)	-0.074 ± 0.39	0.25[b]
V_{out} (ms^{-1})	0.016 ± 0.051	0.08[a]
HC-time (ms)	-0.11 ± 0.45	0.13[b]
DA (mm)	-0.0022 ± 0.065	0.84[b]
$SimK_1$ (D)	-0.080 ± 0.33	0.15[b]
$SimK_2$ (D)	-0.028 ± 0.13	0.19[b]

[a]Wilcoxon signed-rank tests were performed.

[b]Paired samples t-tests were performed.

IOP = intraocular pressure; CCT = central corneal thickness; 1st A-time = time from start until the first applanation; 1st A-length = cord length of the cornea in the first applanation; V_{in} = corneal velocity during the first applanation moment; 2nd A-time = time from start until the second applanation; 2nd A-length = cord length of the cornea in the second applanation; V_{out} = corneal velocity during the second applanation moment; HC-time = time from start until the highest concavity of cornea is reached; DA = maximum deformation amplitude at the corneal apex; $SimK_1$ = simulated flattest corneal curvature; $SimK_2$ = simulated steepest corneal curvature; SD = standard deviation

As the two corneal deformation parameters, DA and 1st A-time, showed good intra-examiner repeatability and no intersession differences, Bland-Altman analyses were conducted accordingly. No significant relationships were found between the mean differences and their means for both parameters ($-0.149 < r < -0.076$, $0.38 < p < 0.66$). The mean differences in DA and 1st A-time were 0.00 mm and -0.03 ms respectively. The 95 % limits of agreement were +0.13 mm to -0.13 mm for DA and +0.27 ms to -0.33 ms for 1st A-time. Figure 2.3 presents plots of intersession differences of DA and 1st A-time against their means.

The DA was moderately and negatively associated with CCT ($r = -0.53$, $p < 0.001$) (Figure 2.4) while no association with simulated keratometry readings were found ($SimK_1$, $r = 0.13$, $p = 0.46$; $SimK_2$, $r = 0.05$, $p = 0.75$).

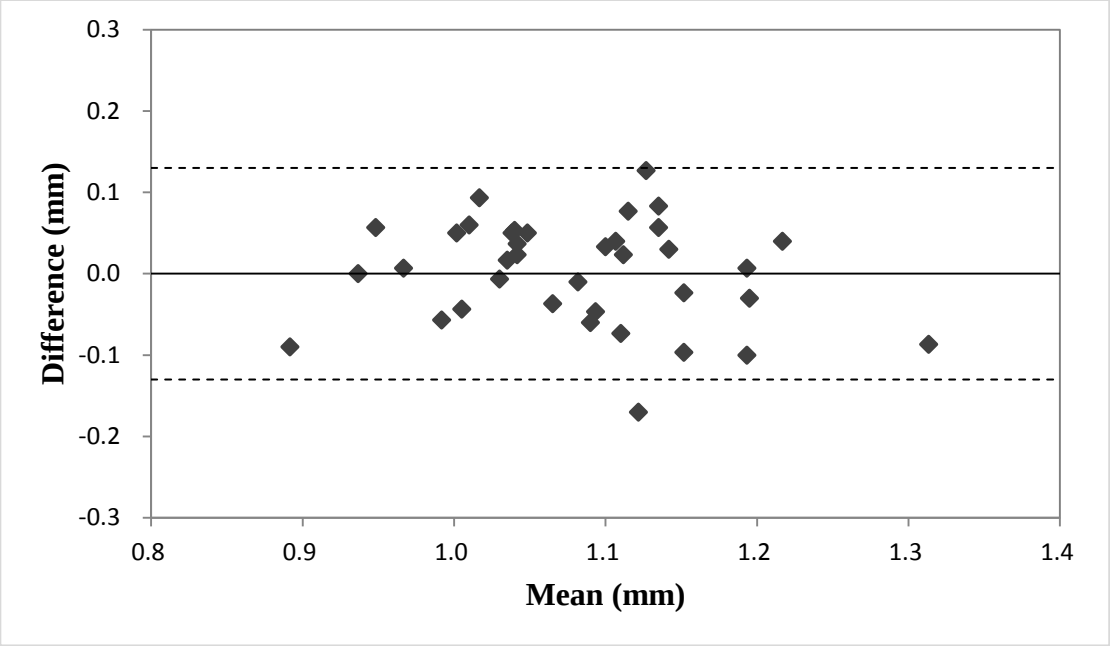

(a)

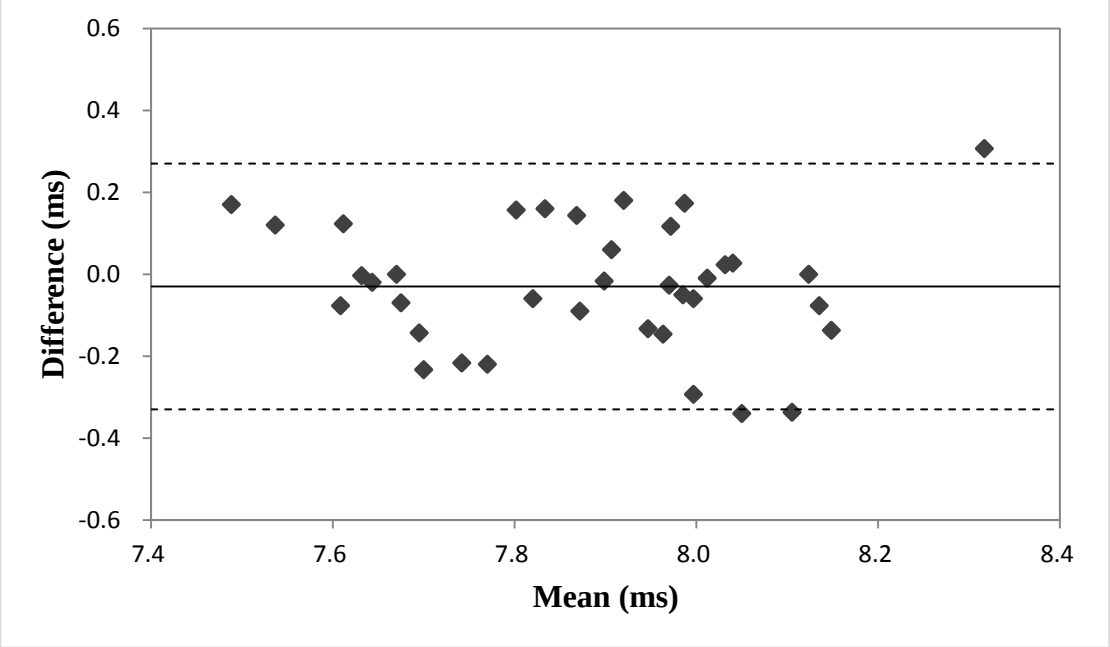

(b)

Figure 2.3 Bland-Altman plots illustrating the intersession reproducibility of **(a)** DA and **(b)** 1st A-time. The upper and lower dotted lines represent the upper and lower limits of agreement (mean difference ± 1.96 x standard deviation of the differences), respectively. The solid line in the middle represents the mean of the differences.

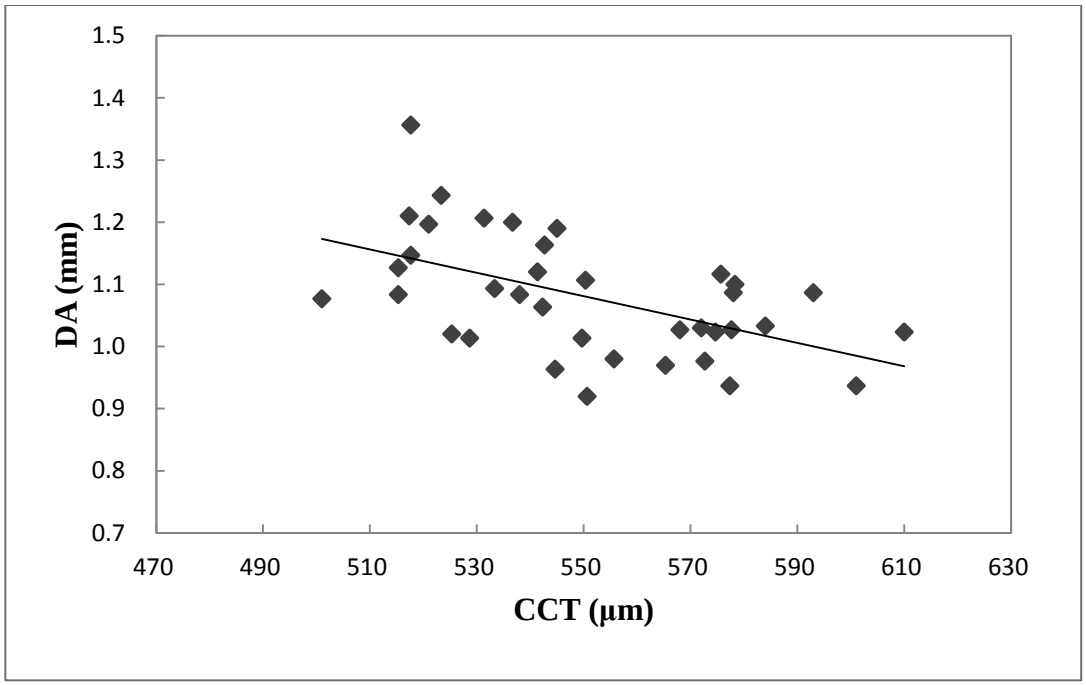

Figure 2.4 Negative correlation between central corneal thickness (CCT) and deformation amplitude (DA) was observed (r = -0.53, $p < 0.001$).

2.5 Discussion

Corvis ST is the first automated NCT incorporating Scheimpflug imaging technique for dynamic corneal deformation measurement. This is the first study investigating the intraexaminer repeatability and intersession reproducibility of Corvis ST after its launch. Among all the Corvis-generated parameters, only CCT, IOP, DA and 1st A-time demonstrated good repeatability. Being one of the commercially available NCTs, the repeatability coefficient (precision) of IOP measured in Corvis ST was 1.4 mmHg. The precision values obtained from other models were slightly higher, which ranged from 2.5 to 3.2 mmHg (Cho & Lui, 1997, Tonnu et al., 2005, AlMubrad & Ogbuehi, 2008). Previous studies reported that precision of CCT varied from 13.4 to 60.5 μm using standard ultrasound pachymeter (Marsich & Bullimore, 2000, Schiano Lomoriello et al., 2011, Reinstein et al., 2012, Maresca et al., 2014). Comparable variability was found using Corvis ST (15.3 μm). Among the corneal deformation parameters, only DA and 1st A-time achieved good repeatability. Large variations were shown in both lengths and corneal velocities in the two applanations. Though 2nd A-time and HC-time had low coefficients of variation, the ICC values were moderate to poor.

During the study period, the early software version in Corvis ST did not include data regarding peak distance and radius of curvature at highest concavity (definitions described by Nemeth et al.(2013)). Subsequent studies evaluated the repeatability of all corneal deformation parameters when a new software version was provided. Results were commonly presented using repeatability (2.77 S_w) and ICC. Regarding the ICC values, good intraexaminer repeatability was consistently shown in IOP, CCT, DA and 1st A-time (Nemeth et al., 2013, Ali et al., 2014, Bak-Nielsen et al., 2015, Ye et al., 2015). In addition, only some studies also found 2nd A-time and V_{out} to be repeatable (Chen et al., 2014, Asaoka et al., 2015, Salvetat et al., 2015). Table 2.5 lists the aforementioned Corvis parameters for comparison. The poor repeatability of the Corvis-generated deformation parameters could be attributed to the poor image quality of corneal capture under fast motion, i.e. within 32 ms, which made surface tracing difficult.

Table 2.5 Comparison of intraexaminer repeatability of selected Corvis ST parameters from different studies.

Study	Repeatability (2.77 S_w)						Intraclass correlation coefficient (ICC)					
	IOP (mmHg)	CCT (μm)	DA (mm)	1st A-time (ms)	2nd A-time (ms)	V_{out} (ms^{-1})	IOP (mmHg)	CCT (μm)	DA (mm)	1st A-time (ms)	2nd A-time (ms)	V_{out} (ms^{-1})
Hon & Lam (2013) (current study)	1.97	15.34	0.13	0.31	0.62	0.14	0.75	0.96	0.80	0.77	0.59	0.40
Nemeth et al. (2013)	n/a	n/a	n/a	n/a	n/a	n/a	0.87	0.97	0.76	0.78	0.31	0.55
Chen et al. (2014)	1.62	12.56	0.11	0.24	0.48	0.10	0.93	0.99	0.88	0.94	0.92	0.65
Ali et al. (2014)	2.30	27.00	0.11	0.28	0.77	0.11	0.73	0.86	0.63	0.73	0.53	0.33
Salvetat et al. (2015)	n/a	n/a	n/a	n/a	n/a	n/a	0.96	0.99	0.96	0.96	0.94	0.80
Bak-Nielsen et al. (2015)	1.20	14.00	0.10	0.20	0.50	0.10	n/a	n/a	n/a	n/a	n/a	n/a
Ye et al. (2015)	3.08	12.84	0.15	n/a	n/a	0.10	0.78	0.99	0.70	n/a	n/a	0.73
Asaoka et al. (2015)	n/a	n/a	n/a	n/a	n/a	n/a	0.97	0.99	0.95	0.95	0.75	0.75

IOP = intraocular pressure; CCT = central corneal thickness; DA = maximum deformation amplitude at the corneal apex; 1st A-time = time from start until the first applanation; 2nd A-time = time from start until the second applanation; V_{out} = corneal velocity during the second applanation moment; n/a = not available

Our study found that Corvis ST parameters remained stable between morning and afternoon sessions except for CCT and 1st A-length. Decreased central thickness and increased 1st applanation length was revealed in the afternoon (Table 2.4). Diurnal variation studies reported that corneal thickness (both central and peripheral) increases immediately after awakening due to overnight corneal swelling of around 2.9 to 5.5 %. These gradually reduced and remained relatively stable after noon (Harper et al., 1996, Read & Collins, 2009). Hence reduction in CCT is expected. Due to the poor intraexaminer repeatability in applanation lengths, no conclusion can be drawn upon significant findings between sessions. Evaluation of intersession reproducibility was conducted using Bland-Altman plots. We concluded that changes within 0.13 mm in DA and 0.33 ms in 1st A-time during Corvis ST measurements are acceptable in healthy individuals.

Correlation analyses found that deformation amplitude was inversely related to corneal thickness, which was echoed by subsequent studies (Leung et al., 2013, Chen et al., 2014). The influence of corneal curvature was found to be insignificant in the current study, as well as in that of Lanza et al. (2014). However, Nemeth et al. (2013) found positive correlation between keratometry values and 10 Corvis-generated parameters. Mechanically a thinner or flatter cornea could be deformed to a greater extent when the same air puff pressure is applied. However, corneal deformation is not solely dependent on corneal geometry but can also be affected by intraocular pressure and corneal biomechanics (Kling & Marcos, 2013). Thus, further investigation is necessary to confirm the various factors influencing the corneal deformation response.

Diurnal variation of ocular parameters in human eyes is common (Hamilton et al., 2007, Chakraborty et al., 2011). The current study is limited to measurements at different time points within the same day. Yet, diurnal variation of Corvis-generated deformation parameters has not been evaluated. Hereby we highlight the importance of assessing intersession reproducibility on different days within the same period of time.

Considering the current sample size of 37 with 3 Corvis ST measurements per eye, the 95 % confidence interval at either side of the estimate of S_w (1.96 / √ [2 x sample size x (number of observation – 1]) is 16.1 %. Thus, adequate accuracy was achieved in the repeatability assessment when the confidence interval is set as below 20 % (Bland, 2010).

The Corvis ST allows visualization and quantification of the corneal deformation response. However, its corneal deformation parameters are raw and do not give direct representation of material properties such as elastic modulus. Although corneal displacement (related to the strain) can be measured by Corvis ST, the stress exerted onto the cornea cannot be precisely measured from air puff indentation. Similar to the ORA, the Corvis ST is also limited to central corneal measurement. Of the 10 corneal biomechanical parameters described in the current study, more than half showed unsatisfactory repeatability, which reduces the usefulness of Corvis ST in characterization of corneal biomechanical properties.

2.6 Conclusion

The current study demonstrated adequate intraexaminer repeatability and intersession reproducibility for Corvis-generated CCT, IOP, DA and 1st A-time in normal subjects. Other *in vivo* devices to measure corneal biomechanics using conventional mechanical terms to be employed at other corneal locations are needed.

Paper published:

Hon, Y. & Lam, A. K. 2013. Corneal deformation measurement using Scheimpflug noncontact tonometry. *Optom Vis Sci*, 90, e1-8.

Chapter 3

Evaluation of a novel corneal indentation device for a clinical corneal biomechanical measurement

3.1 Introduction

Corneal biomechanics, which describes the mechanical behavior of the corneal tissue, is conventionally measured *in vitro*. As discussed in Section 1.2, the most common quantitative expression of corneal biomechanics involves stress, strain, tangent (elastic) modulus and Poisson's ratio (Table 3.1) (Buzard, 1992, Fung, 1993). Standard techniques such as strip extensiometry and pressure inflation have been developed to measure these parameters in mechanical engineering (Woo et al., 1972, Hoeltzel et al., 1992, Zeng et al., 2001). Both methods are destructive because the whole eye is dissected while the corneal tissue has to be prepared as a corneal button or strip. Under controlled stress levels, strain can be measured from a change of shape or length of tissue. A typical stress-strain curve of human corneal tissue (Figure 3.1) revealed increasing slope (increasing elastic modulus) with increasing stress, which indicates that the cornea exhibits non-linear elastic behavior (Elsheikh & Anderson, 2005). Under strip extensiometry, the corneal tissue was found more distensible in keratoconus patients (Andreassen et al., 1980, Nash et al., 1982). Normal corneal tissue was also stiffened after collagen cross-linking, indicated by a 4.5 times increase in elastic modulus (Wollensak et al., 2003).

Table 3.1 Common quantitative descriptive parameters of mechanical properties of material.

Parameters	Description
Stress	Force per unit area, in Nm^{-2}
Strain	Ratio of change in length to original length
Tangent (elastic) modulus	Ratio of stress to strain, in Pa or Nm^{-2}
Poisson's ratio	Absolute value of transverse strain divided by axial strain

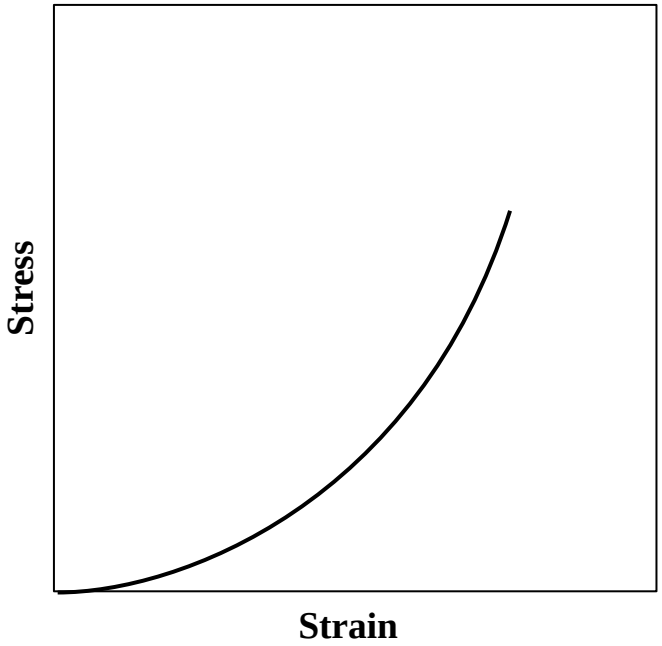

Figure 3.1 Typical stress-strain relationship of human corneal tissue from strip extensiometry (Reproduced from (Elsheikh & Anderson, 2005)).

Currently available commercial devices, the ORA and the Corvis ST, cannot measure corneal biomechanics in terms of standard engineering terminology (McMonnies, 2012, Hon & Lam, 2013) and so, direct description of corneal stiffness measured using these devices is difficult. In addition, confounding factors such as corneal thickness and

curvature, as well as internal pressure of the eye, aggravate the difficulties in characterization of corneal biomechanics.

A novel corneal indentation device (CID) has been developed, which aims to overcome these obstacles in clinical corneal biomechanical measurement (Ko, 2013). The CID measures the force required to displace the cornea to 1 mm depth by a small probe. Corneal tangent (elastic) modulus (Figure 3.2), an instantaneous slope on a stress-strain curve, can be calculated by knowing the force-displacement relationship, thickness, and curvature of the cornea. The corneal indentation method was first validated using a silicone bar and a silicone corneal model that originated from the same material. Tangent modulus obtained from corneal indentation agreed with that obtained from standard three-point bend test on the silicone bar. As the cornea is viscoelastic in nature, the rate of corneal indentation changes the measured value for tangent modulus. Experiments were then performed on *ex vivo* porcine eyes and *in vivo* rabbit eyes in order to establish an ideal indentation rate for measuring rate-independent tangent modulus (Ko et al., 2013). Repeatability of the device and its agreement with UTM were further ratified using porcine eyes (Ko et al., 2014).

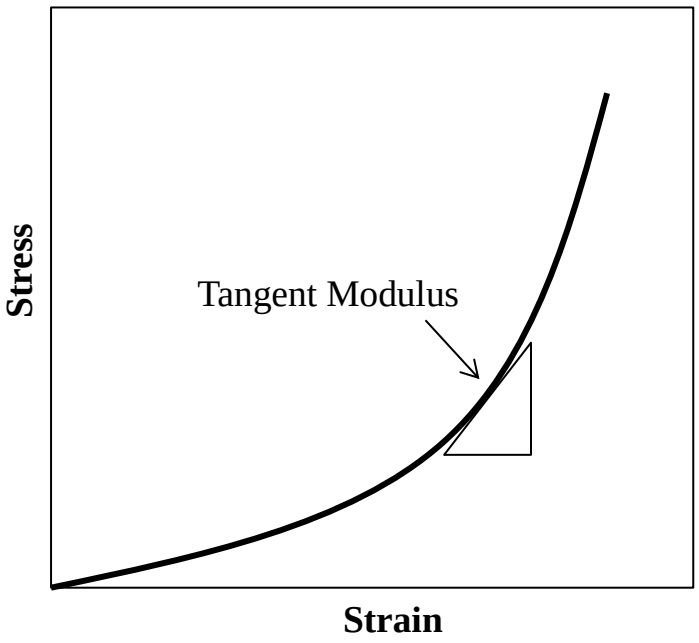

Figure 3.2 Tangent modulus is defined as an instantaneous slope on a non-linear stress-strain curve.

Before the CID can be fully utilized for clinical trials, it was necessary to examine the repeatability and diurnal variation of the CID-derived corneal biomechanical parameters in human subjects.

3.2 Mathematical deviations of corneal tangent modulus

Goldmann applanation tonometry (GAT) is still considered the gold standard for measuring intraocular pressure (IOP) despite the influence on measurements of corneal factors (Liu & Roberts, 2005). The basic principle of GAT comes from the Imbert-Fick law (Ethier & Simmons, 2007) such that

$$\text{IOP} = \frac{F}{A} \ , \tag{3.1}$$

where F is the force applied to the applanation head and A is the flattened area of the cornea. The law is valid when the cornea is infinitely thin, perfectly elastic, spherical and dry at the contact surface. However, none of the assumptions is true for human corneal tissue. When an indentation probe is in contact with the cornea, the actual balance of force is therefore

$$F + s = A \cdot \text{IOP} + b \ , \tag{3.2}$$

where s is the surface tension of the tear film and b is the resistance of the cornea to deformation (Figure 3.3). Disregarding surface tension and IOP, the resistance force b during indentation of a partial spherical shell by a concentrated force can be calculated as

$$b = \frac{E \cdot t^2}{a(R - t/2)\sqrt{1-\nu^2}} \delta \ . \tag{3.3}$$

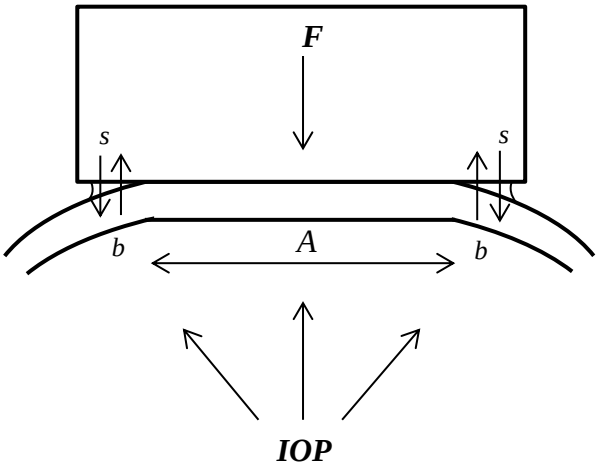

Figure 3.3 A force diagram representing corneal indentation, in which *F* is the applied force, *A* is the contact area of the cornea, *IOP* is the intraocular pressure, *s* is the surface tension of tear film and *b* is the resistance of the cornea to deformation.

The resistance force is dependent on corneal mechanical property (*E*), corneal geometry constant (*a*), corneal thickness (*t*), corneal radius (*R*), Poisson's ratio of the cornea (ν), and indentation depth (δ). The value of *a* is determined from μ (Young & Budynas, 2002),

$$\mu = r_o \left[\frac{12(1-\nu^2)}{(r-t/2)^2 t^2}\right]^{1/4}. \tag{3.4}$$

The radius of a circular flat-surface probe that is in full contact with the cornea is denoted as r_0. The relationship between μ and *a* was derived by Reissner (1946) and reported by Young (2002) (Table 3.2). Ko et al. (2013) deduced corneal stiffness by differentiating equation 3.2 with respect to indentation depth δ and giving:

$$\frac{dF}{d\delta} + \frac{ds}{d\delta} = \frac{d}{d\delta}(A \cdot IOP) + \frac{db}{d\delta}\ . \tag{3.5}$$

Table 3.2 The geometry constant *a* in equation 3.3 is determined from μ calculated using equation 3.4 (Young & Budynas, 2002).

$\boldsymbol{\mu}$	0	0.1	0.2	0.4	0.6	0.8	1.0	1.2	1.4
$\boldsymbol{a}$	0.433	0.431	0.425	0.408	0.386	0.362	0.337	0.311	0.286

When changes in the surface tension *s* are negligible at constant IOP and constant contact area *A*, equation 3.3 can be rearranged and substituted into 3.5 giving corneal stiffness as

$$\frac{dF}{d\delta} = \frac{E \cdot t^2}{a(R - t/2)\sqrt{1-\nu^2}} \quad . \tag{3.6}$$

As corneal tangent modulus is IOP dependent (Elsheikh et al., 2007b, Ko et al., 2013), corneal tangent modulus at specific IOP can be calculated after rearranging equation 3.6 into

$$E = \frac{a(R - t/2)\sqrt{1-\nu^2}}{t^2}\frac{dF}{d\delta} \quad . \tag{3.7}$$

Therefore corneal tangent modulus *E* at specific IOP can be determined by substituting individual corneal thickness and curvature measured using available clinical devices, together with corneal stiffness obtained from CID.

3.3 Preparation and measurement

The CID is designed to work with a slit-lamp biomicroscope. It consists of a main unit, a detachable indentation probe and a foot-switch (Figure 3.4). Prior to measurement, a 2-mm round probe with a flat surface was mounted onto the CID. It was disinfected with 70 % isopropyl alcohol, allowed to air-dry for 1 minute, and rinsed with normal saline. To prepare the subject, topical anaesthetic (one drop of 0.4 % Benoxinate) was applied to the cornea. The subject was instructed to put his/her head and chin firmly against the head and chin rests of the slit-lamp and look at an external fixation target. The reset button on the CID was pressed so that the load cell (force detector) was set at zero, followed by an alignment of the probe to the corneal geometric center using a joystick from the slit-lamp.

When the probe touched the corneal surface at a minimum force of 0.001 – 0.003 N, a low-pitched signal was released indicating the readiness for data acquisition. By pressing the foot-switch, the probe was actuated forward at 12 mms^{-1} to indent the cornea to 1 mm depth. After reaching the set depth, the probe was withdrawn from the cornea at the same rate as the forward actuation. The entire indentation process was completed in approximately 0.2 s. The load cell in the CID recorded the force required for a 1 mm corneal indentation. A force-displacement curve was displayed on the screen immediately after each measurement. A valid measurement featured a smooth and linear slope within a full contact regime (Figure 3.5), in which the slope was defined as corneal stiffness and was readily read on the screen display. The quality of raw data was objectively evaluated immediately after each acquisition with presentation of a quality score (Q) on the screen display. Only "Q = 1" indicated valid measurement such that the coefficient of determinant of the slope regime was 0.95 or more.

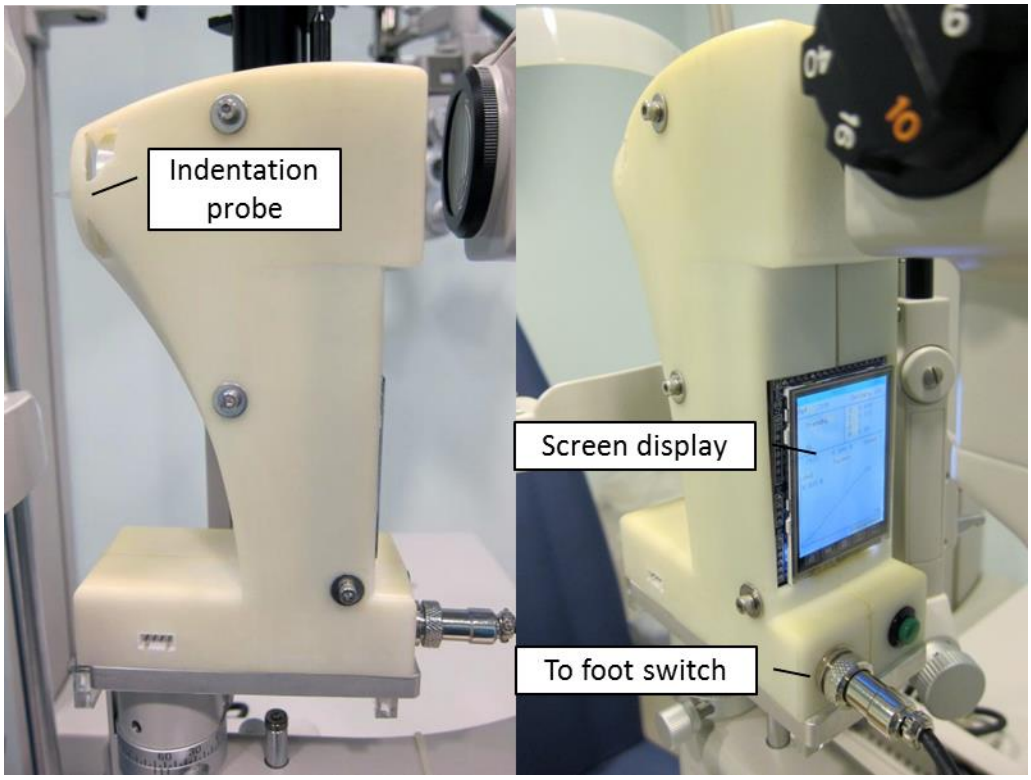

(a) (b)

Figure 3.4 (a) Side view and **(b)** front view of a corneal indentation device (CID) mounted on a slit-lamp unit.

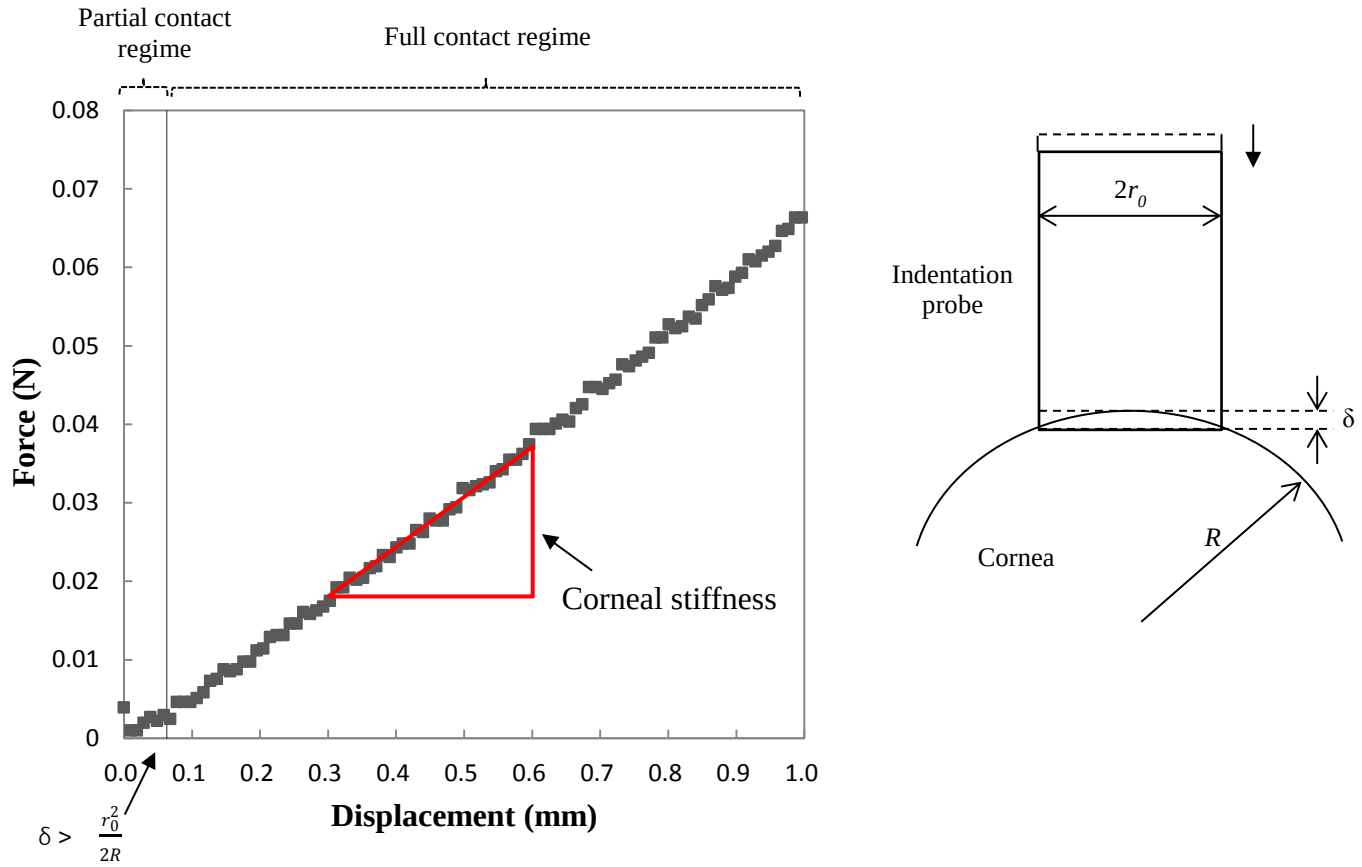

Figure 3.5 An actual force-displacement curve from the corneal indentation device. In this example, corneal stiffness is the average rate of change of force under a corneal displacement between 0.3 - 0.6 mm. The indentation probe is in full contact with the cornea when $\delta > r_0^2 / 2R$, where δ is the indentation depth, r_0 is the radius of curvature of indentation probe and R is the radius of curvature of the cornea.

3.4a Repeatability and reproducibility

3.4a.1 Subjects

Twenty-nine healthy young adults (18 male and 11 female) with a mean ± standard deviation (SD) age of 23.4 ± 1.7 years (range from 20 to 28 years) were enrolled in this study. All subjects had unremarkable general and ocular health. Exclusion criteria included GAT IOP ≥ 21 mmHg, rigid lens wear, currently pregnant, history of refractive surgery or eye diseases, and use of long-term eye or oral medications. Soft lens wearers were required to cease contact lens wear for at least 24 hours before data collection. All procedures followed the Declaration of Helsinki and the protocol was reviewed and approved by the ethics review board of The Hong Kong Polytechnic University. Informed consent was obtained from each subject before commencement of the study.

3.4a.2 Procedures

All subjects were required to visit the campus Optometry Clinic. Noncontact procedures such as measurements of corneal thickness, corneal radius of curvature and axial length (AL) were first performed with anterior segment optical coherence tomography (AS-OCT; Casia SS-1000, Tomey, Japan), corneal topography (Medmont E300, Medmont Pty Ltd., Australia), and optical biometry (IOLMaster 500, Carl Zeiss Meditec, Inc., USA), respectively, in a random order. Two contact procedures requiring topical anesthesia were then performed with CID and followed by GAT.

For noncontact procedures, subjects were asked to blink normally, open the eyes widely and fixate on the internal target during data acquisition. Three pachymetric images were captured using a ‘Topo-Pachy-Map’ scan mode in the AS-OCT. The corneal thickness at the vertex was denoted as central corneal thickness (CCT). Three topographic images with scores higher than 95 were captured using the topographer. The meanK was calculated from averaging the flattest and steepest simulated keratometry readings in each image. Five readings of AL were automatically generated from the IOLMaster. In contact procedures, three valid readings were obtained from the CID and two IOP readings were collected from the GAT using standard protocols. Because CID and GAT are subjective measurements and their parameters are strongly associated with each other

(Ko et al., 2013), the GAT IOP was performed by a masked examiner. Multiple measurements from each device were averaged for analysis. Data collection was first conducted in the right eye followed by the left eye.

Subjects were required to return to the clinic 7-10 days after the first visit and all measurements were repeated for assessing the reproducibility of ocular parameters, except for AL. To prevent diurnal variation, all measurements were conducted at a similar time at both visits.

3.4a.3 Statistical analysis

Statistical analyses and graphics were performed using IBM SPSS (version 18.0, SPSS, Inc., USA) and Microsoft (Excel 2013, Microsoft Corp., USA) software, respectively. Sample size of the repeatability study was evaluated according to Bland's method (2010). All the data were tested for normality using Shapiro-Wilk tests.

Distinct corneal biomechanical parameters from the CID included corneal stiffness and corneal tangent modulus. To compare intrasession repeatability of these parameters, the within-subject standard deviation (S_w), repeatability (2.77 S_w), and within-subject coefficient of variation (CV) of the three consecutive measurements in the first session were calculated. Intraclass correlation coefficient (ICC) was also assessed to evaluate its intrasession reliability. Clinical measurement with ICC $\geq$ 0.75 is indicated as reliable.

When evaluating intersession reproducibility, the required corneal and ocular parameters in each session were averaged and significant differences between sessions were first evaluated by paired samples t-tests. Bland-Altman analyses (Bland & Altman, 1986) were performed to assess the intersession reproducibility of corneal biomechanical parameters from the CID, under the condition that no significant associations were present between the mean differences and the means by Pearson correlations. Limits of agreement were computed as mean difference ± 1.96 x SD of the difference.

3.4b Diurnal variation

3.4b.1 Subjects

Twenty-five healthy young adults (17 male and 8 female) with a mean age of 23.0 ± 1.0 (SD) years (range 21 to 25 years) were enrolled in this study. All subjects had unremarkable general and ocular health. Exclusion criteria and ethics approval were as described in section 3.4a.1. One eye was randomly selected where both eyes were eligible for the study.

3.4b.2 Procedures

The CCT and meanK were first measured using a Scheimpflug imaging system (Pentacam; Oculus, Germany). Each subject was asked to fixate on an internal target while the measurement was automatically completed within 2 seconds upon perfect alignment by the joystick. A 25-image mode was used and 3 valid images were captured in which the Quality Specification (QS) indicated "OK". After that, one drop of topical anaesthetic was applied to the eye. Three valid readings of corneal stiffness were recorded from CID. Lastly, GAT IOP was measured twice by a masked examiner.

Data collection was repeated at 3-hour intervals from 09:00 to 21:00 during waking time, with a 30-minute tolerance before and after the scheduled time. Specifically, the time allowance was from 8:30 to 9:30, 11:30 to 12:30, 14:30 to 15:30, 17:30 to 18:30 and 20:30 to 21:30.

3.4b.3 Statistical analysis

Data analyses and graphical presentation were conducted using IBM SPSS (version 23.0, SPSS, Inc., USA) and GraphPad Prism (version 5, GraphPad Software, Inc., USA), respectively. The statistical power was computed using G-power (version 3.1.7, Franz Faul, Universität Kiel, Germany).

In each time frame, the means of all required parameters were calculated. Corneal tangent modulus was then derived from individual means of CCT, meanK, and corneal stiffness. The distributions of CCT, meanK, IOP, corneal stiffness, and corneal tangent

modulus did not differ significantly from a normal distribution (Shapiro-Wilk tests, $p > 0.05$). Hence, repeated-measures analyses of variance (RMANOVAs) were performed to compare variations over time. In presence of significant differences, paired *t*-tests with Bonferroni adjustment were used for post-hoc comparisons.

3.5a Results (Repeatability and reproducibility)

Repeatability of CID measurement was performed in both eyes of subjects. Since there was no significant between-eye difference in CCT, meanK, AL, GAT IOP, and corneal stiffness in the first session, data from the right eye was selected for analysis (Table 3.3). The mean spherical equivalent refractive error in the right eyes was -3.38 ± 2.63 D. Corneal stiffness (S_w, 0.0058 Nmm^{-1}; repeatability, 0.016 Nmm^{-1}; CV, 7.32 %; ICC, 0.75), and corneal tangent modulus (S_w, 0.046 MPa; repeatability, 0.13 MPa; CV, 7.34 %; ICC, 0.84) demonstrated good intrasession repeatability. Mean corneal tangent modulus calculated in the first session was 0.63 ± 0.11 MPa (range 0.40 – 0.79 MPa).

Table 3.3 Between-eye comparison of ocular parameters for 29 subjects from the first visit. The results are presented as mean ± standard deviation.

Parameters	Right eye	Left eye	Paired t-test
Mean corneal radius (mm)	7.85 ± 0.30	7.85 ± 0.30	$t = 0.30$, $p = 0.77$
Central corneal thickness (μm)	546.4 ± 32.3	547.4 ± 32.1	$t = -1.71$, $p = 0.10$
Axial length (mm)	25.28 ± 1.28	25.22 ± 1.31	$t = 0.80$, $p = 0.43$
Intraocular pressure (mmHg)	13.17 ± 2.37	13.40 ± 2.45	$t = -1.07$, $p = 0.30$
Corneal stiffness† (Nmm^{-1})	0.079 ± 0.011	0.085 ± 0.009	$t = 1.66$, $p = 0.11$

†Corneal stiffness was defined as the average rate of change of force under a corneal displacement of 0.4 – 0.9 mm.

There was no significant intersession difference across most of the corneal and ocular parameters (Table 3.4). Statistically significant difference was present in CCT, although the mean difference was only 1.32 μm. No significant associations were found between the differences and the means for corneal stiffness ($r = 0.09$, $p = 0.64$) and tangent

modulus (r = 0.04, p = 0.85) between the two sessions. Figure 3.6 presents the corresponding Bland and Altman plots for corneal stiffness (mean difference: 0.0010 ± 0.011 Nmm^{-1}; limits of agreement: -0.021 Nmm^{-1} to 0.023 Nmm^{-1}) and corneal tangent modulus (mean difference: 0.0051 ± 0.090 MPa; limits of agreement: -0.17 to 0.18 MPa).

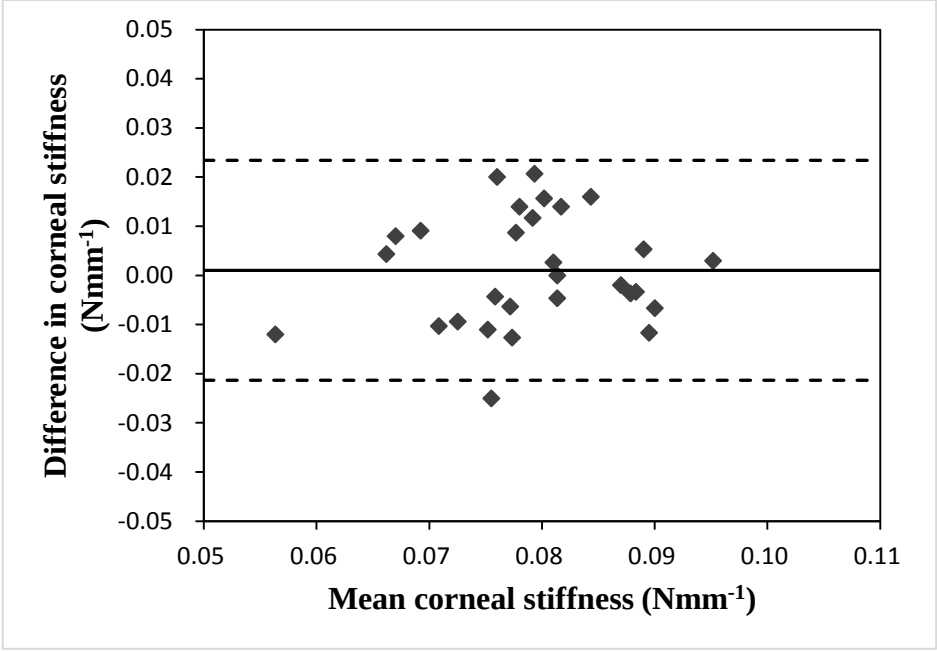

(a)

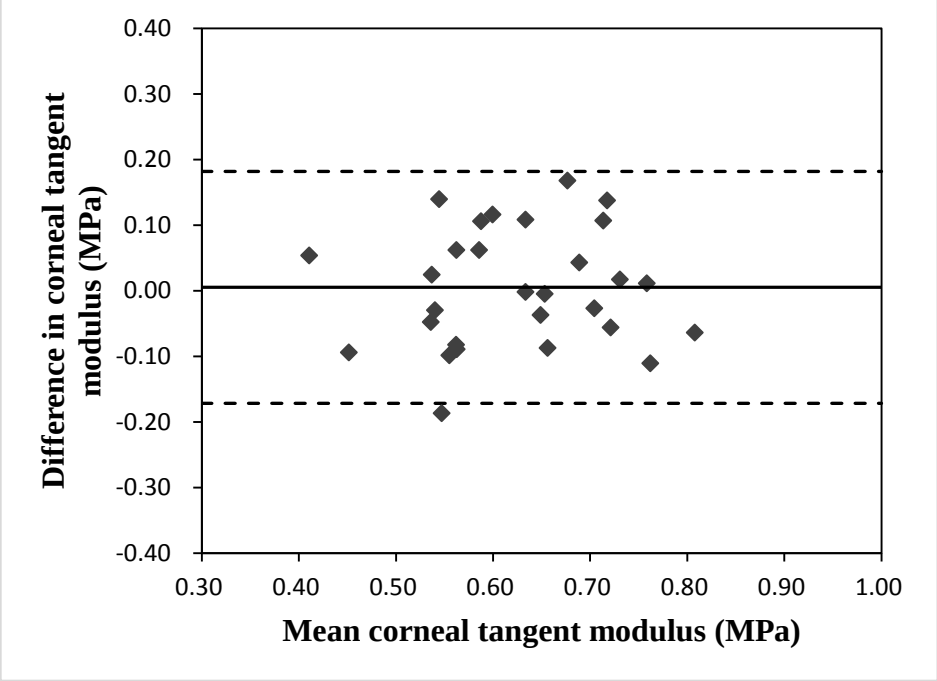

(b)

Figure 3.6 Bland-Altman plots illustrating the intersession reproducibility of **(a)** corneal stiffness and **(b)** corneal tangent modulus. The upper and lower dotted lines represent the upper and lower limits of agreement (mean difference ± 1.96 x standard deviation of the differences), respectively. The solid line in the middle represents the mean of the differences.

Table 3.4 Intersession difference of ocular parameters in the right eyes of 29 subjects. The results are presented as mean ± standard deviation.

Parameters	first session	second session	Paired t-test
Mean corneal radius (mm)	7.85 ± 0.30	7.85 ± 0.30	t = -0.67, p = 0.51
Central corneal thickness (μm)	546.4 ± 32.3	545.0 ± 33.4	t = 2.51, $p < 0.05$
Intraocular pressure (mmHg)	13.17 ± 2.37	13.17 ± 2.37	t = 0.06, p = 0.96
Corneal stiffness† (Nmm^{-1})	0.079 ± 0.011	0.078 ± 0.010	t = 0.49, p = 0.63
Corneal tangent modulus (MPa)	0.63 ± 0.11	0.62 ± 0.10	t = 0.30, p = 0.76

†Corneal stiffness was defined as the average rate of change of force under a corneal displacement of 0.4 – 0.9 mm.

Twenty-nine subjects participated in the repeatability study and 3 CID measurements were taken from each eye. The computed 95 % confidence interval at either side of the estimate of S_w (1.96 / √ [2 x sample size x (number of observation – 1]) is 18.2 %. The current sample size was adequate by achieving an confidence interval below 20 % (Bland, 2010).

3.5b Results (Diurnal variation)

In the diurnal variation study, the mean ± SD of refractive sphere and cylinder of the eyes were -2.16 ± 2.18 D and -0.74 ± 0.66 D respectively. Table 3.5 summarizes the mean values of all parameters at each time frame. Significant reduction in CCT was present (F (4, 96) = 15.77, $p < 0.001$). The maximum CCT, which was observed at 09:00, was significantly higher than the CCT at all subsequent visits (paired t-tests with Bonferroni correction, $p < 0.01$) (Figure 3.7). Although IOP showed a significant decreasing trend during the day (F (4, 96) = 2.91, $p < 0.05$), the readings between early morning and at other time frames were not significantly different (paired t-tests with Bonferroni correction, $p > 0.05$) (Figure 3.8). MeanK was stable at all times (F (4, 96) = 1.37, p = 0.25) (Figure 3.8). Two corneal biomechanical parameters, corneal stiffness (F (4, 96) = 0.82, p = 0.52) and corneal tangent modulus (F (4, 96) = 0.80, p = 0.53), did not demonstrate significant diurnal patterns (Figure 3.9) during the day.

The statistical power of repeated measures on corneal tangent modulus was evaluated. Based on the observed sample effect size of 0.18 and correlation among repeated measures of 0.8, 96 % power was achieved with alpha at 0.05 when the sphericity was assumed.

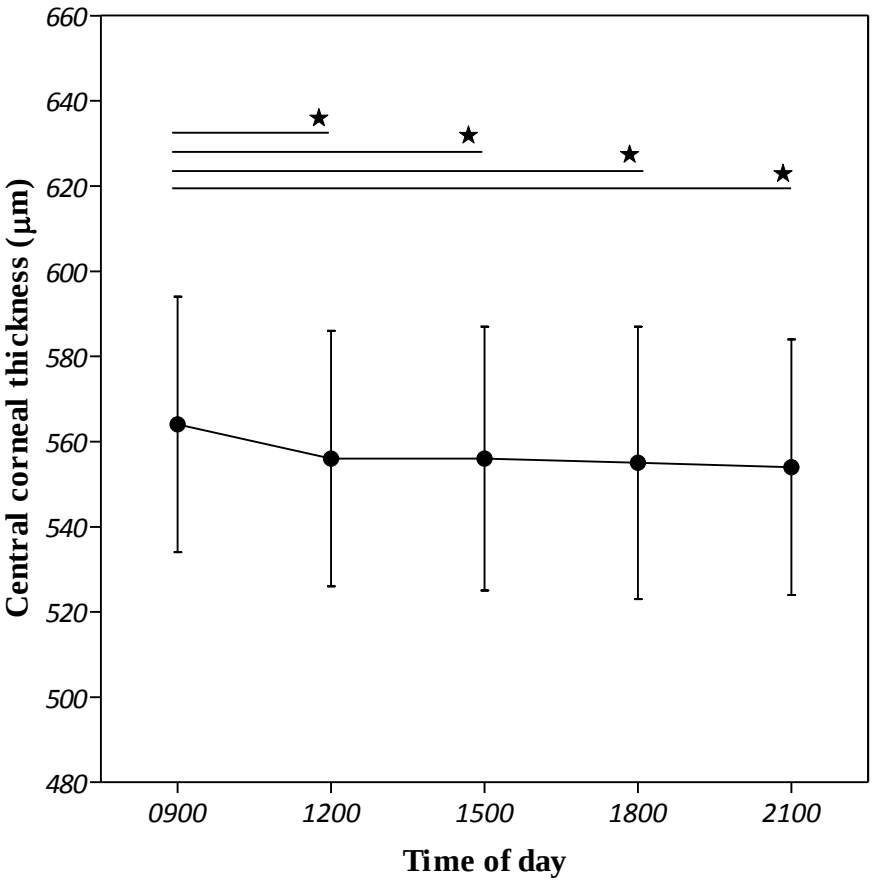

Figure 3.7 Mean and standard deviation (SD) of central corneal thickness over time. ★Indicates significant difference in post-hoc test. Each error bar indicates 1 SD.

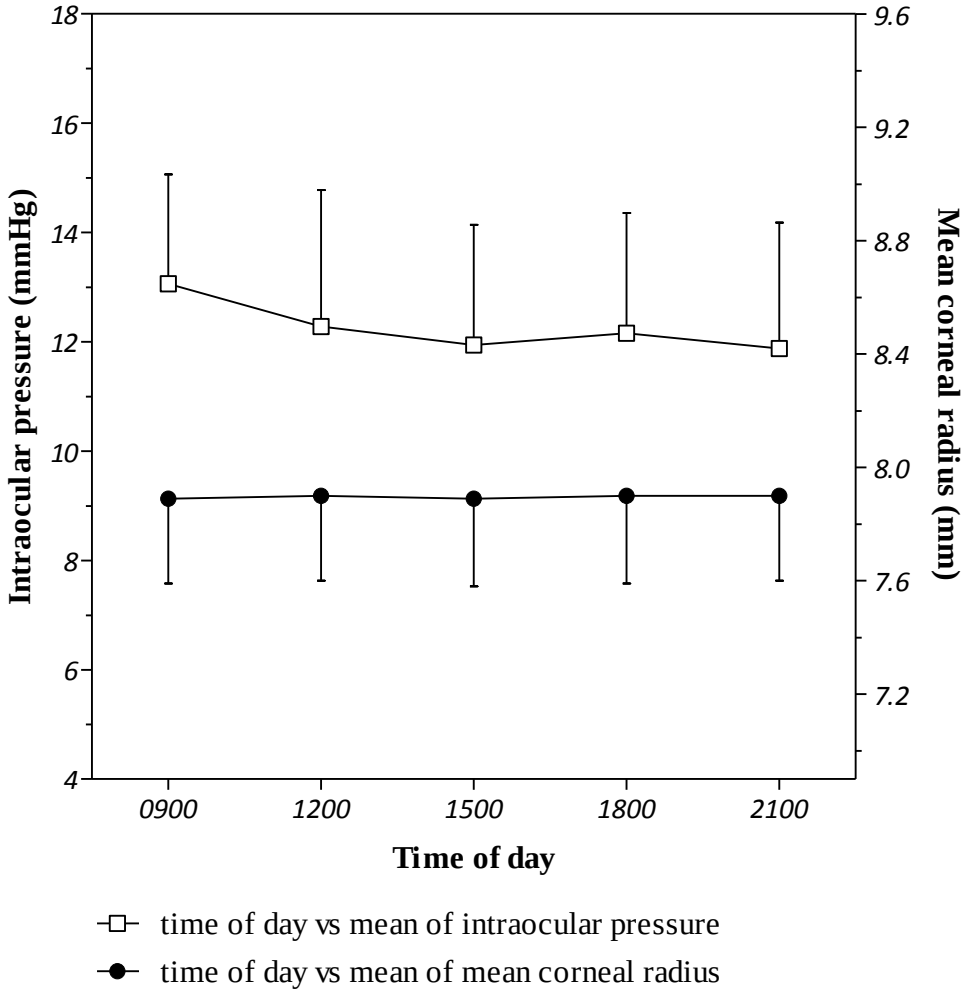

Figure 3.8 Mean and standard deviation (SD) of intraocular pressure and mean corneal radius over time. Each error bar indicates 1 SD.

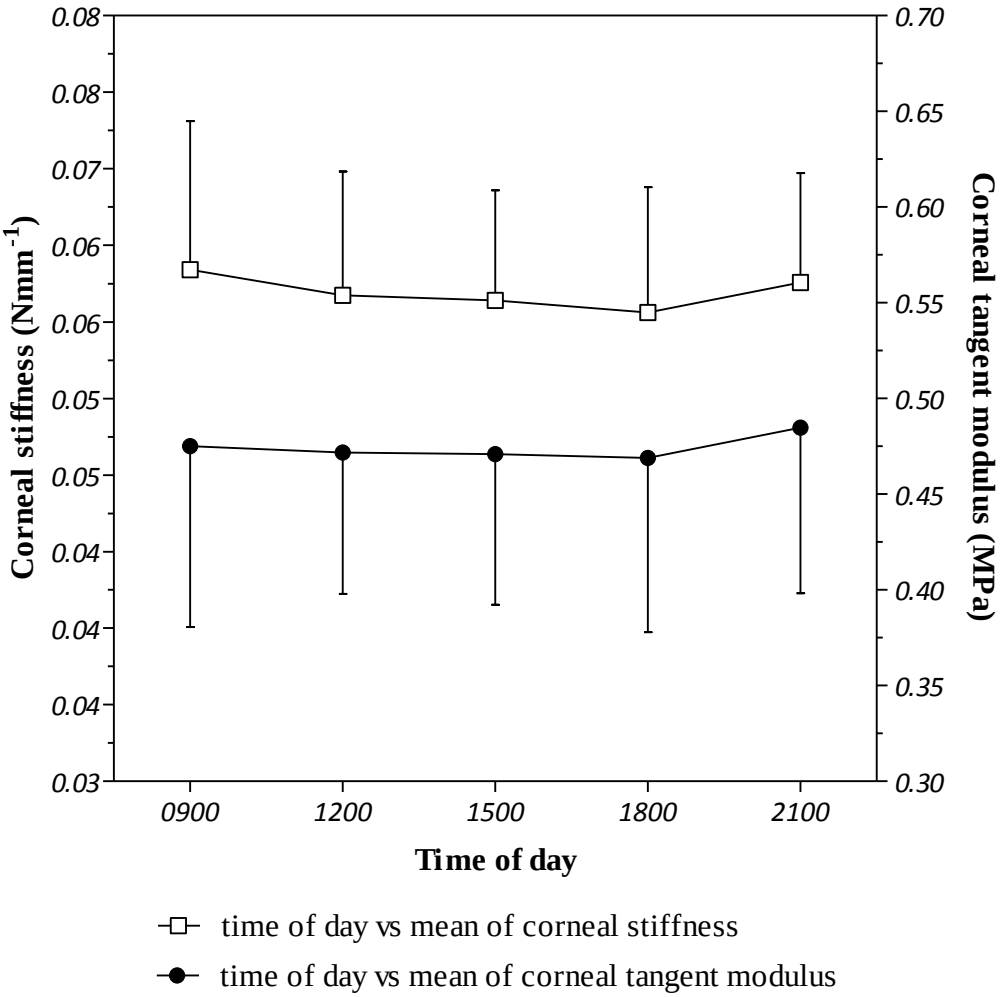

Figure 3.9 Mean and standard deviation (SD) of corneal stiffness and corneal tangent modulus over time. Each error bar indicates 1 SD.

Table 3.5 Mean and standard deviation (SD) of ocular parameters measured throughout the study period.

Time	Central corneal thickness (µm)	Mean corneal radius (mm)	Intraocular pressure (mmHg)	Corneal stiffness[†] (Nmm^{-1})	Corneal tangent modulus (MPa)
9:00	563.6 ± 30.0	7.89 ± 0.30	13.06 ± 1.99	0.063 ± 0.010	0.48 ± 0.094
12:00	556.5 ± 29.6	7.90 ± 0.30	12.28 ± 2.49	0.062 ± 0.008	0.47 ± 0.074
15:00	556.3 ± 30.7	7.89 ± 0.31	11.94 ± 2.20	0.061 ± 0.007	0.47 ± 0.079
18:00	554.7 ± 32.5	7.90 ± 0.31	12.16 ± 2.17	0.061 ± 0.008	0.47 ± 0.091
21:00	554.3 ± 30.1	7.90 ± 0.30	11.88 ± 2.29	0.063 ± 0.007	0.49 ± 0.086
Mean	557.1	7.89	12.26	0.062	0.47
SD	30.3	0.3	2.23	0.008	0.085
P-value[a]	<0.001[b]	0.25	< 0.03[b]	0.52	0.53

[†]Corneal stiffness was defined as the average rate of change of force under a corneal displacement of 0.3 – 0.6 mm.

[a]Significance of the *F* statistic from repeated-measures analysis of variance.

[b]Significant effect within sessions

3.6a Discussion (Repeatability and reproducibility)

Elastic modulus is a standard measure of the elastic property of materials. In laboratory testing, different stress levels can be set and a range of modulus values of corneal tissue can be determined due to its nonlinearity in material behavior (Ahearne et al., 2007, Elsheikh et al., 2008b). Physiologically, laboratory testing is inapplicable in living human corneas as only small stress and strain is affordable. Buzard (1992) introduced tangent modulus, an instantaneous slope at a specific stress or strain level, as a suitable descriptor for the material property of biological tissue. Thus the current study evaluated clinical measurement of corneal tangent modulus in the human cornea using a novel indentation device.

Good intrasession repeatability and intersession reproducibility of the novel CID parameters in human subjects were demonstrated. Ko et al. (2014) examined the repeatability of 5 consecutive CID measurements on *ex vivo* porcine eyes and obtained excellent results on corneal tangent modulus (S_w, 0.006 MPa; repeatability, 0.015 MPa; CV, 4.3 %; ICC, 0.99). Clinically, three repeated measurements per eye were preferable to minimize patient fatigue and corneal staining, if any. It is expected that repeatability tests on *ex vivo* porcine cornea would yield better results than that on *in vivo* human cornea. Fluctuations in corneal biomechanical measurements could be induced from physiological influences such as blinking and involuntary eyeball movement in human subjects.

3.6b Discussion (Diurnal variation)

The diurnal variation study revealed a general reduction of CCT during wake time, in which the extent of changes in a similar measurement period was comparable with previous studies (Shen et al., 2008b, Kotecha et al., 2009, Read & Collins, 2009). A stable meanK was maintained, which was in accord with other studies (Hamilton et al., 2007, Lau & Pye, 2012). Corneal stiffness can be instantly measured by CID and its magnitude can be affected by corneal geometry, such that a thicker cornea results in a higher corneal stiffness reading. However, since the CCT only varied by a mean of 10 μm throughout the study, such negligible changes did not lead to significant variations in corneal stiffness. Diurnal variation in IOP has been extensively reviewed

using various types of tonometers (Liu et al., 2002, Hamilton et al., 2007, Read et al., 2008, Chakraborty et al., 2011, Lau & Pye, 2012). The current study showed a decreasing trend of GAT IOP from mean values of 13.1 mmHg in morning to 11.9 mmHg at night. According to the previous studies on diurnal variation of IOP, the reduction in IOP between 09:00 and 21:00 was also confined to 2 mmHg. No significant diurnal rhythm was observed in corneal tangent modulus during waking time. Corneal tangent modulus is linearly dependent on the internal pressure of the eye (Ko et al., 2013). Since IOP variation was small during waking time, variation in corneal tangent modulus due to IOP changes was also small. This indicated that the elastic property of living human cornea was stable while the subject was awake.

The cornea is a viscoelastic material which consists of both viscous and elastic components. The measured value of elastic modulus changes according to the rate of force applied to the cornea (Elsheikh et al., 2007a). Therefore, measurement of elastic modulus in the human cornea can vary from units of 0.1 to 10 MPa (Woo et al., 1972, Andreassen et al., 1980, Hoeltzel et al., 1992, Hjortdal, 1996, Orssengo & Pye, 1999, Zeng et al., 2001, Wollensak et al., 2003, Elsheikh et al., 2007a). Experimental work was conducted and the measured corneal tangent modulus was found to be independent of indentation rate when its speed was 0.33 mms^{-1} or above (Ko et al., 2013). Above this threshold indentation rate, the time-dependent viscous behavior of the cornea can be negligible and the CID dominantly measures corneal elasticity. The indentation rate of CID in the current clinical trial was 12 mms^{-1}. Such a high speed actuation enhances patient comfort and minimizes influence due to heart beat rate (Ko, 2013).

There are some limitations on the application of the CID. Similar to GAT, CID is operated with the use of topical anaesthetic. Previous studies had demonstrated that tetracaine and oxybuprocaine did not have significant effect on corneal biomechanics in terms of CH and CRF (Ehongo et al., 2009, Ogbuehi, 2012). Measurements of children could be difficult. Experimental work revealed small fluctuations of IOP (less than 3mmHg) during corneal indentation by CID, but the effect on corneal biomechanics was less than 3 % (Leung et al., 2014). Scleral stiffness and backward eye movement can affect corneal deformation response by air puff indentation

(Metzler et al., 2014, Koprowski et al., 2015). The use of a small probe size and concentrated force could minimize the influence to central corneal stiffness measurement using the CID.

Because of the complexity of corneal microstructure, assumptions on corneal tangent modulus derivations are necessary. The cornea is treated as spherical and of uniform thickness. The corneal tissue consists of 5 distinct layers. Due to the lack of understanding of the biomechanical properties in each layer that contribute to the overall corneal biomechanics, the corneal tissue is assumed as homogenous. Therefore, the CID measures bulk corneal biomechanical properties (Ko, 2013).

Evaluation of these distinct corneal biomechanical parameters, corneal stiffness, and corneal tangent modulus, was limited to healthy corneas and was performed during wake time. On the basis of previous diurnal variation studies using the ORA parameters (Kida et al., 2006, Shen et al., 2008b), it was not anticipated there would be any significant changes in corneal tangent modulus over 24 hours. To maintain the corneal integrity before stiffness measurement, noncontact imaging systems were used to measure corneal thickness and curvature. In particular, Pentacam enables acquisition of thickness and curvature simultaneously. Thus, it enhances time control for repeated measures at regular time intervals in diurnal variation studies.

3.7 Conclusion

Corneal biomechanical parameters from the CID were repeatable and reproducible, and stable during wake time in healthy adults. Corneal tangent modulus features the elastic properties of human cornea. This novel indentation device may facilitate clinical investigation in groups with different corneal and ocular statuses.

Papers published:

Lam, A. K., Hon, Y., Leung, L. K. & Lam, D. C. 2015. Repeatability of a novel corneal indentation device for corneal biomechanical measurement. *Ophthalmic Physiol Opt*, 35, 455-61.

Hon, Y., Wan, K., Chen, G. Z., Lu, S. H., Lam, D. C. & Lam, A. K. 2016. Diurnal

Variation of Corneal Tangent Modulus in Normal Chinese. *Cornea*, 35, 1600-1604.

Chapter 4

Comparison of corneal tangent modulus in low and high myopes

4.1 Introduction

Early studies suggested weaker ocular biomechanics in highly myopic eyes. A Schiotz indentation tonometer was used to measure the biomechanical properties of the ocular coats of the human eye (Friedenwald, 1937). Using either 2 plunger weights from the Schiotz tonometer or 1 plunger weight from the Schiotz tonometer and Goldmann applanation tonometry (GAT), two intraocular pressure (IOP) readings were obtained and an ocular rigidity coefficient was derived that could reflect the resistance of the outer tunic (mainly cornea and sclera) to indentation (Stamper, 2011). Myopic eyes could have lower ocular rigidity simply because of a larger ocular volume and vice versa for hyperopic eye (Perkins, 1981). Most of the early studies did report this observation (Castren & Pohjola, 1962, Honmura, 1968, Bonomi et al., 1982), although some more recent studies did not observe this difference (Wong E., 1991, Schmid et al., 2003). Subsequently, other clinical methods, such as direct manometry during ocular surgery and stretching of the ocular shell using weights were used to correlate ocular rigidity with axial length or elongation (Pallikaris et al., 2005, Sergienko & Shargorogska, 2012). However, no consensus was reached. Because of the limitations and measurement errors of Schiotz indentation tonometry (Alguire, 1990, Stamper, 2011), this technique is not recommended among clinicians.

Recently, the relationship between corneal biomechanics and myopia rekindled scientific interest due to the availability of the ORA for *in vivo* corneal biomechanical measurement. Nevertheless, clinical findings are controversial (discussed in Section 1.4.2.7) and interpretation of the empirically-derived ORA parameters is ambiguous (McMonnies, 2012, Sullivan-Mee et al., 2012, Roberts, 2014). Despite the poor repeatability of some corneal deformation parameters from the Corvis ST (discussed in Chapter 3), two studies revealed different corneal deformation profiles in high myopes (Wang et al., 2015, Lee et al., 2016). Methodology for corneal biomechanical measurement using a novel indentation method is introduced in previous chapter

(Section 3.2). The following study aimed to compare corneal tangent modulus between low and high myopes.

4.2 Methodology

4.2.1 Subjects

Thirty-two healthy young adults with low myopia and 32 with high myopia were recruited. Based on a mean axial length (AL) of 24 mm in emmetropic eyes (Khurana, 2008), low myopes were defined as having a spherical equivalent (SE) within -0.50 D and -3.00 D, with an AL $\leq$ 25 mm, whereas high myopes had a SE of < -6.00 D with AL > 26 mm. All subjects had good general health and underwent a comprehensive eye examination, including subjective refraction, slit lamp biomicroscopy, and funduscopy, to confirm their normal ocular health. Exclusion criteria included GAT IOP $\geq$ 21 mmHg, rigid lens wear, pregnancy, history of refractive surgery or eye diseases, and long-term use of ocular or oral medications. Soft lens wearers were required to cease contact lens wear for at least 24 hours before data collection. The study protocol was reviewed and approved by the institutional review board according to the Declaration of Helsinki. Informed consent was obtained from each subject after the study procedures were explained.

4.2.2 Procedures

Subjects first underwent non-contact measurements which included central corneal thickness (CCT) by anterior segment optical coherence tomography (AS-OCT; Casia SS-1000, Tomey, Japan), central corneal radius of curvature by corneal topography (Medmont E300, Medmont Pty Ltd., Australia), and AL by partial coherence interferometry (IOLMaster 500, Carl Zeiss, Germany). Three images of the pachymetry map were obtained using the "Topo-Pachy-Map" scan mode in AS-OCT. The corneal thickness at the vertex was denoted as the CCT. In corneal topography, three images with scores higher than 95 were captured. The mean value of the simulated steepest and flattest keratometry readings (meanK) was used for analysis. Five readings of AL were taken by IOLMaster.

Subsequently, corneal biomechanics were measured using the ORA, followed by the corneal indentation device (CID). A five-minute lapse was allowed between the ORA

and CID measurements. Three ORA measurements with waveform scores of at least 6.0 were accepted (Mandalos et al., 2013). The ORA provides corneal hysteresis (CH), corneal resistance factor (CRF), Goldmann-correlated intraocular pressure (IOPg) and corneal-compensated IOP (IOPcc) in one measurement. The CH, CRF and IOPcc were selected for data analysis. After instillation of topical anaesthetic (one drop of 0.4 % Benoxinate) into the eye, three valid readings of corneal stiffness were acquired using the CID. As corneal tangent modulus is strongly associated with IOP (Ko et al., 2013), the GAT IOP was measured twice by a masked examiner. Only one eligible eye of the subject was selected for data analysis. When both eyes were eligible, the eye with the shorter AL (low myopia group) or the longer one (high myopia group) was selected. Multiple measurements from each device were averaged for statistical analysis. Corneal tangent modulus was computed by substituting subject-specific corneal stiffness, thickness and radius of curvature into equation 3.7.

4.3 Statistical analysis

Data analyses and graphical presentation were conducted using IBM SPSS (version 23.0, SPSS, Inc., USA) and GraphPad Prism (version 5, GraphPad Software, Inc., USA), respectively. The statistical power was computed using G-power (version, 3.1.7, Franz Faul, Universität Kiel, Germany). A p-value < 0.05 was considered statistically significant.

The Shapiro-Wilk tests were used to assess data normality. Most measured parameters were not significantly different from a normal distribution, thus, parametric statistical tests were used to analyze the data. As age and AL were not normally distributed, nonparametric statistical tests were used on these parameters. Corneal biomechanical measurements have been shown to be confounded by physical properties of the cornea, such as its thickness and radius, as well as the internal pressure of the eye (Sullivan-Mee et al., 2012, Asaoka et al., 2015). Bivariate correlation analyses were performed to investigate the associations between corneal biomechanical parameters (corneal stiffness, CH and CRF) and ocular parameters (meanK, CCT, GAT IOP and IOPcc). Considering corneal stiffness as a novel corneal parameter from the CID, multiple linear regression analysis was further constructed to determine which aforementioned

ocular parameters dominantly affect corneal stiffness measurement. These ocular parameters (as independent variables) must have a linear relationship with corneal stiffness (as dependent variable) and must not show multicollinearity with each other. The independence of observations was checked using the Durbin-Watson statistic and the homoscedasticity was assessed by plotting the standardized residuals against the unstandardized predicted values. For corneal radius, only mean values were used for statistical analysis. It remains unknown whether corneal toricity affects corneal stiffness, thus, correlation analyses were also conducted to investigate the association.

Animal studies have confirmed a strong relationship between corneal tangent modulus and IOP (Ko et al., 2013). It has been shown that IOPcc is less affected by CCT than is GAT IOP (Medeiros & Weinreb, 2006). The associations between the two IOP readings (namely GAT IOP and IOPcc) and CCT were analyzed to check their CCT dependence. The means of each parameter between the two refractive groups were compared.

4.4 Results

Significant correlations were observed between corneal stiffness and ocular parameters (Table 4.1). In particular, corneal stiffness was positively associated with meanK (r = 0.28, p < 0.05) and CCT (r = 0.26, p < 0.05), as well as GAT IOP (r = 0.57, p < 0.001) and IOPcc (r = 0.46, p < 0.001). Both CH (r = 0.67, p < 0.001) and CRF (r = 0.78, p < 0.001) were positively associated with CCT. CRF was positively associated with GAT IOP (r = 0.37, p < 0.01). Conversely, CH was negatively associated with IOPcc (r = -0.40, p < 0.01). MeanK, CCT and IOPcc were significantly correlated with corneal stiffness and did not violate multicollinearity, so they were treated as the independent variables. Multiple linear regression analysis reported a significant overall result (F(3, 60) = 8.57, p < 0.001) with an R^2 of 0.30. Only IOPcc correlated significantly with corneal stiffness but not for meanK and CCT (Table 4.2). Corneal toricity, which ranged from 0.5 to 3.5 D in the current study, did not affect corneal biomechanical measurements from the CID and the ORA (Table 4.1). Corneal tangent modulus increased significantly with increasing GAT-IOP (r = 0.28, p < 0.05) (Figure 4.1) and IOPcc (r = 0.34, p < 0.001) (Figure 4.2). GAT IOP was positively

associated with the CCT (r = 0.28, p < 0.05), whereas IOPcc was independent of the CCT (r = 0.087, p = 0.49).

Table 4.1 Factors affecting corneal stiffness, corneal hysteresis (CH) and corneal resistance factor (CRF) measurements.

	Corneal stiffness	**CH**	**CRF**
meanK			
r	0.28*	-0.07	-0.01
CCT			
r	0.26*	0.67***	0.78***
toricity			
r	-0.11	-0.10	<-0.002
GAT IOP			
r	0.57***	0.01	0.37**
IOPcc			
r	0.46***	-0.40**	0.13

meanK = mean corneal radius; GAT IOP = intraocular pressure from Goldmann applanataion tonometry; IOPcc = corneal-compensated intraocular pressure; *r* = correlation coefficient

*Significance of p-value < 0.05.

**Significance of p-value < 0.01.

***Significance of p-value < 0.001.

Table 4.2 Multiple linear regression of parameters affecting corneal stiffness measurement (n = 64).

	Standardized	**Partial correlation**	**P-value**
meanK	0.20	0.22	0.08
CCT	0.18	0.21	0.11
IOPcc	0.43	0.45	<0.001

meanK = mean corneal radius; CCT = central corneal thickness; IOPcc = corneal-compensated intraocular pressure

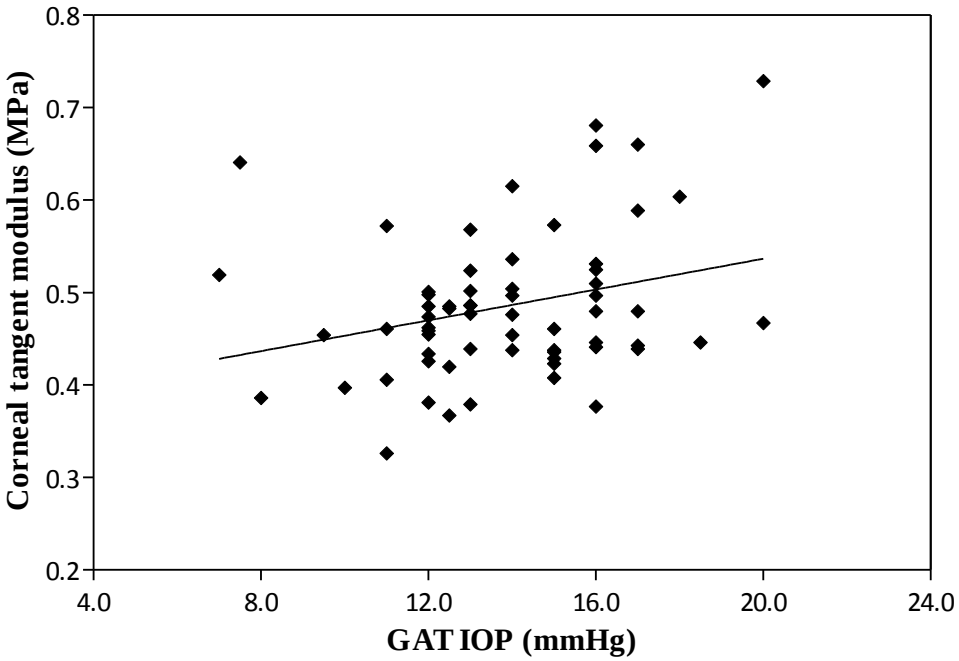

Figure 4.1 Presence of positive correlation between corneal tangent modulus and Goldmann applanation tonometry (GAT IOP) ($r = 0.28$, $p < 0.05$).

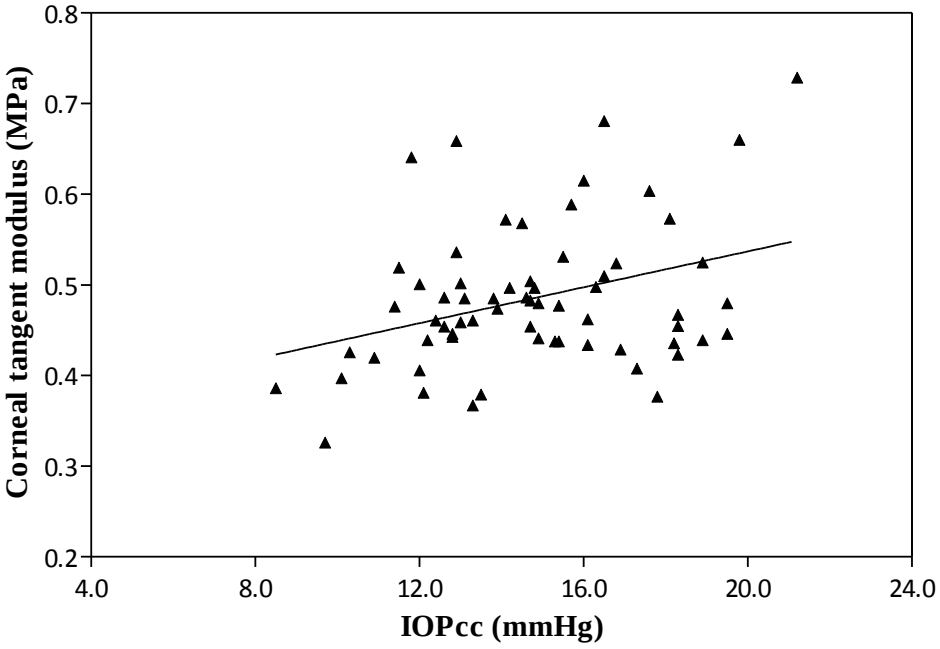

Figure 4.2 Presence of positive correlation between corneal tangent modulus and corneal-compensated intraocular pressure (IOPcc) ($r = 0.34$, $p < 0.01$).

Statistical comparisons of the demographic data and biomechanical parameters for the two refractive groups are presented in Table 4.3. There were no significant differences between the two groups in age (U = 461.00, p = 0.49) and sex (U = 496.00, p = 0.80). Because of the inclusion criteria, the low and high myopia groups exhibited distinct differences in SE (t = 21.62, p < 0.001) and AL (U = 0.00, p < 0.001). Both groups showed a similar CCT (t = 0.89, p = 0.38) and meanK (t = -0.0064, p = 0.99). In addition, a significant difference was observed in corneal toricity between the two groups (t = -4.23, p < 0.001). The low myopia group exhibited significantly lower tonometry results, in terms of IOPcc (t = -5.57, p < 0.001) and GAT IOP (t = -2.60, p < 0.05), than the high myopia group.

The low and high myopia groups had a similar CRF (t = 0.35, p = 0.73) and corneal stiffness (t = -0.11, p = 0.92). The high myopia group showed a significantly lower CH than the low myopia group (t = 2.92, p < 0.01) (Figure 4.3a). However, corneal tangent modulus calculated using subject-specific IOP was not significantly different between the two groups. As corneal biomechanical parameters in the present study were significantly associated with IOP, the modulus value of each subject was normalized to 15.5mmHg (the mean IOP of normal eyes (King et al., 2013)) using IOPcc. The high myopia group demonstrated a significantly lower normalized corneal tangent modulus (0.47 ± 0.087 MPa) than the low myopia group (0.57 ± 0.099 MPa) (t = 4.17, p < 0.001) (Figure 4.3b). On the basis of the observed effect size of 1.04 on normalized tangent modulus, 98 % power was achieved with an alpha of 0.05.

Table 4.3 Differences in the demographic data and corneal biomechanical parameters between low and high myopia groups. Parametric data are presented as mean ± standard deviation while nonparametric data are presented as median (range).

Parameters	Low myopes	High myopes	P-value
Age (year)	23.5 (range: 19.0 - 31.0)	24.5 (range: 19.0 - 36.0)	0.49[a]
Sex (M/F)	15 / 17	15 / 17	0.80[a]
Spherical equivalent (D)	1.37 ± 0.60	9.08 ± 1.92	<0.001
Axial length (mm)	22.87 (range: 22.87 - 24.94)	27.28 (range: 26.04 - 29.65)	<0.001[a]
Central corneal thickness (μm)	553.3 ± 32.8	545.8 ± 34.8	0.38
Mean corneal radius (mm)	7.77 ± 0.21	7.77 ± 0.18	0.99
Corneal toricity (D)	1.21 ± 0.46	1.82 ± 0.68	<0.001
Intraocular pressure from Goldmann applanation tonometry (mmHg)	12.98 ± 2.57	14.66 ± 2.57	<0.05
Corneal-compensated intraocular pressure (mmHg)	13.13 ± 1.96	16.38 ± 2.51	<0.001
Corneal hysteresis (mmHg)	10.56 ± 1.38	9.52 ± 1.51	<0.01
Corneal resistance factor (mmHg)	9.62 ± 1.58	9.46 ± 1.90	0.73
Corneal stiffness (Nmm^{-1})	0.063 ± 0.0085	0.063 ± 0.0079	0.92
Corneal tangent modulus (MPa)	0.48 ± 0.076	0.49 ± 0.084	0.42
Normalized corneal tangent modulus (MPa)[†]	0.57 ± 0.099	0.47 ± 0.087	<0.001

†The corneal tangent modulus was normalized to the mean intraocular pressure of normal eyes (15.5 mmHg).

[a]Mann-Whitney U tests were performed.

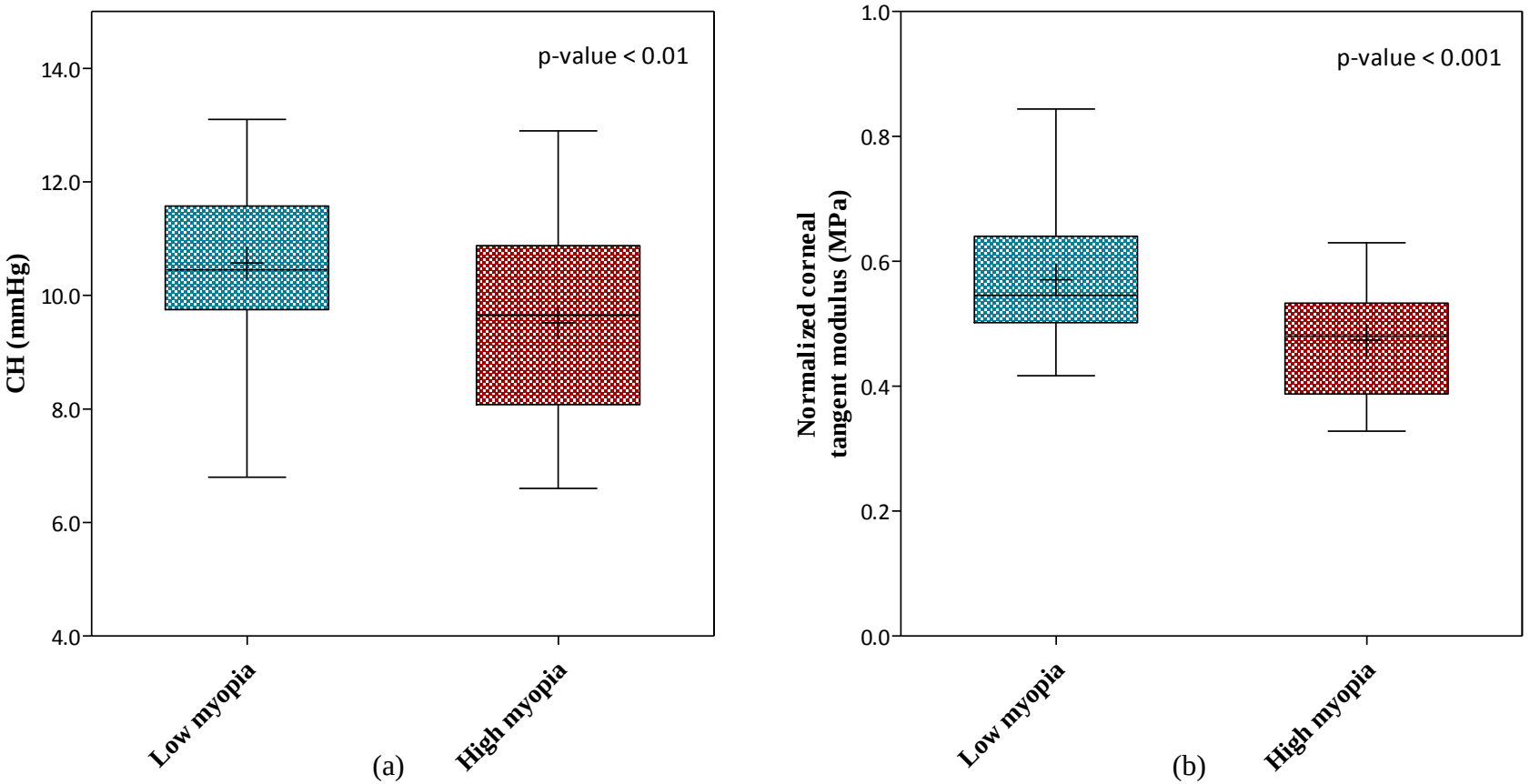

Figure 4.3 Box-and-whisker plots for **(a)** corneal hysteresis (CH) and **(b)** corneal tangent modulus in the two refractive groups. The cross and the middle line in each box represent the mean and median respectively. The height of the box represents the upper and lower quartiles. The whiskers represent the maximum and minimum values respectively.

4.5 Discussion

This is the first study establishing corneal tangent modulus in two distinct refractive groups. Among a total of 64 subjects in the current study pool, corneal tangent modulus at subject-specific IOP ranged from 0.33 to 0.73 MPa. Orssengo and Pye (1999) developed a mathematical algorithm to calculate elastic modulus of the human cornea *in vivo*. The principle of this algorithm involved modeling of corneal deformation by the GAT probe. The elastic modulus from 100 subjects aged 18 to 30 years ranged from 0.13 to 0.43 MPa (Hamilton & Pye, 2008). Despite the same order of magnitude from the current study, the CID gave higher modulus values in low and high myopia subjects at subject-specific IOP. Nevertheless, direct comparison of elastic modulus from different methodologies is difficult due to the difference in the applied stress. Moreover, elastic modulus from Orssengo and Pye (1999) was derived in a static condition while the CID provides tangent modulus which is rate-dependent (Ko et al., 2013). From preliminary experiments on porcine eyes, tangent modulus measured from the CID could be double that of the static elastic modulus (Ko et al., 2013).

Corneal stiffness is directly measured from the CID and it represents a force-displacement relationship of the corneal tissue during corneal indentation. From the mechanical perspective, the force required to indent the cornea to the same depth differs between individual eyes, depending on the physical properties of the cornea (thickness, radius, and elasticity) and internal pressure of the eye. According to the present findings, corneal stiffness measurement was predominately influenced by IOP. The ORA parameters, CH and CRF, were positively correlated with CCT, but did not vary with meanK or corneal toricity. On the other hand, CH demonstrated an inverse relationship with IOPcc while CRF had a positive relationship with GAT IOP. The influence of corneal thickness, curvature, and IOP on the two ORA parameters coincides well with the literature, which is fully discussed in Section 1.4.2.4 to 1.4.2.6.

The CID measures corneal biomechanics in terms of corneal stiffness and tangent (elastic) modulus. A clear understanding of their biomechanical meanings is essential to interpret the present findings. Using a real-life comparison, a thick wood chopstick is more difficult

to bend than a thin wood chopstick. Thus the thick wood chopstick can be called stiffer. However, both chopsticks originate from the same material (i.e. wood) and they have the same elastic modulus. Therefore, corneal stiffness measurement is affected by corneal geometries, such that a higher corneal stiffness can be obtained in a thicker cornea. Only tangent (elastic) modulus represents an intrinsic material property which is independent of corneal geometry changes.

The two refractive groups had a similar CCT and central corneal radius, but the high myopia group had a higher measured IOP. The positive association between high myopia and IOP has been reported elsewhere (Jensen, 1992, Nomura et al., 2004, Joseph et al., 2016), but the causal role is yet to be confirmed (Pruett, 1988, Quinn et al., 1995). Corneal stiffness and tangent modulus were similar between the groups, however, both factors are highly IOP-dependent (Kurita et al., 2008, Ko et al., 2013). These linear and positive correlations were consistent in our study. Hence, corneal tangent modulus could not be directly compared when high myopic eyes had a significantly higher IOP. To tackle the problem, normalization of corneal tangent modulus to the mean IOP in normal eyes was performed on each subject. It is well known that significant errors in applanation tonometry can be induced by different corneal properties (Whitacre et al., 1993, Liu & Roberts, 2005). The IOPcc from the ORA is empirically derived from a set of pre- and post-laser in situ keratomileusis (LASIK) data, which was used to minimize the difference in applanation pressures between pre- and post-LASIK patients (Luce, 2006). Thus, the IOPcc can give an IOP reading which is less affected by corneal properties (Luce, 2006, Medeiros & Weinreb, 2006, Lam et al., 2007). Our results revealed no association between IOPcc and CCT. Other studies also found less reduction in IOPcc than IOPg and GAT IOP upon alteration of corneal biomechanics from corneal refractive surgeries (Ortiz et al., 2007, Chen et al., 2008, Shin et al., 2015a). In animal studies, corneal tangent modulus is linearly dependent on the true IOP regulated by manometry (Ko et al., 2013). Corneal tangent modulus was therefore normalized to 15.5mmHg (King et al., 2013) using IOPcc rather than using GAT IOP. After normalization, the low myopia group revealed a significantly higher corneal tangent modulus than the high myopia group, indicating stiffer corneas.

The two refractive groups showed statistically significant difference in CH. The CH was higher in low myopes compared with high myopes, which coincided with previous findings (Jiang et al., 2011, Altan et al., 2012, Bueno-Gimeno et al., 2014b, Del Buey et al., 2014). However, as shown in Figure 4.3a, inter-subject variation of CH was considerable within groups. Direct relationship between corneal biomechanical parameters from the ORA and myopia remains unclear. Low CH might indicate a low viscous damping capacity in the corneas of high myopes (Bueno-Gimeno et al., 2014b). Although corneal toricity showed significant difference between the two refractive groups, no association was observed between corneal stiffness and toricity. As the CID measures corneal stiffness when the indenter is under full contact at the central cornea, the effect of corneal toricity could be minimal.

Early studies attempted to measure the ocular biomechanics in eyes with different refractive error. Friedenwald (1937) reported that myopes had lower coefficient of rigidity compared with hyperopes, whereas Sergienko and Shargorogska (2012) observed more expandable eyes with increasing myopia. Both studies performed corneoscleral indentation. The air puff systems (ORA and Corvis ST) are designed for measuring corneal biomechanical parameters. Robert et al. (2014) used ORA waveform data and suggested that hyperopic eyes are stiffer than myopic eyes. To differentiate distinct corneal biomechanics from the influence of confounding factors, they performed vigorous matching of CCT, IOPcc and age on the two refractive groups. Consequently, even though a large number of subjects were recruited only around 20 % were eligible. This methodology could be clinically inapplicable. On the other hand, a stiffer sclera could produce a stiffer corneal response by using an air puff (Metzler et al., 2014). The advantages of CID include calculation of corneal tangent modulus that takes corneal thickness, radius of curvature and IOP into account and thus allows a clear delineation of corneal biomechanics in human subjects. The effect of the scleral properties on corneal biomechanical measurement could be minimized by the small area of central corneal contact that is sufficiently far from the limbus.

Myopia is associated with thinner and mechanically weakened sclera (McBrien et al., 2009). Scleral biomechanical changes could be involved in both the cause and the consequence of axial elongation (McMonnies, 2016). It is interesting to learn that corneal biomechanics might be relevant to the expansion of the whole eyeball, as shown in the current study. Finite element model simulation also revealed increased stress at the lamina cribosa with increasing corneal tangent modulus without IOP change, implying a risk for glaucoma development (Ko, 2013). The cornea and sclera are derived from the same mesoderm. A recent microscopic study reinforced the presence of a network of elastic fibers in the central cornea which originated from the limbus and possibly the sclera (Lewis et al., 2015). These elastic fibers could play an important role in corneal deformation and recovery. Although axial elongation predominantly alters scleral biomechanics (McMonnies, 2016), changes of corneal biomechanics might come along with myopia development.

Normalization of corneal tangent modulus was performed in the data analysis due to the linear dependency between corneal tangent modulus and true IOP, which has been confirmed in animal experiments (Ko et al., 2013). However, true IOP in human subjects can only be measured using an intracameral method (Feltgen et al., 2001, Boehm et al., 2008). Regarding this limitation, the use of IOPcc for normalization could be justified.

4.6 Conclusion

The present study demonstrates different corneal tangent modulus in low and high myopia groups. Corneas in high myopes showed lower tangent modulus. A material with lower tangent (elastic) modulus is considered as less stiff. More work is needed to confirm the association between corneal and scleral biomechanics and their roles in myopia. To determine the cause or effect of the altered corneal biomechanics in highly myopic eyes, monitoring of corneal tangent modulus in children during active myopia development is warranted.

Paper published:

Hon, Y., Chen, G. Z., Lu, S. H., Lam, D. C. & Lam, A. K. 2017. High myopes have

lower normalised corneal tangent modulus (less ‘stiff’ corneas) than low myopes. *Ophthalmic Physiol Opt*, 37, 42-50.

Conference presentation:

Hon, Y., Lam, A. K., Lam, D. C. Corneal stiffness and tangent elastic modulus in low and high myopes. The 11th Joint Eye Research Day 2015, Hong Kong. Oral presentation.

Hon, Y., Lam, A. K., Chen, G. Z., Lu, S. H., Lam, D. C. Corneal stiffness and tangent modulus in low and high myopes. The 10th Asia Cornea & Contact Lens Conference 2016, Hong Kong. Poster presentation.

Chapter 5

Influence of short-term orthokeratology on corneal stiffness and corneal tangent modulus – a pilot study

5.1 Introduction

Orthokeratology (ortho-k), or corneal reshaping therapy, is a clinical technique that reshapes the cornea temporarily to reduce myopia with the use of specially designed rigid contact lenses (Caroline, 2001). Following publication of the evidence that ortho-k can effectively reduce myopia progression in children (Cho & Cheung, 2012, Santodomingo-Rubido et al., 2012), the demand for myopia control using ortho-k has inevitably been increasing. Thus, there is a need to achieve a better understanding of corneal behavior and improve the effectiveness of ortho-k treatment.

Ortho-k modifies corneal geometry. It causes a flattening of anterior corneal curvature and a thinning of the central corneal thickness. This allows light rays to be redirected onto the retina, hence reducing myopia. The refractive and biometric changes due to ortho-k are well documented (Swarbrick, 2006, Cheung & Cho, 2013). Yet, the effect on corneal biomechanics is unclear. As discussed in Section 1.4.3.5, although corneal hysteresis (CH) or corneal resistance factor (CRF) were found to be reduced under short-term ortho-k, the changes were not clinically significant (Mao et al., 2010, Chen, 2011, Yeh et al., 2013). Whether CH and CRF truly represent the mechanical behavior of the corneal tissue remains controversial (McMonnies, 2012, Roberts, 2014). Therefore, it is desirable to explore new techniques and provide understandable terminology to quantify corneal biomechanics *in vivo*.

The aim of this pilot study was to investigate the changes in corneal stiffness and corneal tangent modulus with short-term ortho-k treatment using a novel corneal indentation device (CID).

5.2 Methodology

5.2.1 Subjects

Eighteen young Chinese myopes (6 male and 12 female), aged from 18 to 25 years, were recruited. The inclusion criteria for refractive error included refractive sphere between -2.00 D to -4.00 D, refractive cylinder within 1.00 D and corneal toricity within 2.00 D in each eye. The difference in myopia between the two eyes was within 1.00 D for both the sphere and cylinder components. Spherical equivalent refraction (SER) was therefore fallen between -2.00 D to -4.50 D. All subjects had good ocular and general health and no history of ocular surgeries or diseases. Previous Rigid lens wearers were excluded while soft contact lens wearers were required to cease lens wear for at least 7 days before any measurements. The study protocol was reviewed and approved by the institutional review board according to the Declaration of Helsinki. Informed consent was obtained from each subject before the commencement of the study.

5.2.2 Ortho-k fitting and aftercares

The reverse geometry rigid lens used in the study was Paragon Corneal Reshaping Therapy (CRT, Paragon Vision Sciences, AZ), which has an oxygen permeability (Dk) of 100. The total lens diameter was 10.5 mm with a 6-mm optic zone diameter. The lens thickness at the centre was 0.18 mm. Ortho-k fitting and aftercare were conducted by an experienced ortho-k practitioner.

The initial trial lens was selected using a Lens Selector Slide Rule provided by the manufacturer, based on the flat keratometry reading and manifest refractive sphere of the subject. Lens fitting was assessed with fluorescein, whereby an optimal fluorescein pattern consisted of 3 – 4 mm of central touch, 1 - 1.5 mm of mid-peripheral pooling and 1 - 1.5 mm of peripheral alignment (Figure 5.1). When acceptable fit was obtained with the trial lenses, the subject was asked to close their eyes for approximately 1 hour. After that, the trial lenses were removed and corneal topography (Medmont E300, Medmont Pty Ltd., Australia) was performed to assess lens centration. Good lens centration was revealed by a typical bull’s eye topography on a tangential subtractive map (Figure 5.2).

This topographic pattern consists of a centrally flattened zone surrounded by a steepened annulus. A lens order was placed after fluorescein and topographic evaluation.

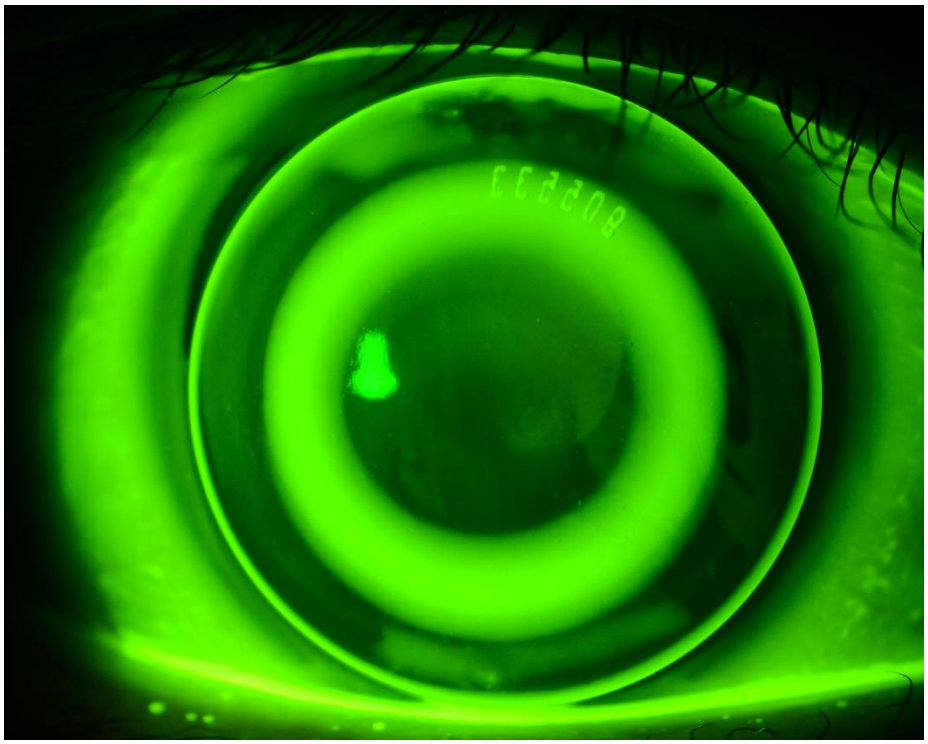

Figure 5.1 Optimal fluorescein pattern of a reverse geometry rigid lens on the eye, which was observed under a slit-lamp with a yellow filter.

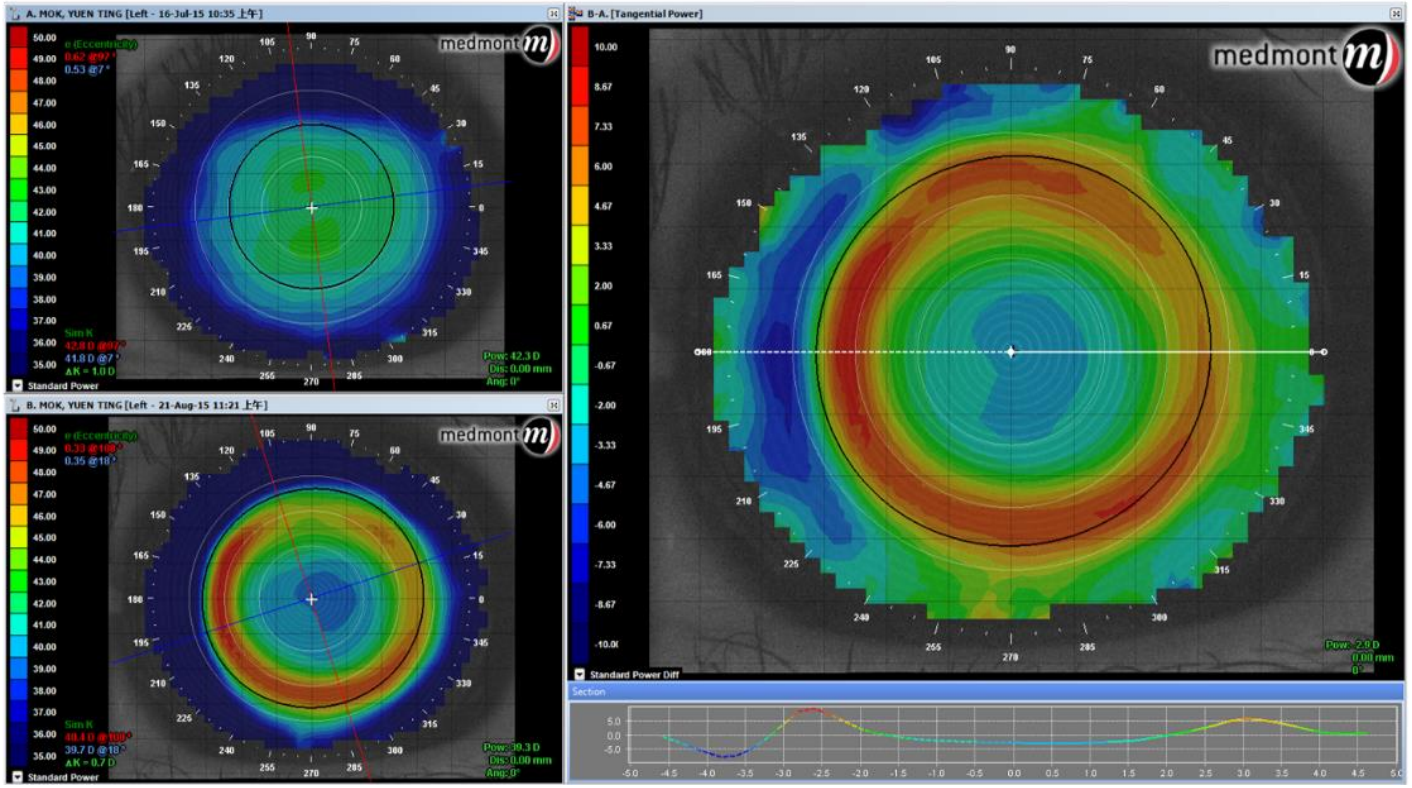

Figure 5.2 Tangential subtractive map of an eye from an ortho-k subject. Pre- and post-treatment topography are shown on the top left and bottom left, respectively. The subtractive map is presented on the right-hand side, revealing a bull's eye topography.

Subjects were instructed to wear the ortho-k lenses during sleep for a 1 month period. Lens care regimen materials were provided, which included Boston Advance Conditioning Solution, Boston Advance Cleaner and saline solution for daily soaking, cleaning and rinsing of the lenses respectively. Scheduled ortho-k aftercare included first overnight visit, first week visit, first month visit, and three months after cessation of lens wear. All aftercare was conducted in the morning between 9 to 11 am and within 2 hours of awakening. At the first overnight visit, subjects were asked to visit the Optometry Clinic with the lenses *in situ* in order to evaluate the possibility of lens binding and associated ocular response. At other visits within the 1 month period, subjects returned to the clinic after lens removal. Following the clinical protocol of the Optometry Clinic at the School of Optometry, anterior ocular health, corneal topography, visual acuity, residual refractive error, patient compliance and lens condition were strictly monitored by the ortho-k practitioner.

5.2.3 Procedures

Data collection was performed by a separate practitioner. Subjects underwent non-contact measurements which included corneal topography, pachymetry and biomechanics using the Medmont E300, anterior segment optical coherence tomography (Casia SS-1000, Tomey, Japan) and the Ocular Response Analyzer (ORA, Reichert Ophthalmic Instruments, NY), respectively. Biometric measurements were always arranged to be performed first and in a random order, followed by biomechanical measurement. The subject was seated behind the instrument and was asked to blink normally, open the eyes widely and fixate on the internal target during image acquisitions. In corneal topography, three images with scores higher than 95 were captured. The simulated steepest and flattest anterior corneal curvatures in the central 3.0mm zone were used for analysis. Three images of the pachymetry map were obtained using the "Topo-Pachy-Map" scan mode in AS-OCT. The corneal thickness at the vertex was denoted as the CCT. Three ORA measurements with waveform scores of at least 6.0 were accepted (Mandalos et al., 2013). Corneal hysteresis (CH), corneal resistance factor (CRF) and corneal-compensated intraocular pressure (IOPcc) were extracted for analysis.

Distance uncorrected visual acuity (UCVA) was measured using the Early Treatment Diabetic Retinopathy Study visual acuity chart (ETDRS, Prevision Vision, IL) under normal room lighting. Recording was done in Bailey-Lovie logarithm of the minimum angle of resolution (logMAR) unit.

Contact procedures included corneal indentation and Goldmann applanation tonometry (GAT). After topical anaesthesia (one drop of 0.4 % Benoxinate), three valid readings of corneal stiffness were acquired using the CID. Intraocular pressure (IOP) was measured twice by a masked examiner. Corneal tangent modulus was calculated using Equation 3.7 in Chapter 3. The simulated steepest and flattest anterior corneal curvatures in each subject were averaged for the computation.

All measurements were conducted immediately after regular orthok aftercares. Baseline data taking was arranged within 3 days before the first overnight visit. Subsequent time points of data collection included first overnight visit, first week visit, first month visit and three months after cessation of lens wear. Because the treatment efficacy can be different between eyes, the eye with a better UCVA after 1 month of treatment was treated as the good response eye, and its data was used for analysis. When both eyes achieved equal UCVAs, the right eye was selected.

5.3 Statistical analysis

Statistical analyses and graphics were performed using SPSS (version 18.0, SPSS, Inc., USA) and GraphPad Prism (version 5, GraphPad Software, Inc., USA), respectively. The statistical power was computed using G-power (version 3.1.7, Franz Faul, Universität Kiel, Germany). All the data were tested for normality using Shapiro-Wilk tests. Appropriate parametric or nonparametric statistical tests were used for further analyses. The level of significance chosen was 5 %.

Repeated measures analyses of variance (RMANOVAs) were used to compare the changes in all measured parameters over all visits. In the presence of significant differences, post-hoc comparisons were conducted using paired *t*-tests with Bonferroni adjustment. For non-parametric data, Friedman tests were conducted to evaluate the overall significant differences between visits. Whenever positive results

were found, Wilcoxon signed-rank tests with Bonferroni adjustment were used to determine the significant pairs. The observed power of the sample size was examined using SPSS software.

5.4 Results

The mean ± standard deviation (SD) age of the subjects was 20.7 ± 1.6 years. Their baseline SER in the good response eyes were -3.13 ± 0.71 D (range -2.00 D to -4.38 D).

Detailed changes of all required measurements during the study period are tabulated in Table 5.1. Upon good treatment response, the resultant SER became -0.10 ± 0.22 D and the UCVA was -0.068 ± 0.073 at one month. Significant and temporary central corneal thinning and flattening (including the flattest and steepest meridians) were observed across a 1 month treatment period (RMANOVAs, all $p < 0.001$). The average reduction in CCT after 1 month was 11.8 ± 6.6 μm. Similarly, the flattest and steepest corneal curvatures were flattened by 1.79 ± 0.73 D and 1.89 ± 0.76 D, respectively. The GAT IOP showed a trend of statistically significant reduction due to the corneal changes in the lens wearing period, whereas the reduction in IOPcc was insignificant (RMANOVAs, GAT IOP, $p < 0.05$; IOPcc, $p = 0.059$).

Table 5.1 Ocular parameters of the good response eyes in the study period. Data are presented as mean ± standard deviation.

Parameter / **Visit**	**Baseline**	**1st overnight**	**1st week**	**1st month**	**3 months after lens cessation**
SER (D)	-3.13 ± 0.71	-1.49 ± 0.77**	-0.26 ± 0.55**	-0.10 ± 0.22**	-3.09 ± 0.66
UCVA (logMAR)	0.88 ± 0.26	0.38 ± 0.20**	-0.02 ± 0.11**	-0.068 ± 0.073**	0.90 ± 0.15
Flat K (D)	42.55 ± 1.98	41.45 ± 1.81**	41.03 ± 1.73**	40.77 ± 1.60**	42.34 ± 1.75
Steep K (D)	43.71 ± 2.13	42.68 ± 1.86**	42.18 ± 2.04**	41.82 ± 1.82**	43.58 ± 2.10
CCT (μm)	570.4 ± 30.3	567.5 ± 32.0	562.1 ± 33.5	558.6 ± 33.3**	570.7 ± 31.7
GAT-IOP (mmHg)	14.25 ± 2.62	13.19 ± 2.41	13.06 ± 2.16	12.53 ± 1.62	13.31 ± 2.07
Corneal stiffness (Nmm^{-1})	0.064 ± 0.0093	0.063 ± 0.0087	0.063 ± 0.0070	0.065 ± 0.0073	0.065 ± 0.0055
Corneal tangent modulus (MPa)	0.47 ± 0.093	0.48 ± 0.088	0.50 ± 0.088	0.52 ± 0.080*	0.48 ± 0.072
CH (mmHg)	10.51 ± 1.46	10.76 ± 1.16	10.69 ± 0.99	10.39 ± 1.02	10.93 ± 1.20
CRF (mmHg)	10.32 ± 1.36	10.45 ± 1.11	10.17 ± 1.07	9.79 ± 0.97	10.49 ± 1.33
IOPcc (mmHg)	15.32 ± 2.79	14.77 ± 2.53	14.32 ± 2.06	14.28 ± 2.34	14.34 ± 2.00

SER = spherical equivalent refraction; UCVA = uncorrected visual acuity; Flat K = flattest anterior corneal curvature; Steep K = steepest anterior corneal curvature; CCT = central corneal thickness; GAT IOP = intraocular pressure from Goldmann applanation tonometry; CH = corneal hysteresis; CRF = corneal resistance factor; IOPcc = corneal-compensated intraocular pressure

*Significance of p-value < 0.05 compared with the baseline result.

**Significance of p-value < 0.001 compared with the baseline result.

For the corneal biomechanical properties, there were no significant changes in CH throughout the study (RMANOVAs, $p = 0.082$), whilst CRF was reduced temporarily (RMANOVAs, $p < 0.05$) (Figure 5.3). Compared with the baseline, however, the mean CRF reduction from these 18 eyes was 4.3 % only after 1 month of treatment (from 10.32 to 9.79 mmHg) (paired *t*-test with Bonferroni adjustment, $p = 0.28$). No significant changes were observed in corneal stiffness (RMANOVA, $p = 0.33$) (Figure 5.4). Corneal tangent modulus was increased significantly in the lens wearing period (RMANOVA, $p < 0.001$) (Figure 5.5). The mean increment was 12.1 % (from 0.47 to 0.52 MPa) (paired *t*-test with Bonferroni adjustment, $p < 0.05$).

Measurements were repeated 3 months after discontinuation of lens wear. In general, all physical parameters of the eyes returned to the baseline values (post-tests with Bonferroni adjustment, all $p > 0.05$). Less than 0.25 D residual corneal flattening was observed. The SER in the good response eyes returned to -3.09 ± 0.66 D (range -2.00 D to -4.38 D). The statistical power of repeated measures on corneal tangent modulus during ortho-k was evaluated. Based on the observed sample effect size of 0.57 and correlation among repeated measures of 0.8, 100 % power was achieved with alpha at 0.05 when the sphericity was assumed.

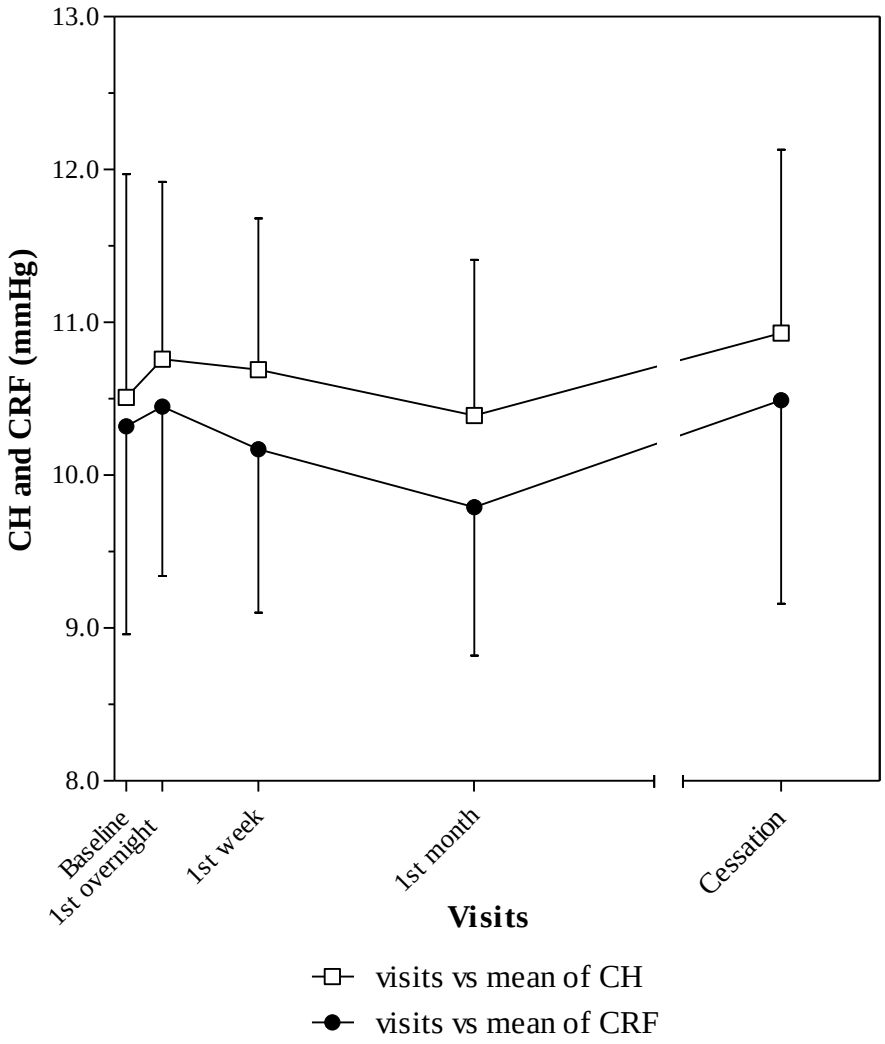

Figure 5.3 Corneal hysteresis (CH, RMANOVA, $p = 0.082$) and corneal resistance factor (CRF, RMANOVA, $p < 0.05$) changes over the study period. Each error bar indicates 1 standard deviation.

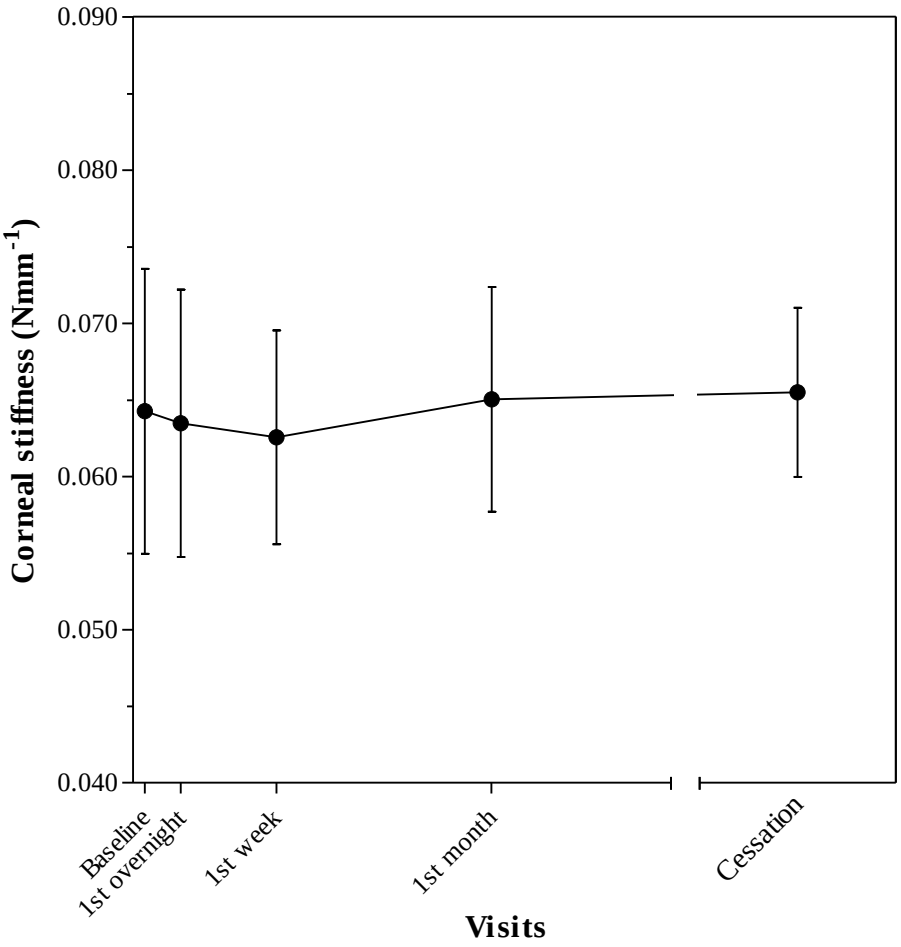

Figure 5.4 Corneal stiffness over the study period (RMANOVA, p = 0.33). Each error bar indicates 1 standard deviation.

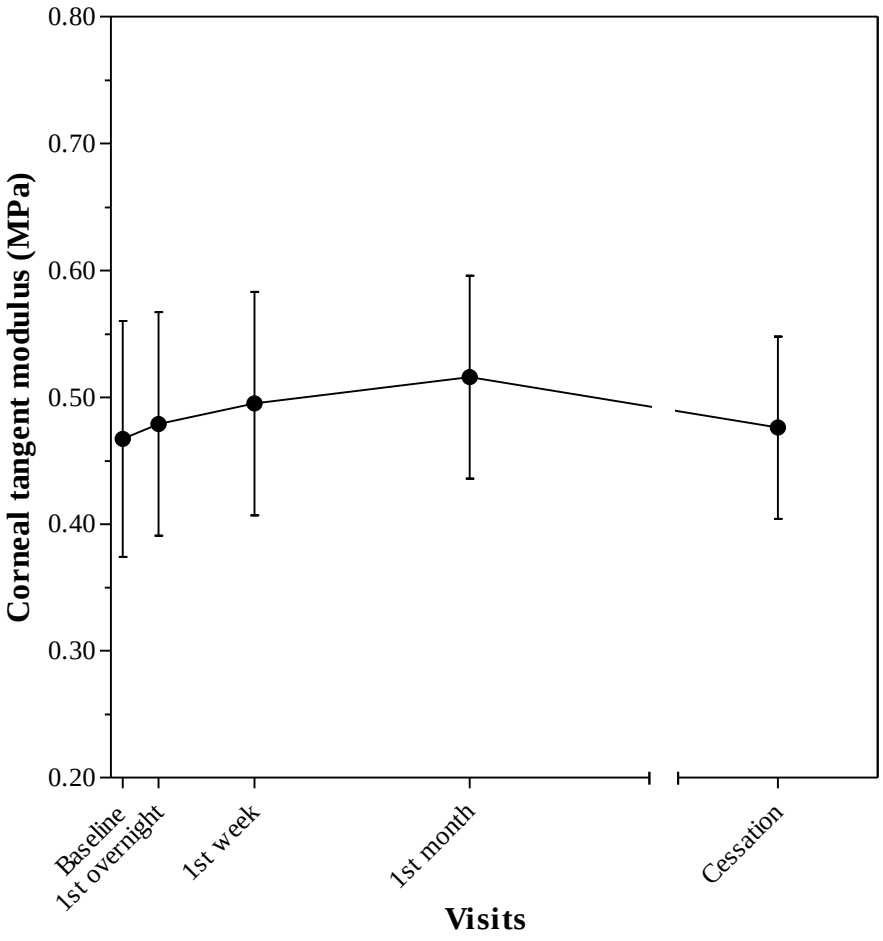

Figure 5.5 Corneal tangent modulus over the study period (RMANOVA, $p < 0.001$). Each error bar indicates 1 standard deviation.

5.5 Discussion

Reverse geometry lens wear causes central flattening and thinning to the cornea (Swarbrick et al., 1998, Caroline, 2001, Sridharan & Swarbrick, 2003). Previous clinical studies agreed that most of the corneal and refractive changes in low myopes (> -4.00 D) were beginning to plateau after 10 nights of lens wear and stabilized at 1 month (Nichols et al., 2000, Alharbi & Swarbrick, 2003, Owens et al., 2004, Kang et al., 2007, Chen et al., 2010a). The corneal reshaping is temporary and reversible after lens cessation (Sridharan, 2001, Soni et al., 2004). Central corneal flattening is the major contributor to myopia reduction, thus the amount of flattening correlates with the amount of refractive correction in ortho-k treatment (Mountford, 1997, Chan et al., 2010). Accordingly, the

changes of corneal thickness have been evaluated by different studies (Swarbrick et al., 1998, Nichols et al., 2000, Alharbi & Swarbrick, 2003, Soni et al., 2003, Haque et al., 2004, Owens et al., 2004, Zhong et al., 2009, Chen, 2011, Nieto-Bona et al., 2011b). Comparing the results between baseline and after one month of treatment, central corneal thinning ranged between 3 – 16 µm (Nichols et al., 2000, Alharbi & Swarbrick, 2003, Owens et al., 2004, Chen, 2011, Nieto-Bona et al., 2011b). Our findings fit well into the reported range.

Corneal stiffness did not undergo any significant changes throughout the study period. As discussed in Section 4.5, corneal stiffness measurement is dependent on the physical properties of the cornea (e.g. thickness, radius and elasticity) and IOP. It was speculated that flattening and thinning of the cornea would lead to a lower corneal stiffness; however, statistically insignificant changes of corneal stiffness were detected. Underestimation of IOP from applanation tonometry or non-contact tonometry is expected due to modification of corneal geometry by ortho-k (Ishida et al., 2011, Chang et al., 2013). As a result, the GAT IOP showed significant reduction across the lens wearing period. Interestingly, no studies have reported changes of IOPcc during ortho-k treatment. The IOPcc showed little reduction which was statistically insignificant. The use of strict control of diurnal variation in the experimental design, has revealed that the true IOP is unlikely to vary by the corneal reshaping therapy in these healthy and young subjects. Thus the effect of IOP on corneal stiffness could be minimal.

The influence of corneal reshaping therapy on corneal biomechanics remains unclear. From the microstructural view, the biomechanical contribution of the cornea is dominated by the stroma which contains lamellae of collagen fibrils and extracellular matrix (discussed in Section 1.1). Hence, corneal biomechanical changes could be induced accompanying alteration of cornea stromal components. In short-term ortho-k, Alharbi and Swarbrick (2003) found no change in stromal thickness at the central cornea, but stromal thickening (10.9 ± 5.9 µm) was present at the mid-peripheral cornea. Following longer wear, Nieto-Bona et al. (2011a) observed stromal thickening of around 3 % in the central cornea, although Zhong et al. (2009) reported stable central stromal thickness.

Some clinical studies concluded the reduction of total corneal thickness was mostly as a result of epithelial thinning (Soni et al., 2003, Nieto-Bona et al., 2011b). In the cellular level, research is limited. Nieto-Bona et al. (2011b) reported an increased number of keratocytes in the stroma, but Zhong and colleagues (2009) reported a decrease in cell number. Structural modification of stromal collagen fibrils in ortho-k has not been investigated. Existing microstructural information is insufficient to suggest corneal biomechanical alteration resulting from ortho-k treatment.

We attempted to derive the corneal tangent modulus using corneal stiffness, thickness, and curvature data acquired at different stages of the treatment. A substantial increase in the corneal tangent modulus from baseline to 1 month of lens wear was observed. However increased modulus values after commencement of treatment should be interpreted with caution. Due to the lack of evidence regarding the corneal stromal changes in ortho-k, it was unclear what constituted changes of corneal tangent modulus within the treatment period.

Results from ORA revealed a decreasing trend of CRF across the treatment period, but CH remaining stable. There are few clinical studies on the corneal biomechanical changes in ortho-k. These have reported CRF reduced by less than 7.2% after 1 month of lens wear (Mao et al., 2010, Chen, 2011, Yeh et al., 2013, Chen, 2014). However, the mechanical meaning of CRF remains unclear. The CRF is heavily weighted by CCT (Luce, 2006, Shah et al., 2006, Touboul et al., 2008), and hence the reduction of CRF may be partly explained by the reduction of CCT in ortho-k. Due to the lack of microstructural and mechanical evidence, more experimental and clinical work is needed to elucidate the corneal biomechanical changes in ortho-k treatment.

As ortho-k involves corneal deformation when the corneal tissue is subject to a compressive force under a reverse geometry lens, it has become important to determine the corneal response from a biomechanical perspective. During short-term ortho-k with a controlled target reduction (i.e. same compressive force exerted), inter-subject variation of the corneal response, in terms of curvature and thickness changes, was observed in

subjects with similar age and between different age groups (Jayakumar & Swarbrick, 2005, Lu et al., 2008, Villa-Collar et al., 2009). Correspondingly, it appears that pre-treatment corneal biomechanics could play a role in corneal reshaping. In a single and small sample study, González-Méijome and colleagues (2008b) found that greater pre-treatment CH was associated with less corneal topographic and pachymetric changes and hypothesized that corneas with higher resistance would respond and recover more slowly. However, a higher CH value does not necessarily represent higher corneal resistance (Roberts, 2014). The CH and CRF do not accurately predict corneal changes in ortho-k, as demonstrated in a later study (Glavine, 2009).

The predictive value of the ortho-k response using baseline corneal tangent modulus was found to be limited in the current study, because changes of corneal curvature depend on different refractive targets (Mountford, 1997, Soni et al., 2003, Villa-Collar et al., 2009, Chan et al., 2010) which confounds the corneal biomechanical effect. It is necessary to confine the target reduction of ortho-k and conduct studies involving larger sample sizes in order to elucidate the mechanisms involved.

5.6 Conclusion

One-month orthokeratology showed insignificant changes in corneal stiffness and increased corneal tangent modulus in a group of healthy young adults. Measurement of corneal tangent modulus deserves more attention because it signifies a different biomechanical implication than the ORA-derived corneal viscoelastic parameters. Further study is warranted to investigate whether corneal tangent modulus is predictive of successful corneal reshaping. Clinically, it is useful to offer an additional tool for patient screening for suitability of corneal reshaping therapy and effective intervention for arresting myopia progression.

Conference presentation:

Lam, A. K., Hon, Y., Wong, C. K., Tse, S. H., Chen, G. Z., Lu, S. H., Lam, D. C. Short-term orthokeratology on corneal tangent elastic modulus – a pilot study. ARVO Annual Meeting 2016, Seattle, USA. Poster presentation.

Chapter 6

Corneal stiffness measurement at different corneal locations

6.1 Introduction

Clinical interest regarding corneal disease diagnosis and treatment should not be limited to the central corneal area (Li et al., 2008, Jinabhai et al., 2011, Lam et al., 2015). Localized corneal biomechanical alterations may be more sensitive than geometrical changes in detecting a diseased cornea (Roberts & Dupps, 2014).

It has recently become possible to measure corneal biomechanics *in vivo* (Luce, 2005, Ambrósio Jr et al., 2013). Devices such as the ORA and the Corvis ST are basically modified pneumotonomers that record moments of applanation and quantify deformation responses at the corneal centre. Regional corneal biomechanical properties have been investigated in *in vitro* experiments (Reichel et al., 1989, Hjortdal, 1996, Shin et al., 1997, Sloan et al., 2014), but cannot be assessed by existing clinical devices.

The newly developed CID provides a way to measure scleral biomechanics (Leung et al., 2014). The device has the potential to measure corneal biomechanics at different corneal locations due to its direct working principle and flexibility in device alignment.

The present study aimed to investigate the feasibility of corneal stiffness measurement at the peripheral cornea in human subjects, which was defined as 3mm from the temporal limbus. Peripheral corneal measurements were performed when subjects separately maintained primary and nasal gazes. Central corneal measurement was also measured for comparison.

6.2 Methodology

6.2.1 Subjects

Twenty-five healthy young adults (14 male and 11 female) with mean ± standard deviation (SD) age of 22.8 ± 1.3 years were recruited (range 21 to 26 years). All subjects

had unremarkable general and ocular health. Exclusion criteria included Goldmann applanation tonometry ≥ 21 mmHg, rigid lens wear, current pregnancy, history of refractive surgery or eye disease, and use of long-term eye or oral medications. Soft lens wearers were required to cease contact lens wear for at least 24 hours before the data taking. All procedures followed the Declaration of Helsinki and the protocol was reviewed and approved by the ethics review board of The Hong Kong Polytechnic University. Informed consent was obtained from each subject before the commencement of the study.

6.2.2 Procedures

Data was collected at a single visit. Noncontact procedures were conducted before contact procedures. Corneal thickness and radius of curvature both at the centre and at 3 mm from the temporal limbus were measured using available clinical instruments, in a random order. The corneal thickness profile was captured using anterior segment optical coherence tomography (AS-OCT; Casia SS-1000, Tomey, Japan). Both the "3D Corneal Map" scan and the "2D Anterior Segment" scan were used for data collection. Three automated measurements were obtained using each scan mode while the subject focused on a central target inside the instrument. The corneal thickness at the vertex was directly read from the measurement output of the Corneal Map and was denoted as the central corneal thickness (CCT). Corneal radius profile was imaged using corneal topography (Medmont E300, Medmont Pty Ltd., Australia). Three topography images with scores higher than 95 were captured while the subject looked into the centre of the ring pattern inside the instrument. Central mean corneal radius (meanK) was calculated from averaging the simulated flattest and steepest keratometry readings in each image. Measurements of temporal corneal thickness and radius of curvature are described in Section 6.2.3.

Corneal stiffness measurement using the CID was conducted after the abovementioned noncontact procedures. Following corneal anaesthesia with one drop of 0.4 % Benoxinate, corneal stiffness was measured at central and peripheral corneal locations. During the central corneal measurement ($Stiff_{cent}$), the subject was instructed to look

straight ahead and fixate on an external target. The measurement was carried out at the corneal geometric centre (Figure 6.1a). Peripheral corneal measurement was conducted using two protocols. In the first protocol (Figure 6.1b), the CID was placed at the temporal side of subject's eye while the subject looked straight ahead. The CID was positioned by the practitioner such that the indentation probe was normal to the corneal surface. The location of measurement was 3 mm from the temporal limbus. This was achieved by placing the CID probe (2 mm in diameter) at the temporal cornea away from the limbus at 1-probe size. The "3 mm from the temporal limbus" refers to the distance from the temporal limbus to the centre of the CID probe ($Stiff_{prim}$). In the second protocol (Figure 6.1c), the CID was aligned with the slit-lamp unit while the illumination system was placed at the nasal side of subject's eye. The distance between the CID and the illumination system was fixed. The subject was instructed to look nasally and fixate on a target on the illumination system. The location of measurement was the same as in the first protocol, despite the difference in direction of gaze ($Stiff_{nasal}$).

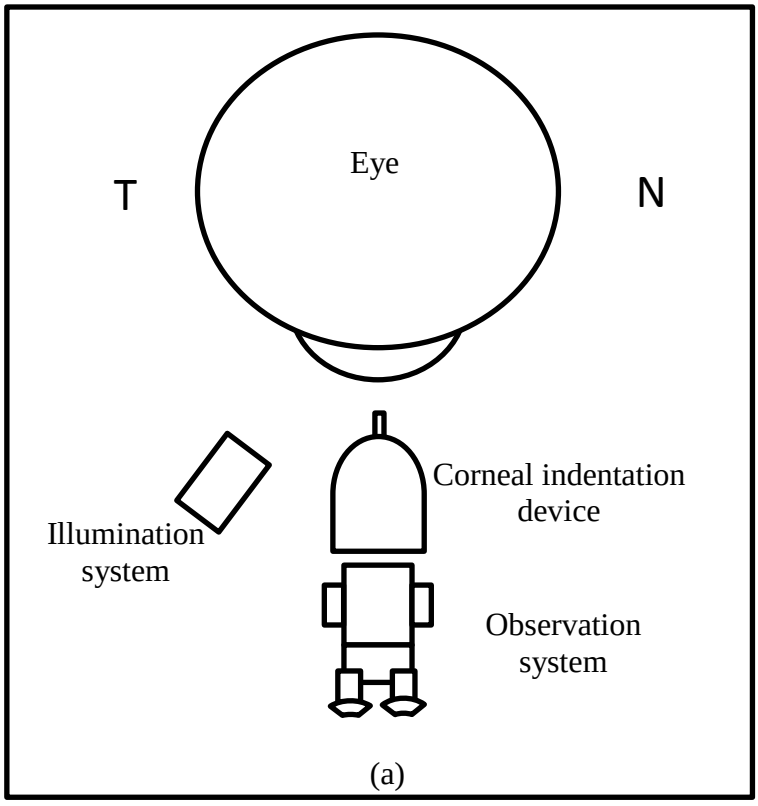
Eye
T
N
Illumination system
Corneal indentation device
Observation system

(a)

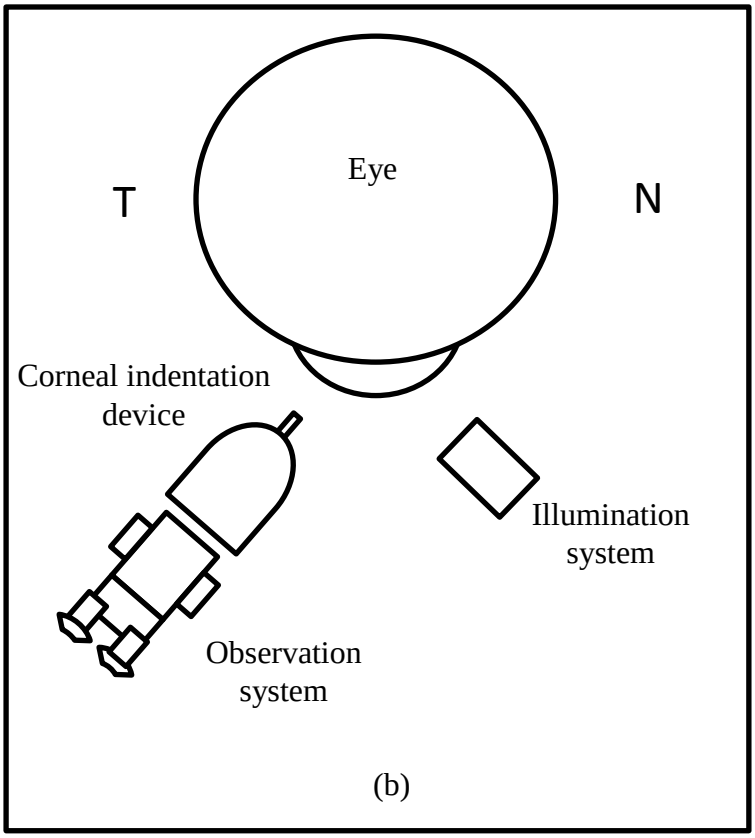
Eye
T
N
Corneal indentation device
Illumination system
Observation system

(b)

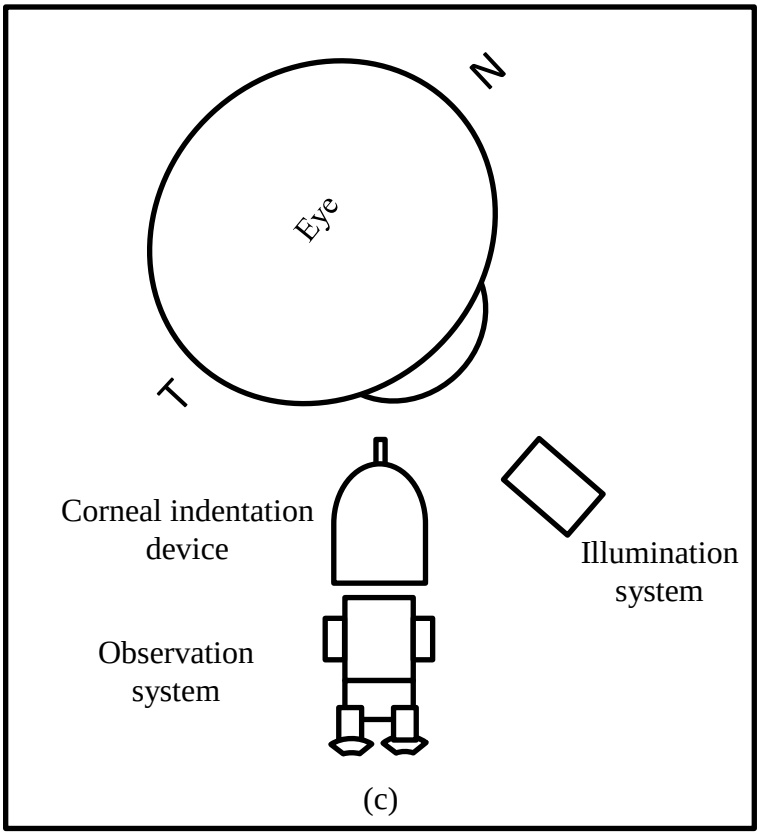

Figure 6.1 Schematic representations of corneal stiffness measurements at different corneal locations. The corneal indentation device was seated on a slit-lamp unit. **(a)** Central corneal stiffness was measured at the corneal geometric centre while the subject looked straight ahead. **(b)** Peripheral corneal stiffness was measured at 3 mm from the temporal limbus while the subject looked straight ahead. **(c)** Peripheral corneal stiffness was measured at 3 mm from the temporal limbus while the subject looked towards the nasal side. T, temporal; N, nasal.

The contact measurements, $Stiff_{cent}$, $Stiff_{prim}$ and $Stiff_{nasal}$ were performed in random order. Three valid readings were taken for each method. Consecutive readings were averaged for statistical analysis. Both eyes were measured.

6.2.3 Measurements of peripheral corneal thickness and radius of curvature

Both $Stiff_{prim}$ and $Stiff_{nasal}$ were measured at 3 mm from the temporal limbus. At the location of indentation, corneal thickness and radius of curvature were also retrieved for subsequent analysis (Appendices).

In the AS-OCT, a front view of the anterior eye was captured from the measurement output of a "2D Anterior Segment" scan. The temporal limbus was visible and could be located using the scale bar along the x-axis of the image (Appendix A). Upon locating the limbus, a "2D Analysis" button was clicked on the tool bar where a horizontal cross-sectional image of the anterior segment of an eye was displayed (Appendix B). The limbus was located using the same scale bar along the x-axis of the image. A 3-mm chord from the limbus towards the central cornea was drawn using a ruler tool, which indicated the location of corneal indentation from the CID. The shortest horizontal distance between the limbus and the indentation location was measured. Subsequently, the pachymetry map from a "3D Corneal Map" scan was selected where the temporal limbus was again visible (Appendix C). The ruler tool was applied to find the location of corneal indentation using the shortest horizontal distance measured from the 2D image. Corneal thickness at 3 mm from the temporal limbus (PCT) was read from the pachymetry map.

Peripheral corneal radius of curvature was obtained using a topography image from the Medmont topographer. A tangential curvature map was selected (Appendix D). Similarly, a ruler was used to locate the site of corneal indentation by using the shortest horizontal distance measured from the 2D image in the AS-OCT. The corneal radius of curvature at 3 mm from the temporal limbus (K_p) was read from the topography map.

6.3 Statistical analysis

Statistical analyses and graphics were performed using SPSS (version 18.0, SPSS, Inc., USA). Statistical power was computed using G-power (version 3.1.7, Franz Faul, Universität Kiel, Germany). The level of significance chosen was 5 %. The distributions of all physical parameters of the cornea were not significantly different from normal distribution (Shapiro-Wilk tests, $p > 0.05$). Hence, parametric statistical tests were used to analyze the data.

Between-eye differences in all measured parameters were tested using paired sample t-tests. Data in right eyes were selected for analysis when no between-eye differences were present. Paired sample t-tests were performed to compare the differences in corneal geometry measured centrally and peripherally. Repeated measures analyses of variance (RMANOVAs) were used to compare the differences of $Stiff_{cent}$, $Stiff_{prim}$ and $Stiff_{nasal}$. Whenever significant differences were found, post-hoc comparisons were conducted with Bonferroni adjustment.

6.4 Results

There was no significant between-eye difference in CCT, PCT, meanK, K_p, $Stiff_{cent}$, $Stiff_{prim}$ and $Stiff_{nasal}$, so only the right eye results were used for analysis (Table 6.1). The mean spherical equivalent refractive error in the right eyes was -3.73 ± 2.10 D.

Table 6.1 Between-eye comparison of ocular parameters for 25 subjects. The results are presented as mean ± standard deviation.

Parameter	**Right eye**	**Left eye**	**Paired t-test**	
Central corneal thickness (μm)	536.7 ± 36.7	538.9 ± 35.6	t = -1.44,	p = 0.16
Peripheral corneal thickness (μm)	625.6 ± 36.3	620.4 ± 36.4	t = 2.06,	p = 0.05
Mean corneal radius (mm)	7.86 ± 0.25	7.86 ± 0.24	t = -0.20,	p = 0.85
Peripheral corneal radius (mm)	8.41 ± 0.26	8.45 ± 0.24	t = -1.15,	p = 0.26
Central corneal stiffness (Nmm^{-1})	0.07 ± 0.0065	0.068 ± 0.0068	t = 1.63,	p = 0.12
Peripheral corneal stiffness in primary gaze (Nmm^{-1})	0.074 ± 0.0074	0.072 ± 0.0087	t = 1.30,	p = 0.21
Peripheral corneal stiffness in nasal gaze (Nmm^{-1})	0.0803 ± 0.0067	0.079 ± 0.011	t = 0.38,	p = 0.71

Peripheral corneal measurements were conducted at 3 mm from temporal limbus.

Corneal thickness and radius of curvature were significantly different between the central and peripheral regions. The corneal geometry was found to be thicker (t = -29.05, p < 0.001) and flatter (t = -13.01, p < 0.001) at the temporal periphery. The mean central corneal stiffness was 0.070 Nmm^{-1}. The mean peripheral corneal stiffness was 0.074 Nmm^{-1} and 0.080 Nmm^{-1} when the subjects maintained primary gaze and nasal gaze, respectively. Significant differences were observed in corneal stiffness measurements (RMANOVA, p < 0.001). In primary gaze, peripheral readings ($Stiff_{prim}$) were significantly higher than the central readings ($Stiff_{cent}$) (paired t-test with Bonferroni adjustment, p = 0.019). In respect of peripheral measurements, significantly higher stiffness was observed in nasal gaze ($Stiff_{nasal}$) than in primary gaze ($Stiff_{prim}$) (paired t-test with Bonferroni adjustment, p = 0.007).

With an observed sample effect size of 0.96 and correlation of 0.4 among repeated measures on corneal stiffness, 100 % power was achieved with alpha at 0.05 when sphericity was assumed.

6.5 Discussion

Use of recently introduced specialized imaging devices allows straightforward mapping of corneal thickness and radius of curvature. The Casia AS-OCT provides high-resolution, cross-sectional images of the anterior segment without contacting the ocular surface. It is equipped with several scan types depending on the purpose of measurement. Central and peripheral corneal thickness was acquired from a pachymetry map which was generated using automated corneal topography scan. Several studies have evaluated CCT measurements using various clinical devices (Nakagawa et al., 2011, Szalai et al., 2012, Fukuda et al., 2013, Kumar et al., 2015, Lee et al., 2015). Overall, the Casia AS-OCT provided more consistent measurements and a higher rate of successful acquisitions than Scheimpflug imaging in both normal and keratoconic eyes. Neri et al. (2012) reported excellent repeatability for the entire pachymetry map using the Casia AS-OCT, including central, paracentral, and peripheral zones. The corneal curvature map, however, received little attention. Central and peripheral corneal radius of curvature was acquired using the Medmont corneal topography as it provides accurate and reliable measurement of corneal shape (Tang et al., 2000, Cho et al., 2002).

Conforming to normal corneal architecture, the human cornea becomes thicker and flatter from centre to periphery. These geometrical variations contribute to the heterogeneity of corneal biomechanical properties. Applying a novel corneal indentation technique, a higher corneal stiffness was obtained in the peripheral cornea compared with the central area. Although it is expected that a thicker or steeper material is more difficult to deform than a thinner or flatter one, corneal indentation could be more influenced by changes in thickness than radius, resulting in a higher stiffness measurement. Apart from the geometrical factors, the corneal boundary may also affect corneal stiffness measurement. Corneal indentation was performed at 3 mm from the limbus in the current study. According to Roark's formula (Young & Budynas, 2002), deformation due to indentation of a partial spherical shell by a concentrated force is not effected when the boundary is around 2 mm or more from the site of indentation. Moreover, with an indentation probe as small as 2 mm and the presence of flexible boundaries without a distinct transition (i.e. limbus and sclera), the effect on stiffness measurement could be reduced. Nevertheless,

more experimental work is required to further investigate the influence of corneal boundary on peripheral corneal biomechanics measurements.

Peripheral corneal stiffness increased further in nasal gaze. The extraocular muscles create an external force on the eye globe in different directions of gaze. During adduction, contraction of the medial rectus is accompanied by relaxation of the lateral rectus. However, tonic contraction of the lateral rectus and its stretching force at the muscle insertion, which is located about 6.9 mm from the corneal limbus (Millodot 2009), could stress the scleral tissue resulting in an increased corneal stiffness at the temporal region. Hence, in an attempt to measure corneal biomechanics using the CID at regions other than the central cornea, practitioners should take the direction of fixation into account in order to eliminate unwanted effects from muscle force.

As discussed in Section 1.4.3.1, corneal hysteresis and corneal resistance factor determined by the ORA cannot discriminate keratoconus (KC) or suspected KC from normal eyes due to the wide overlap in their values (Ortiz et al., 2007, Shah et al., 2007, Kirwan et al., 2008, Fontes et al., 2011a). It is hypothesized that localized reduction of corneal thickness and radius of curvature in KC could be secondary signs occurring due to an initial and localized reduction in elastic modulus (tissue weakening) (Roberts & Dupps, 2014). Thus central corneal biomechanical measurements might not be helpful in characterizing corneal diseases which affect the eccentric corneal region, such as keratoconus. A preliminary investigation using a mechanical imaging method called Brillouin light-scattering has been described (Scarcelli et al., 2012) in an attempt to illustrate the spatial variations of Brillouin modulus in KC corneas (Scarcelli et al., 2015). On the other hand, it is interesting to note that rebound tonometry demonstrated less reduction in IOP after LASIK when it was performed at the peripheral cornea (Lam et al., 2015). These readings after LASIK with corneal collagen crosslinking remained similar compared to those taken pre-LASIK (Lam et al., 2015). With increasing popularity of corneal refractive surgeries, conventional tonometry for glaucoma screening and management is less accurate because of the measurement error induced by an alteration of corneal properties at the central region (Ortiz et al., 2007, Pepose et al., 2007, Chen et

al., 2008). Corneal biomechanics outside the treatment zone might be preserved in the surgical process and thus peripheral tonometry might give a more predictable preoperative IOP. It would be ideal if corneal biomechanics could be measured at various corneal locations accompanied with peripheral tonometry.

The current study compared corneal stiffness, the direct force-displacement responses, between central and peripheral corneal locations. However, derivation of corneal tangent modulus in the peripheral region was not comparable to that in the central region because an asymmetry of surrounding corneal geometry violated one of the assumptions for Equation 4.7. More work should be done to deduce the status of corneal tangent modulus in the peripheral region. Peripheral corneal measurements were limited at the temporal cornea in the current study. Practitioner should be aware of the effect from direction of gaze in peripheral corneal measurements. In early years, techniques for measuring regional elastic modulus of the cornea included strip extensiometry and pressure inflation (Reichel et al., 1989, Hjortdal, 1996). Experimental results varied and were affected by methodology utilized. Corneal indentation is a technique that can be applied in clinical setting.

6.6 Conclusion

The current study demonstrated the feasibility of the CID to measure corneal stiffness at the peripheral cornea. The increased stiffness from corneal centre to periphery, during primary gaze and nasal gaze fixations could be considerably affected by tissue thickening. Stretching of extraocular muscles away from primary gaze position could induce unexpected changes in corneal stiffness at the peripheral cornea.

Chapter 7 Summary and future work

7.1 Summary

This study has applied and evaluated new clinical devices for corneal biomechanical measurement *in vivo*.

In Chapter 2, repeatability of the Corneal Visualization Scheimpflug Technology (Corvis ST) for corneal biomechanical measurement was evaluated in normal subjects. Of eight customized corneal deformation parameters, only deformation amplitude and the time to first applanation demonstrated clinically acceptable repeatability. The Corvis ST uses the captured images from a Scheimpflug camera to derive corneal deformation parameters. Poor image quality could contribute to substantial measurement variability. Other limitations are also present. For example, standard assessment of mechanical properties, such as stress and strain, could not be achieved by air puff indentation. Moreover, the Corvis measurements are restricted to the central cornea. A novel measurement method to overcome these limitations would be valuable.

In Chapter 3, repeatability and diurnal variation of a novel corneal indentation device (CID) for corneal biomechanical measurement was evaluated in normal subjects. Corneal stiffness and tangent (elastic) modulus, as obtained by the CID, demonstrated good repeatability and minimal diurnal variation. Upon a direct working principle to measure the force (related to stress) and displacement (related to strain) on the cornea, the CID provides a standard measure of the elastic properties of the cornea in terms of tangent modulus. The CID is an alternative device for *in vivo* corneal biomechanical evaluation. Further investigation is recommended to explore the clinical usefulness of corneal tangent modulus measurement on different aspects such as age and ocular diseases.

In Chapter 4, a clinical study was conducted to compare the difference of corneal tangent modulus in low and high myopes. The IOP-dependence of corneal tangent modulus was demonstrated. Because high myopes were presented with a significantly higher IOP, between-group comparison could only be achieved when individual corneal tangent

modulus was normalized to IOP of normal eyes (such as 15.5 mmHg). A significantly lower corneal tangent modulus was revealed in the high myopia group. Myopia development is associated with a thinner and mechanically weakened sclera. The corneas of high myopes could also be considered mechanically weakened. Due to the inherent continuity between cornea and sclera, corneal tangent modulus might serve as an index for the strength of the scleral coat.

In Chapter 5, a pilot study was conducted to investigate the effect of one-month orthokeratology on corneal stiffness and corneal tangent modulus. Corneal stiffness did not show significant changes during the treatment period and after lens cessation. It could be the result of an equilibrium of forces exerted onto the cornea despite the alteration of corneal geometry during corneal reshaping. However, an increase of corneal tangent modulus was observed during the treatment period which might indicate an increase of intrinsic stiffness of the corneal tissue. More experimental work is needed to support this clinical observation. Upon lens cessation, corneal tangent modulus showed no significant difference to its baseline value. In view of the popularity of orthokeratology, it may be worthwhile to study if corneal stiffness or corneal tangent modulus has any predictive value for successful orthokeratology treatment.

In Chapter 6, the feasibility of the CID for corneal biomechanical measurement at peripheral cornea was demonstrated. A higher corneal stiffness was obtained in the peripheral cornea (3 mm from the temporal limbus) compared with the central one during central fixation, attributing to tissue thickening at the peripheral cornea. Peripheral corneal stiffness increased further when subjects looked towards the nasal side, which might be the result of additional stress exerted by the recti muscles. Therefore, it is recommended to maintain central fixation during peripheral measurement of corneal biomechanics. More work should be done to deduce the status of corneal tangent modulus at the peripheral cornea.

7.2 Future work

The corneal indentation device (CID) is a new tool which provides standard measurement of corneal biomechanical properties *in vivo*. The current study results enable better understanding of corneal biomechanical behavior in normal eyes.

The current CID prototype is designed to take single measurement of corneal tangent modulus at specific IOP and specific loading rate. To enhance its clinical or research usefulness, it is ideal to obtain a complete corneal deformation response under different loading rates. A complete characterization of corneal biomechanics could provide valuable information for exploring disease development such as keratoconus and improving surgical outcomes such as corneal refractive surgeries. Due to the flexibility in device alignment, the CID could also be applied to measure scleral biomechanics, which is speculated to be more relevant to development of myopia and glaucoma.

In the meantime, a long-term clinical study has been commenced to investigate the predictive value of corneal tangent modulus for corneal response in orthokeratology. It is hoped that the CID can offer an additional tool to aid patient screening for suitability of orthokeratology.

Appendices

Measurement of peripheral corneal thickness at 3 mm from temporal limbus

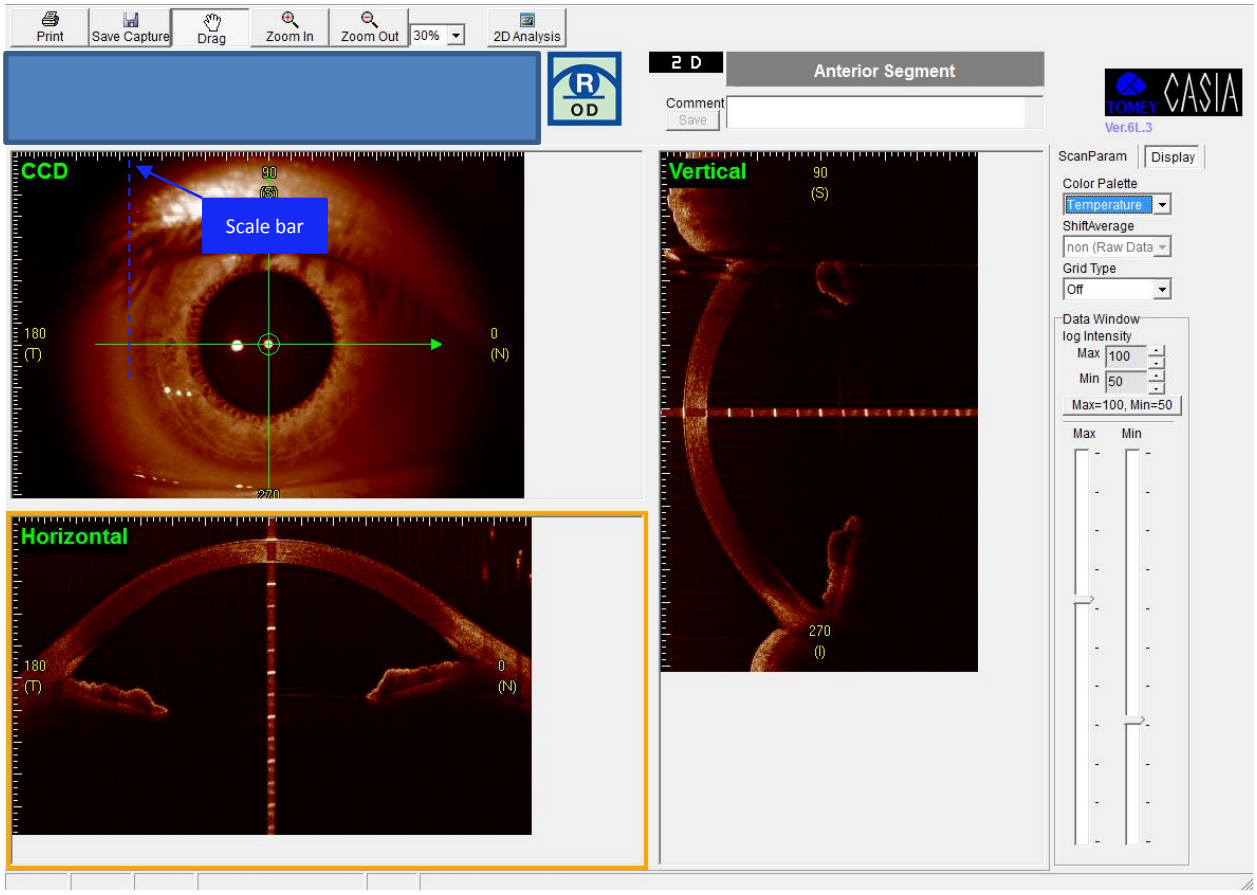

Appendix A Main viewer screen from a "2D Anterior Segment" scan in the AS-OCT. An infrared image is shown in the top left corner. The visible temporal limbus (*blue dash line*) was located using a scale bar.

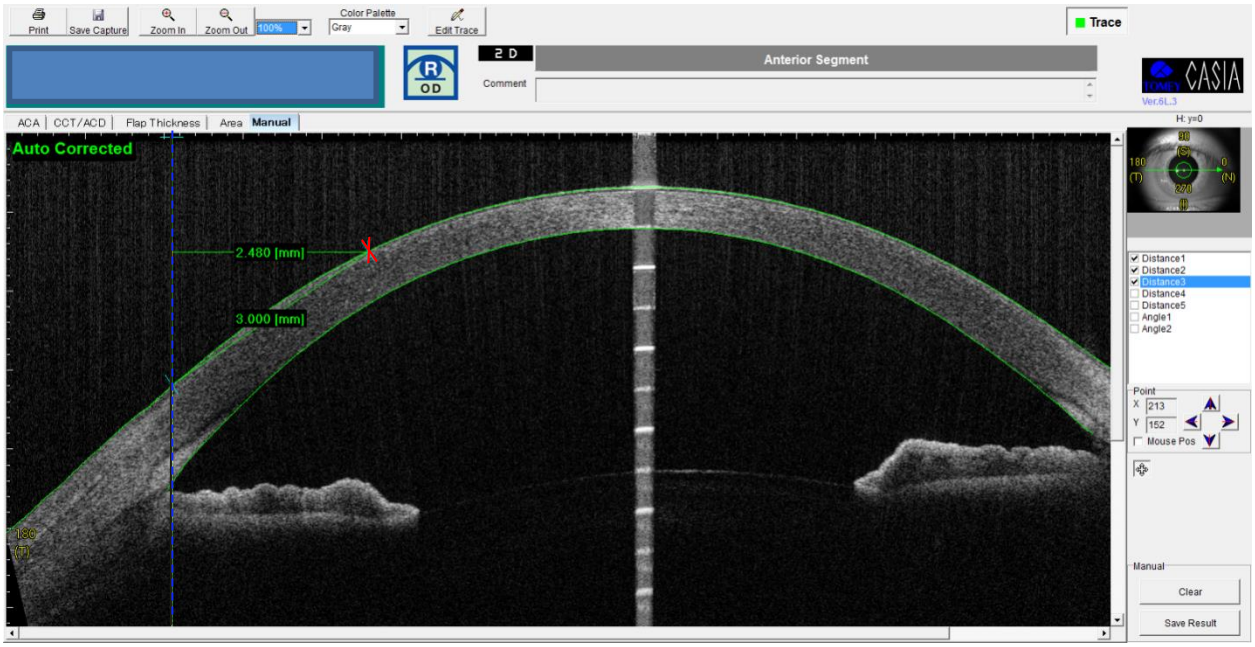

Appendix B "2D Analysis" screen from a "2D Anterior Segment" scan in the AS-OCT. A horizontal cross-sectional image of the anterior segment of an eye is shown. The temporal limbus was re-located using the scale bar (*blue dash line*). A 3-mm chord from the limbus into the cornea was drawn to indicate the location of corneal indentation from the CID (*red cross*). The shortest horizontal distance from the limbus to the indentation location was measured as 2.48 mm.

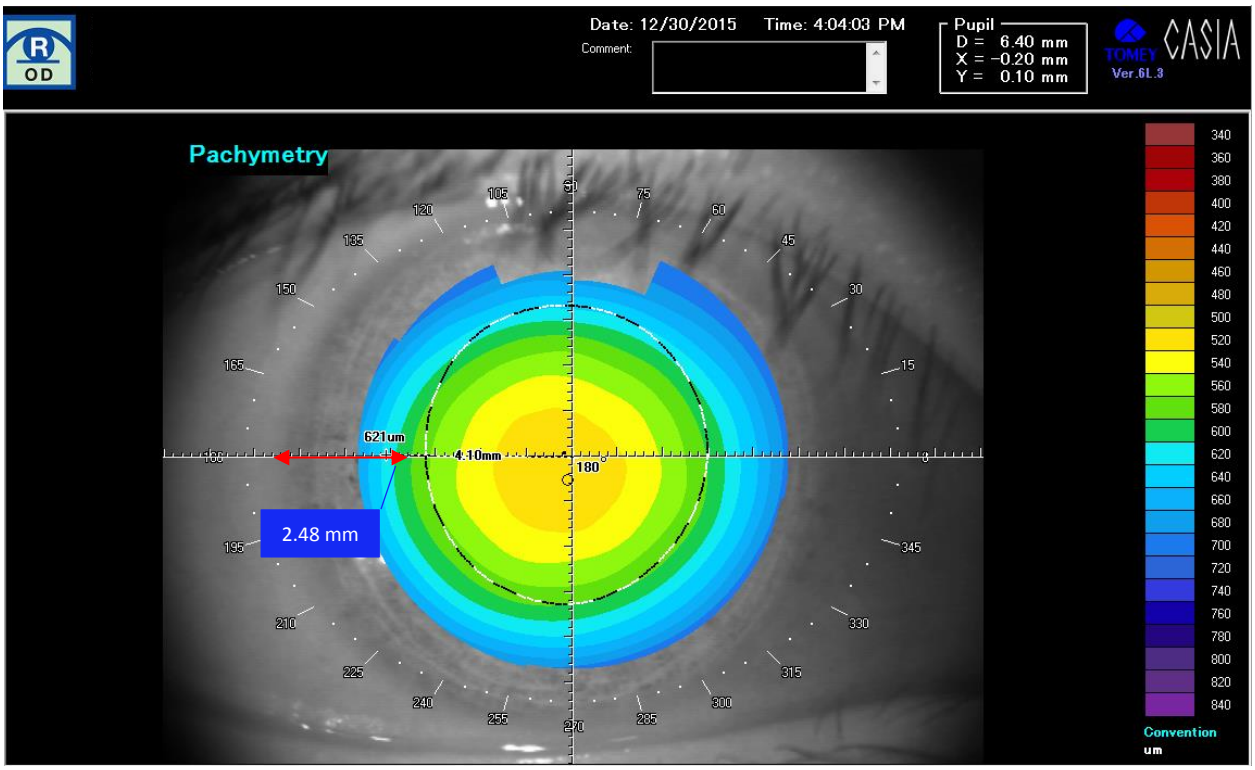

Appendix C A single pachymetry map from a "3D Corneal Map" scan in the AS-OCT. Peripheral corneal thickness at the location of corneal indentation was obtained by measuring 2.48 mm from the visible temporal limbus towards the central cornea using distance measurement function. The current example shows a peripheral corneal thickness of 621 µm measured 2.48 mm from the temporal limbus.

Measurement of peripheral corneal radius of curvature at 3 mm from temporal limbus

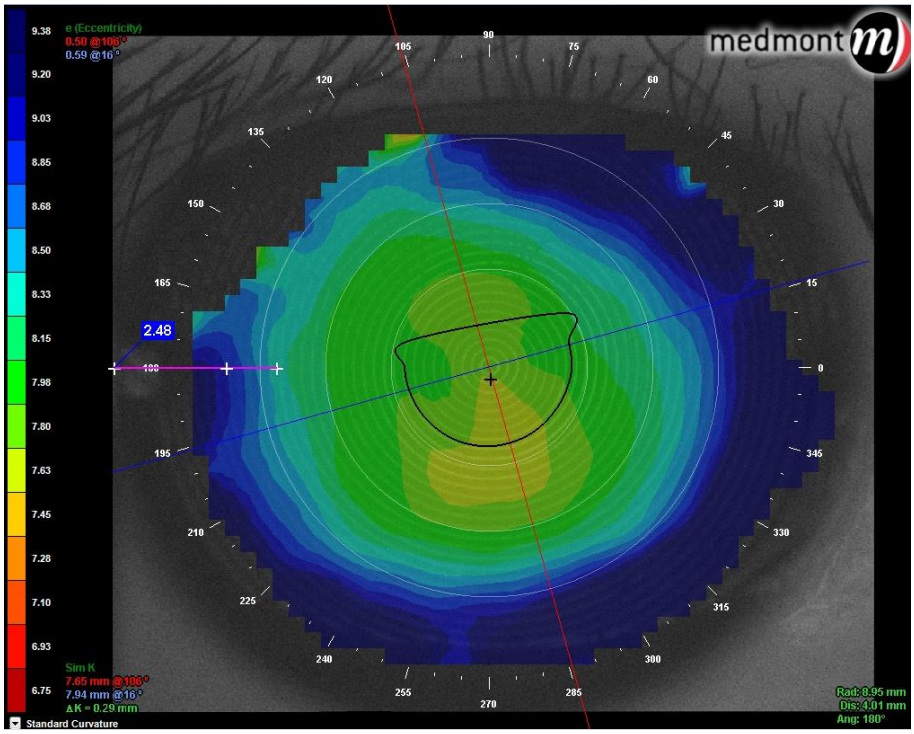

Appendix D A single tangential curvature map from Medmont topography. Peripheral corneal radius of curvature at the location of corneal indentation was obtained by measuring 2.48 mm from the visible temporal limbus into the cornea using ruler annotation. The value is shown inn bottom right corner. The peripheral corneal radius is 8.95 mm in this example.

References

Ahearne, M., Yang, Y., Then, K. Y. & Liu, K. K. 2007. An indentation technique to characterize the mechanical and viscoelastic properties of human and porcine corneas. *Ann Biomed Eng,* 35**,** 1608-16.

Alguire, P. C. 1990. Tonometry. *In:* Walker, H. K., Hall, W. D. & Hurst, J. W. (eds.) *Clinical Methods: The History, Physical, and Laboratory Examinations.* 3rd ed. Boston.

Alhamad, T. A. & Meek, K. M. 2011. Comparison of factors that influence the measurement of corneal hysteresis in vivo and in vitro. *Acta Ophthalmol,* 89**,** e443-50.

Alharbi, A. & Swarbrick, H. A. 2003. The effects of overnight orthokeratology lens wear on corneal thickness. *Invest Ophthalmol Vis Sci,* 44**,** 2518-23.

Ali, N. Q., Patel, D. V. & McGhee, C. N. 2014. Biomechanical responses of healthy and keratoconic corneas measured using a noncontact scheimpflug-based tonometer. *Invest Ophthalmol Vis Sci,* 55**,** 3651-9.

AlMubrad, T. M. & Ogbuehi, K. C. 2008. The effect of repeated applanation on subsequent IOP measurements. *Clin Exp Optom,* 91**,** 524-9.

Alonso-Caneiro, D., Karnowski, K., Kaluzny, B. J., Kowalczyk, A. & Wojtkowski, M. 2011. Assessment of corneal dynamics with high-speed swept source optical coherence tomography combined with an air puff system. *Opt Express,* 19**,** 14188-99.

Altan, C., Demirel, B., Azman, E., Satana, B., Bozkurt, E., Demirok, A. & Yilmaz, O. F. 2012. Biomechanical properties of axially myopic cornea. *Eur J Ophthalmol,* 22 Suppl 7**,** S24-8.

Ambrósio Jr, R., Ramos, I., Luz, A., Faria, F. C., Steinmueller, A., Krug, M., Belin, M. W. & Roberts, C. J. 2013. Dynamic ultra high speed Scheimpflug imaging for assessing corneal biomechanical properties. *Revista Brasileira de Oftalmologia,* 72**,** 99-102.

Ambrosio, R., Jr., Dawson, D. G., Salomao, M., Guerra, F. P., Caiado, A. L. & Belin, M. W. 2010. Corneal ectasia after LASIK despite low preoperative risk: tomographic and biomechanical findings in the unoperated, stable, fellow eye. *J*

Refract Surg, 26**,** 906-11.

Ambrosio, R., Jr. & Randleman, J. B. 2013. Screening for ectasia risk: what are we screening for and how should we screen for it? *J Refract Surg,* 29**,** 230-2.

Anand, A., De Moraes, C. G., Teng, C. C., Tello, C., Liebmann, J. M. & Ritch, R. 2010. Corneal hysteresis and visual field asymmetry in open angle glaucoma. *Invest Ophthalmol Vis Sci,* 51**,** 6514-8.

Andreassen, T. T., Simonsen, A. H. & Oxlund, H. 1980. Biomechanical properties of keratoconus and normal corneas. *Exp Eye Res,* 31**,** 435-41.

Ang, G. S., Bochmann, F., Townend, J. & Azuara-Blanco, A. 2008. Corneal biomechanical properties in primary open angle glaucoma and normal tension glaucoma. *J Glaucoma,* 17**,** 259-62.

Ang, R. T., Dartt, D. A. & Tsubota, K. 2001. Dry eye after refractive surgery. *Curr Opin Ophthalmol,* 12**,** 318-22.

Asaoka, R., Nakakura, S., Tabuchi, H., Murata, H., Nakao, Y., Ihara, N., Rimayanti, U., Aihara, M. & Kiuchi, Y. 2015. The Relationship between Corvis ST Tonometry Measured Corneal Parameters and Intraocular Pressure, Corneal Thickness and Corneal Curvature. *PLoS One,* 10**,** e0140385.

Ayala, M. & Chen, E. 2012. Measuring corneal hysteresis: threshold estimation of the waveform score from the Ocular Response Analyzer. *Graefes Arch Clin Exp Ophthalmol,* 250**,** 1803-6.

Bak-Nielsen, S., Pedersen, I. B., Ivarsen, A. & Hjortdal, J. 2015. Repeatability, reproducibility, and age dependency of dynamic Scheimpflug-based pneumotonometer and its correlation with a dynamic bidirectional pneumotonometry device. *Cornea,* 34**,** 71-7.

Bayoumi, N. H., Bessa, A. S. & El Massry, A. A. 2010. Ocular response analyzer and goldmann applanation tonometry: a comparative study of findings. *J Glaucoma,* 19**,** 627-31.

Bland, J. M. 2010. *How can I decide the sample size for a repeatability study?* [Online]. Available: https://www-users.york.ac.uk/~mb55/meas/sizerep.htm [Accessed 20 Feb, 2016].

Bland, J. M. & Altman, D. G. 1986. Statistical methods for assessing agreement

between two methods of clinical measurement. *Lancet,* 1**,** 307-10.

Bland, J. M. & Altman, D. G. 1996. Measurement error. *BMJ,* 313**,** 744.

Bochmann, F., Ang, G. S. & Azuara-Blanco, A. 2008. Lower corneal hysteresis in glaucoma patients with acquired pit of the optic nerve (APON). *Graefes Arch Clin Exp Ophthalmol,* 246**,** 735-8.

Boehm, A. G., Weber, A., Pillunat, L. E., Koch, R. & Spoerl, E. 2008. Dynamic contour tonometry in comparison to intracameral IOP measurements. *Invest Ophthalmol Vis Sci,* 49**,** 2472-7.

Bonomi, L., Mecca, E. & Massa, F. 1982. Intraocular pressure in myopic anisometropia. *Int Ophthalmol,* 5**,** 145-8.

Broman, A. T., Congdon, N. G., Bandeen-Roche, K. & Quigley, H. A. 2007. Influence of corneal structure, corneal responsiveness, and other ocular parameters on tonometric measurement of intraocular pressure. *J Glaucoma,* 16**,** 581-8.

Bueno-Gimeno, I., Espana-Gregori, E., Gene-Sampedro, A., Lanzagorta-Aresti, A. & Pinero-Llorens, D. P. 2014a. Relationship among corneal biomechanics, refractive error, and axial length. *Optom Vis Sci,* 91**,** 507-13.

Bueno-Gimeno, I., Gene-Sampedro, A., Pinero-Llorens, D. P., Lanzagorta-Aresti, A. & Espana-Gregori, E. 2014b. Corneal biomechanics, retinal nerve fiber layer, and optic disc in children. *Optom Vis Sci,* 91**,** 1474-82.

Buzard, K. A. 1992. Introduction to biomechanics of the cornea. *Refract Corneal Surg,* 8**,** 127-38.

Cankaya, A. B., Beyazyildiz, E., Ileri, D. & Ozturk, F. 2012. The effect of contact lens usage on corneal biomechanical parameters in myopic patients. *Cornea,* 31**,** 764-9.

Carbonaro, F., Hysi, P. G., Fahy, S. J., Nag, A. & Hammond, C. J. 2014. Optic disc planimetry, corneal hysteresis, central corneal thickness, and intraocular pressure as risk factors for glaucoma. *Am J Ophthalmol,* 157**,** 441-6.

Caroline, P. J. 2001. Contemporary orthokeratology. *Cont Lens Anterior Eye,* 24**,** 41-6.

Castren, J. A. & Pohjola, S. 1962. Myopia and scleral rigidity. *Acta Ophthalmol (Copenh),* 40**,** 33-6.

Chakraborty, R., Read, S. A. & Collins, M. J. 2011. Diurnal variations in axial length,

choroidal thickness, intraocular pressure, and ocular biometrics. *Invest Ophthalmol Vis Sci,* 52**,** 5121-9.

Chan, B., Cho, P. & Mountford, J. 2010. Relationship between corneal topographical changes and subjective myopic reduction in overnight orthokeratology: a retrospective study. *Clin Exp Optom,* 93**,** 237-42.

Chang, C. J., Yang, H. H., Chang, C. A., Wu, R. & Tsai, H. Y. 2013. The influence of orthokeratology on intraocular pressure measurements. *Semin Ophthalmol,* 28**,** 210-5.

Chang, P. Y., Chang, S. W. & Wang, J. Y. 2010. Assessment of corneal biomechanical properties and intraocular pressure with the Ocular Response Analyzer in childhood myopia. *Br J Ophthalmol,* 94**,** 877-81.

Chang, S. W., Tsai, I. L., Hu, F. R., Lin, L. L. & Shih, Y. F. 2001. The cornea in young myopic adults. *Br J Ophthalmol,* 85**,** 916-20.

Chee, R. I., Silva, F. Q., Ehrlich, J. R. & Radcliffe, N. M. 2013. Agreement of flicker chronoscopy for structural glaucomatous progression detection and factors associated with progression. *Am J Ophthalmol,* 155**,** 983-990 e1.

Chen, C. 2014. *Toric orthokeratology for slowing eye elongation (TO-SEE) in myopic and astigmatic children.* PhD, Hong Kong Polytechnic University.

Chen, D. 2011. *The changes of posterior corneal curvature, topographic corneal thickness and corneal biomechanical properties from overnight orthokeratology lens wear and recoveries of these parameters.* Ph.D., Hong Kong Polytechnic University.

Chen, D., Lam, A. K. & Cho, P. 2010a. Posterior corneal curvature change and recovery after 6 months of overnight orthokeratology treatment. *Ophthalmic Physiol Opt,* 30**,** 274-80.

Chen, M., Yu, M. & Dai, J. 2016. Comparison of biomechanical effects of small incision lenticule extraction and laser-assisted subepithelial keratomileusis. *Acta Ophthalmol*.

Chen, M. C., Lee, N., Bourla, N. & Hamilton, D. R. 2008. Corneal biomechanical measurements before and after laser in situ keratomileusis. *J Cataract Refract Surg,* 34**,** 1886-91.

Chen, S., Chen, D., Wang, J., Lu, F., Wang, Q. & Qu, J. 2010b. Changes in ocular response analyzer parameters after LASIK. *J Refract Surg,* 26**,** 279-88.

Chen, X., Stojanovic, A., Hua, Y., Eidet, J. R., Hu, D., Wang, J. & Utheim, T. P. 2014. Reliability of corneal dynamic scheimpflug analyser measurements in virgin and post-PRK eyes. *PLoS One,* 9**,** e109577.

Cheung, S. W. & Cho, P. 2013. Validity of axial length measurements for monitoring myopic progression in orthokeratology. *Invest Ophthalmol Vis Sci,* 54**,** 1613-5.

Cho, P. & Cheung, S. W. 2012. Retardation of myopia in Orthokeratology (ROMIO) study: a 2-year randomized clinical trial. *Invest Ophthalmol Vis Sci,* 53**,** 7077-85.

Cho, P., Lam, A. K., Mountford, J. & Ng, L. 2002. The performance of four different corneal topographers on normal human corneas and its impact on orthokeratology lens fitting. *Optom Vis Sci,* 79**,** 175-83.

Cho, P. & Lui, T. 1997. Comparison of the performance of the Nidek NT-2000 noncontact tonometer with the Keeler Pulsair 2000 and the Goldmann applanation tonometer. *Optom Vis Sci,* 74**,** 51-8.

Cohen, E. J. 2009. Keratoconus and normal-tension glaucoma: a study of the possible association with abnormal biomechanical properties as measured by corneal hysteresis (An AOS Thesis). *Trans Am Ophthalmol Soc,* 107**,** 282-99.

Congdon, N. G., Broman, A. T., Bandeen-Roche, K., Grover, D. & Quigley, H. A. 2006. Central corneal thickness and corneal hysteresis associated with glaucoma damage. *Am J Ophthalmol,* 141**,** 868-75.

Dawson, D. G., Ubels, J. L. & Edelhauser, H. F. 2011. Cornea and sclera. *In:* Levin, L. A., Nilsson, S. F. E., Ver Hoeve, J. & Wu, S. M. (eds.) *Adler's physiology of the eye.* 11th ed. London ; New York: Saunders/Elsevier.

Daxer, A., Misof, K., Grabner, B., Ettl, A. & Fratzl, P. 1998. Collagen fibrils in the human corneal stroma: structure and aging. *Invest Ophthalmol Vis Sci,* 39**,** 644-8.

de Medeiros, F. W., Sinha-Roy, A., Alves, M. R., Wilson, S. E. & Dupps, W. J., Jr. 2010. Differences in the early biomechanical effects of hyperopic and myopic laser in situ keratomileusis. *J Cataract Refract Surg,* 36**,** 947-53.

De Moraes, C. V., Hill, V., Tello, C., Liebmann, J. M. & Ritch, R. 2012. Lower corneal hysteresis is associated with more rapid glaucomatous visual field progression. *J*

Glaucoma, 21**,** 209-13.

Del Buey, M. A., Lavilla, L., Ascaso, F. J., Lanchares, E., Huerva, V. & Cristobal, J. A. 2014. Assessment of corneal biomechanical properties and intraocular pressure in myopic spanish healthy population. *J Ophthalmol,* 2014**,** 905129.

Detry-Morel, M., Jamart, J., Hautenauven, F. & Pourjavan, S. 2012. Comparison of the corneal biomechanical properties with the Ocular Response Analyzer(R) (ORA) in African and Caucasian normal subjects and patients with glaucoma. *Acta Ophthalmol,* 90**,** e118-24.

Detry-Morel, M., Jamart, J. & Pourjavan, S. 2011. Evaluation of corneal biomechanical properties with the Reichert Ocular Response Analyzer. *Eur J Ophthalmol,* 21**,** 138-48.

Dienes, L., Kiss, H. J., Perenyi, K., Nagy, Z. Z., Acosta, M. C., Gallar, J. & Kovacs, I. 2015. Corneal Sensitivity and Dry Eye Symptoms in Patients with Keratoconus. *PLoS One,* 10**,** e0141621.

Dorronsoro, C., Pascual, D., Perez-Merino, P., Kling, S. & Marcos, S. 2012. Dynamic OCT measurement of corneal deformation by an air puff in normal and cross-linked corneas. *Biomed Opt Express,* 3**,** 473-87.

Dua, H. S., Faraj, L. A., Said, D. G., Gray, T. & Lowe, J. 2013. Human corneal anatomy redefined: a novel pre-Descemet's layer (Dua's layer). *Ophthalmology,* 120**,** 1778-85.

Dupps, W. J., Jr. 2007. Hysteresis: new mechanospeak for the ophthalmologist. *J Cataract Refract Surg,* 33**,** 1499-501.

Dupps, W. J., Jr., Netto, M. V., Herekar, S. & Krueger, R. R. 2007. Surface wave elastometry of the cornea in porcine and human donor eyes. *J Refract Surg,* 23**,** 66-75.

Dupps, W. J., Jr. & Wilson, S. E. 2006. Biomechanics and wound healing in the cornea. *Exp Eye Res,* 83**,** 709-20.

Ehongo, A., De Maertelaer, V. & Pourjavan, S. 2009. Effect of topical corneal anaesthesia on ocular response analyzer parameters: pilot study. *Int Ophthalmol,* 29**,** 325-8.

Elsheikh, A., Alhasso, D. & Rama, P. 2008a. Assessment of the epithelium's contribution

to corneal biomechanics. *Exp Eye Res,* 86**,** 445-51.

Elsheikh, A., Alhasso, D. & Rama, P. 2008b. Biomechanical properties of human and porcine corneas. *Exp Eye Res,* 86**,** 783-90.

Elsheikh, A. & Anderson, K. 2005. Comparative study of corneal strip extensometry and inflation tests. *J R Soc Interface,* 2**,** 177-85.

Elsheikh, A., Brown, M., Alhasso, D., Rama, P., Campanelli, M. & Garway-Heath, D. 2008c. Experimental assessment of corneal anisotropy. *J Refract Surg,* 24**,** 178-87.

Elsheikh, A., Geraghty, B., Rama, P., Campanelli, M. & Meek, K. M. 2010. Characterization of age-related variation in corneal biomechanical properties. *J R Soc Interface,* 7**,** 1475-85.

Elsheikh, A., Wang, D., Brown, M., Rama, P., Campanelli, M. & Pye, D. 2007a. Assessment of corneal biomechanical properties and their variation with age. *Curr Eye Res,* 32**,** 11-9.

Elsheikh, A., Wang, D. & Pye, D. 2007b. Determination of the modulus of elasticity of the human cornea. *J Refract Surg,* 23**,** 808-18.

Ertan, A., Kamburoglu, G. & Colin, J. 2009. Location of steepest corneal area of cone in keratoconus stratified by age using Pentacam. *J Refract Surg,* 25**,** 1012-6.

Ethier, C. R. & Simmons, C. A. 2007. *Inroductory biomechanics: from cells to organisms.* Cambridge, England, Cambridge University Press.

Feltgen, N., Leifert, D. & Funk, J. 2001. Correlation between central corneal thickness, applanation tonometry, and direct intracameral IOP readings. *Br J Ophthalmol,* 85**,** 85-7.

Fontes, B. M., Ambrosio Jr, R., Velarde, G. C. & Nose, W. 2011a. Corneal biomechanical evaluation in healthy thin corneas compared with matched keratoconus cases. *Arq Bras Oftalmol,* 74**,** 13-6.

Fontes, B. M., Ambrosio Junior, R., Jardim, D., Velarde, G. C. & Nose, W. 2010. Ability of corneal biomechanical metrics and anterior segment data in the differentiation of keratoconus and healthy corneas. *Arq Bras Oftalmol,* 73**,** 333-7.

Fontes, B. M., Ambrosio, R., Jr., Alonso, R. S., Jardim, D., Velarde, G. C. & Nose, W. 2008. Corneal biomechanical metrics in eyes with refraction of -19.00 to +9.00

D in healthy Brazilian patients. *J Refract Surg,* 24**,** 941-5.

Fontes, B. M., Ambrosio, R., Jr., Velarde, G. C. & Nose, W. 2011b. Ocular response analyzer measurements in keratoconus with normal central corneal thickness compared with matched normal control eyes. *J Refract Surg,* 27**,** 209-15.

Ford, M. R., Roy, A. S., Rollins, A. M. & Dupps, W. J. 2009. Spatially-Resolved Biomechanical Effects of Riboflavin/uv Collagen Crosslinking in the Human Cornea With Optical Coherence Elastography. *Investigative Ophthalmology & Visual Science,* 50**,** 5478-5478.

Foster, P. J., Broadway, D. C., Garway-Heath, D. F., Yip, J. L., Luben, R., Hayat, S., Dalzell, N., Wareham, N. J. & Khaw, K. T. 2011. Intraocular pressure and corneal biomechanics in an adult British population: the EPIC-Norfolk eye study. *Invest Ophthalmol Vis Sci,* 52**,** 8179-85.

Franco, S. & Lira, M. 2009. Biomechanical properties of the cornea measured by the Ocular Response Analyzer and their association with intraocular pressure and the central corneal curvature. *Clin Exp Optom,* 92**,** 469-75.

Fratzl, P. 2008. Collagen: strucutre and mechanics, an introduction. *In:* Fratzl, P. (ed.) *Collagen : structure and mechanics.* New York: Springer.

Friedenwald, J. S. 1937. Contribution to the theory and practice of tonometry. *Am J Ophthalmol,* 20**,** 985-1024.

Fukuda, R., Usui, T., Miyai, T., Mori, Y., Miyata, K. & Amano, S. 2013. Corneal thickness and volume measurements by swept source anterior segment optical coherence tomography in normal subjects. *Curr Eye Res,* 38**,** 531-6.

Fung, Y. C. 1993. Introduction: a sketch of the history and scope of the field. *Biomechanics: mechanical properties of living tissues.* 2nd ed. New York: Springer-Verlag.

Galletti, J. G., Pfortner, T. & Bonthoux, F. F. 2012. Improved keratoconus detection by ocular response analyzer testing after consideration of corneal thickness as a confounding factor. *J Refract Surg,* 28**,** 202-8.

Garcia-Porta, N., Fernandes, P., Queiros, A., Salgado-Borges, J., Parafita-Mato, M. & Gonzalez-Meijome, J. M. 2014. Corneal biomechanical properties in different ocular conditions and new measurement techniques. *ISRN Ophthalmol,* 2014**,**

724546.

Gatinel, D., Chaabouni, S., Adam, P. A., Munck, J., Puech, M. & Hoang-Xuan, T. 2007. Corneal hysteresis, resistance factor, topography, and pachymetry after corneal lamellar flap. *J Refract Surg,* 23**,** 76-84.

Girard, M. J. A., Tan, D., Ang, M., Mehta, J. S., Zhang, L., Chung, C. W., Mani, B., Tun, T. A. & Aung, T. 2015. An Engineering-based Methodology to Characterize the In Vivo Nonlinear Biomechanical Properties of the Cornea with Application to Glaucoma Subjects. *Investigative Ophthalmology & Visual Science,* 56**,** 1099-1099.

Gkika, M., Labiris, G., Giarmoukakis, A., Koutsogianni, A. & Kozobolis, V. 2012. Evaluation of corneal hysteresis and corneal resistance factor after corneal cross-linking for keratoconus. *Graefes Arch Clin Exp Ophthalmol,* 250**,** 565-73.

Glass, D. H., Roberts, C. J., Litsky, A. S. & Weber, P. A. 2008. A viscoelastic biomechanical model of the cornea describing the effect of viscosity and elasticity on hysteresis. *Invest Ophthalmol Vis Sci,* 49**,** 3919-26.

Glavine, K. A. 2009. *Using corneal characteristics to predict corneal change in overnight orthokeratology.* MSc, The New England College.

Goebels, S. C., Seitz, B. & Langenbucher, A. 2012. Precision of ocular response analyzer. *Curr Eye Res,* 37**,** 689-93.

Goldich, Y., Barkana, Y., Pras, E., Fish, A., Mandel, Y., Hirsh, A., Tsur, N., Morad, Y., Avni, I. & Zadok, D. 2011. Variations in corneal biomechanical parameters and central corneal thickness during the menstrual cycle. *J Cataract Refract Surg,* 37**,** 1507-11.

Goldich, Y., Barkana, Y., Wussuku Lior, O., Marcovich, A. L., Hirsh, A., Avni, I. & Zadok, D. 2014. Corneal collagen cross-linking for the treatment of progressive keratoconus: 3-year prospective outcome. *Can J Ophthalmol,* 49**,** 54-9.

Goldich, Y., Marcovich, A. L., Barkana, Y., Mandel, Y., Hirsh, A., Morad, Y., Avni, I. & Zadok, D. 2012. Clinical and corneal biomechanical changes after collagen cross-linking with riboflavin and UV irradiation in patients with progressive keratoconus: results after 2 years of follow-up. *Cornea,* 31**,** 609-14.

Gonzalez-Meijome, J. M., Queiros, A., Jorge, J., Diaz-Rey, A. & Parafita, M. A. 2008a.

Intraoffice variability of corneal biomechanical parameters and intraocular pressure (IOP). *Optom Vis Sci,* 85**,** 457-62.

Gonzalez-Meijome, J. M., Villa-Collar, C., Queiros, A., Jorge, J. & Parafita, M. A. 2008b. Pilot study on the influence of corneal biomechanical properties over the short term in response to corneal refractive therapy for myopia. *Cornea,* 27**,** 421-6.

Gordon, M. O., Beiser, J. A., Brandt, J. D., Heuer, D. K., Higginbotham, E. J., Johnson, C. A., Keltner, J. L., Miller, J. P., Parrish, R. K., 2nd, Wilson, M. R. & Kass, M. A. 2002. The Ocular Hypertension Treatment Study: baseline factors that predict the onset of primary open-angle glaucoma. *Arch Ophthalmol,* 120**,** 714-20; discussion 829-30.

Goss, D. A., Van Veen, H. G., Rainey, B. B. & Feng, B. 1997. Ocular components measured by keratometry, phakometry, and ultrasonography in emmetropic and myopic optometry students. *Optom Vis Sci,* 74**,** 489-95.

Grabner, G., Eilmsteiner, R., Steindl, C., Ruckhofer, J., Mattioli, R. & Husinsky, W. 2005. Dynamic corneal imaging. *J Cataract Refract Surg,* 31**,** 163-74.

Greenstein, S. A., Fry, K. L. & Hersh, P. S. 2012. In vivo biomechanical changes after corneal collagen cross-linking for keratoconus and corneal ectasia: 1-year analysis of a randomized, controlled, clinical trial. *Cornea,* 31**,** 21-5.

Grise-Dulac, A., Saad, A., Abitbol, O., Febbraro, J. L., Azan, E., Moulin-Tyrode, C. & Gatinel, D. 2012. Assessment of corneal biomechanical properties in normal tension glaucoma and comparison with open-angle glaucoma, ocular hypertension, and normal eyes. *J Glaucoma,* 21**,** 486-9.

Guirao, A. 2005. Theoretical elastic response of the cornea to refractive surgery: risk factors for keratectasia. *J Refract Surg,* 21**,** 176-85.

Hallahan, K. M., Rocha, K., Roy, A. S., Randleman, J. B., Stulting, R. D. & Dupps, W. J., Jr. 2014. Effects of corneal cross-linking on ocular response analyzer waveform-derived variables in keratoconus and postrefractive surgery ectasia. *Eye Contact Lens,* 40**,** 339-44.

Hamilton, K. E. & Pye, D. C. 2008. Young's modulus in normal corneas and the effect on applanation tonometry. *Optom Vis Sci,* 85**,** 445-50.

Hamilton, K. E., Pye, D. C., Aggarwala, S., Evian, S., Khosla, J. & Perera, R. 2007. Diurnal variation of central corneal thickness and Goldmann applanation tonometry estimates of intraocular pressure. *J Glaucoma,* 16**,** 29-35.

Haque, S., Fonn, D., Simpson, T. & Jones, L. 2004. Corneal and epithelial thickness changes after 4 weeks of overnight corneal refractive therapy lens wear, measured with optical coherence tomography. *Eye Contact Lens,* 30**,** 189-93; discussion 205-6.

Harper, C. L., Boulton, M. E., Bennett, D., Marcyniuk, B., Jarvis-Evans, J. H., Tullo, A. B. & Ridgway, A. E. 1996. Diurnal variations in human corneal thickness. *Br J Ophthalmol,* 80**,** 1068-72.

Haseltine, S. J., Pae, J., Ehrlich, J. R., Shammas, M. & Radcliffe, N. M. 2012. Variation in corneal hysteresis and central corneal thickness among black, hispanic and white subjects. *Acta Ophthalmol,* 90**,** e626-31.

Helmy, H., Leila, M. & Zaki, A. A. 2016. Corneal biomechanics in asymmetrical normal-tension glaucoma. *Clin Ophthalmol,* 10**,** 503-10.

Hirneiss, C., Neubauer, A. S., Yu, A., Kampik, A. & Kernt, M. 2011. Corneal biomechanics measured with the ocular response analyser in patients with unilateral open-angle glaucoma. *Acta Ophthalmol,* 89**,** e189-92.

Hjortdal, J. O. 1996. Regional elastic performance of the human cornea. *J Biomech,* 29**,** 931-42.

Hoeltzel, D. A., Altman, P., Buzard, K. & Choe, K. 1992. Strip extensiometry for comparison of the mechanical response of bovine, rabbit, and human corneas. *J Biomech Eng,* 114**,** 202-15.

Hollman, K. W., Emelianov, S. Y., Neiss, J. H., Jotyan, G., Spooner, G. J., Juhasz, T., Kurtz, R. M. & O'Donnell, M. 2002. Strain imaging of corneal tissue with an ultrasound elasticity microscope. *Cornea,* 21**,** 68-73.

Hon, Y. & Lam, A. K. 2013. Corneal deformation measurement using Scheimpflug noncontact tonometry. *Optom Vis Sci,* 90**,** e1-8.

Hon, Y., Wan, K., Chen, G. Z., Lu, S. H., Lam, D. C. & Lam, A. K. 2016. Diurnal Variation of Corneal Tangent Modulus in Normal Chinese. *Cornea*.

Honmura, S. 1968. [Studies on the relationship between ocular tension and myopia. II.

Ocular tension, ocular rigidity, aqueous outflow and aqueous secretion in myopic eyes]. *Nihon Ganka Gakkai Zasshi,* 72**,** 688-96.

Huang, Y., Huang, C., Li, L., Qiu, K., Gong, W., Wang, Z., Wu, X., Du, Y., Chen, B., Lam, D. S., Zhang, M. & Congdon, N. 2011. Corneal biomechanics, refractive error, and axial length in Chinese primary school children. *Invest Ophthalmol Vis Sci,* 52**,** 4923-8.

Huang, Y., Lin, S., Ma, D., Wang, Z., Du, Y., Lu, X. & Zhang, M. 2013. Corneal biomechanical properties and associated factors in school-age children. *Eye Sci,* 28**,** 34-9.

Hutchings, N., Simpson, T. L., Hyun, C., Moayed, A. A., Hariri, S., Sorbara, L. & Bizheva, K. 2010. Swelling of the human cornea revealed by high-speed, ultrahigh-resolution optical coherence tomography. *Invest Ophthalmol Vis Sci,* 51**,** 4579-84.

Insull, E., Nicholas, S., Ang, G. S., Poostchi, A., Chan, K. & Wells, A. 2010. Optic disc area and correlation with central corneal thickness, corneal hysteresis and ocular pulse amplitude in glaucoma patients and controls. *Clin Experiment Ophthalmol,* 38**,** 839-44.

Ishida, Y., Yanai, R., Sagara, T., Nishida, T., Toshida, H. & Murakami, A. 2011. Decrease in intraocular pressure following orthokeratology measured with a noncontact tonometer. *Jpn J Ophthalmol,* 55**,** 190-5.

Jayakumar, J. & Swarbrick, H. A. 2005. The effect of age on short-term orthokeratology. *Optom Vis Sci,* 82**,** 505-11.

Jaycock, P. D., Lobo, L., Ibrahim, J., Tyrer, J. & Marshall, J. 2005. Interferometric technique to measure biomechanical changes in the cornea induced by refractive surgery. *J Cataract Refract Surg,* 31**,** 175-84.

Jensen, H. 1992. Myopia progression in young school children and intraocular pressure. *Doc Ophthalmol,* 82**,** 249-55.

Jiang, Z., Shen, M., Mao, G., Chen, D., Wang, J., Qu, J. & Lu, F. 2011. Association between corneal biomechanical properties and myopia in Chinese subjects. *Eye (Lond),* 25**,** 1083-9.

Jinabhai, A., Radhakrishnan, H. & O'Donnell, C. 2011. Pellucid corneal marginal

degeneration: A review. *Cont Lens Anterior Eye,* 34**,** 56-63.

Johnson, R. D., Nguyen, M. T., Lee, N. & Hamilton, D. R. 2011. Corneal biomechanical properties in normal, forme fruste keratoconus, and manifest keratoconus after statistical correction for potentially confounding factors. *Cornea,* 30**,** 516-23.

Joseph, D. S., Thampi, B., Joosadima, A. & Mohan, A. 2016. A study on association between intraocular pressure and myopia *Int J Res med Sci,* 4**,** 2202-2205.

Jue, B. & Maurice, D. M. 1986. The mechanical properties of the rabbit and human cornea. *J Biomech,* 19**,** 847-53.

Kamiya, K., Hagishima, M., Fujimura, F. & Shimizu, K. 2008. Factors affecting corneal hysteresis in normal eyes. *Graefes Arch Clin Exp Ophthalmol,* 246**,** 1491-4.

Kamiya, K., Shimizu, K. & Ohmoto, F. 2009a. Comparison of the changes in corneal biomechanical properties after photorefractive keratectomy and laser in situ keratomileusis. *Cornea,* 28**,** 765-9.

Kamiya, K., Shimizu, K. & Ohmoto, F. 2009b. Effect of aging on corneal biomechanical parameters using the ocular response analyzer. *J Refract Surg,* 25**,** 888-93.

Kamma-Lorger, C. S., Boote, C., Hayes, S., Moger, J., Burghammer, M., Knupp, C., Quantock, A. J., Sorensen, T., Di Cola, E., White, N., Young, R. D. & Meek, K. M. 2010. Collagen and mature elastic fibre organisation as a function of depth in the human cornea and limbus. *J Struct Biol,* 169**,** 424-30.

Kang, S. Y., Kim, B. K. & Byun, Y. J. 2007. Sustainability of orthokeratology as demonstrated by corneal topography. *Korean J Ophthalmol,* 21**,** 74-8.

Kara, N., Altinkaynak, H., Baz, O. & Goker, Y. 2013. Biomechanical evaluation of cornea in topographically normal relatives of patients with keratoconus. *Cornea,* 32**,** 262-6.

Kaushik, S., Pandav, S. S., Banger, A., Aggarwal, K. & Gupta, A. 2012. Relationship between corneal biomechanical properties, central corneal thickness, and intraocular pressure across the spectrum of glaucoma. *Am J Ophthalmol,* 153**,** 840-849 e2.

Kerautret, J., Colin, J., Touboul, D. & Roberts, C. 2008. Biomechanical characteristics of the ectatic cornea. *J Cataract Refract Surg,* 34**,** 510-3.

Khawaja, A. P., Chan, M. P., Broadway, D. C., Garway-Heath, D. F., Luben, R., Yip, J.

L., Hayat, S., Khaw, K. T. & Foster, P. J. 2014. Corneal biomechanical properties and glaucoma-related quantitative traits in the EPIC-Norfolk Eye Study. *Invest Ophthalmol Vis Sci,* 55**,** 117-24.

Khurana 2008. Errors of Refraction and Binocular Optical Defects. *Theory And Practice Of Optics And Refraction.* 2nd ed.: Elsevier India Pvt. Limited.

Kida, T., Liu, J. H. & Weinreb, R. N. 2006. Effect of 24-hour corneal biomechanical changes on intraocular pressure measurement. *Invest Ophthalmol Vis Sci,* 47**,** 4422-6.

Kida, T., Liu, J. H. & Weinreb, R. N. 2008. Effects of aging on corneal biomechanical properties and their impact on 24-hour measurement of intraocular pressure. *Am J Ophthalmol,* 146**,** 567-572.

Kiely, P. M., Smith, G. & Garney, L. G. 1982. The Mean Shape of the Human Cornea. *Optica Acta: International Journal of Optics* 29**,** 1027-1040.

King, A., Azuara-Blanco, A. & Tuulonen, A. 2013. Glaucoma. *BMJ,* 346**,** f3518.

Kirwan, C. & O'Keefe, M. 2008. Corneal hysteresis using the Reichert ocular response analyser: findings pre- and post-LASIK and LASEK. *Acta Ophthalmol,* 86**,** 215-8.

Kirwan, C., O'Keefe, M. & Lanigan, B. 2006. Corneal hysteresis and intraocular pressure measurement in children using the reichert ocular response analyzer. *Am J Ophthalmol,* 142**,** 990-2.

Kirwan, C., O'Malley, D. & O'Keefe, M. 2008. Corneal hysteresis and corneal resistance factor in keratoectasia: findings using the Reichert ocular response analyzer. *Ophthalmologica,* 222**,** 334-7.

Kling, S. 2014. *Corneal biomechanics: measurement, modification and simulation.* Ph.D., University of Valladolid.

Kling, S. & Marcos, S. 2013. Contributing factors to corneal deformation in air puff measurements. *Invest Ophthalmol Vis Sci,* 54**,** 5078-85.

Knox Cartwright, N. E., Tyrer, J. R. & Marshall, J. 2011. Age-related differences in the elasticity of the human cornea. *Invest Ophthalmol Vis Sci,* 52**,** 4324-9.

Knox Cartwright, N. E., Tyrer, J. R. & Marshall, J. 2012. In vitro quantification of the stiffening effect of corneal cross-linking in the human cornea using radial

shearing speckle pattern interferometry. *J Refract Surg,* 28**,** 503-8.

Ko, M. W. 2013. *Characterization of corneal biomechanical properties and applications in glaucoma risk assessment.* Doctor of Philosophy, The Hong Kong University of Science and Technology.

Ko, M. W., Leung, L. K. & Lam, D. C. 2014. Comparative study of corneal tangent elastic modulus measurement using corneal indentation device. *Med Eng Phys,* 36**,** 1115-21.

Ko, M. W., Leung, L. K., Lam, D. C. & Leung, C. K. 2013. Characterization of corneal tangent modulus in vivo. *Acta Ophthalmol,* 91**,** e263-9.

Kohlhaas, M., Spoerl, E., Schilde, T., Unger, G., Wittig, C. & Pillunat, L. E. 2006. Biomechanical evidence of the distribution of cross-links in corneas treated with riboflavin and ultraviolet A light. *J Cataract Refract Surg,* 32**,** 279-83.

Koprowski, R., Wilczynski, S., Nowinska, A., Lyssek-Boron, A., Teper, S., Wylegala, E. & Wrobel, Z. 2015. Quantitative assessment of responses of the eyeball based on data from the Corvis tonometer. *Comput Biol Med,* 58**,** 91-100.

Kotecha, A. 2007. What biomechanical properties of the cornea are relevant for the clinician? *Surv Ophthalmol,* 52 Suppl 2**,** S109-14.

Kotecha, A., Crabb, D. P., Spratt, A. & Garway-Heath, D. F. 2009. The relationship between diurnal variations in intraocular pressure measurements and central corneal thickness and corneal hysteresis. *Invest Ophthalmol Vis Sci,* 50**,** 4229-36.

Kotecha, A., Elsheikh, A., Roberts, C. R., Zhu, H. & Garway-Heath, D. F. 2006. Corneal thickness- and age-related biomechanical properties of the cornea measured with the ocular response analyzer. *Invest Ophthalmol Vis Sci,* 47**,** 5337-47.

Kotecha, A., Russell, R. A., Sinapis, A., Pourjavan, S., Sinapis, D. & Garway-Heath, D. F. 2014. Biomechanical parameters of the cornea measured with the Ocular Response Analyzer in normal eyes. *BMC Ophthalmol,* 14**,** 11.

Kumar, M., Shetty, R., Jayadev, C. & Dutta, D. 2015. Comparability and repeatability of pachymetry in keratoconus using four noncontact techniques. *Indian J Ophthalmol,* 63**,** 722-7.

Kurita, Y., Kempf, R., Iida, Y., Okude, J., Kaneko, M., Mishima, H. K., Tsukamoto, H., Sugimoto, E., Katakura, S., Kobayashi, K. & Kiuchi, Y. 2008. Contact-based

stiffness sensing of human eye. *IEEE Trans Biomed Eng,* 55**,** 739-45.

Laiquzzaman, M., Bhojwani, R., Cunliffe, I. & Shah, S. 2006. Diurnal variation of ocular hysteresis in normal subjects: relevance in clinical context. *Clin Experiment Ophthalmol,* 34**,** 114-8.

Lam, A., Chen, D., Chiu, R. & Chui, W. S. 2007. Comparison of IOP measurements between ORA and GAT in normal Chinese. *Optom Vis Sci,* 84**,** 909-14.

Lam, A. K., Chen, D. & Tse, J. 2010. The usefulness of waveform score from the ocular response analyzer. *Optom Vis Sci,* 87**,** 195-9.

Lam, A. K. C., Tam, K., Kwok, P., Lee, V., Wang, Z., Wu, R. T., Chan, E. C., Chau, R. C., Au, D. C. & Woo, V. C. 2015. Central and peripheral rebound tonometry in myopic LASIK without and with corneal collagen crosslinking. *Investigative Ophthalmology & Visual Science,* 56**,** 2026-2026.

Landoulsi, H., Saad, A., Haddad, N. N., Guilbert, E. & Gatinel, D. 2013. Repeatability of Ocular Response Analyzer waveform parameters in normal eyes and eyes after refractive surgery. *J Refract Surg,* 29**,** 709-14.

Lanza, M., Cennamo, M., Iaccarino, S., Irregolare, C., Rechichi, M., Bifani, M. & Gironi Carnevale, U. A. 2014. Evaluation of corneal deformation analyzed with Scheimpflug based device in healthy eyes and diseased ones. *Biomed Res Int,* 2014**,** 748671.

Last, J. A., Thomasy, S. M., Croasdale, C. R., Russell, P. & Murphy, C. J. 2012. Compliance profile of the human cornea as measured by atomic force microscopy. *Micron,* 43**,** 1293-8.

Lau, W. & Pye, D. 2011a. Changes in corneal biomechanics and applanation tonometry with induced corneal swelling. *Invest Ophthalmol Vis Sci,* 52**,** 3207-14.

Lau, W. & Pye, D. 2011b. A clinical description of Ocular Response Analyzer measurements. *Invest Ophthalmol Vis Sci,* 52**,** 2911-6.

Lau, W. & Pye, D. C. 2012. Associations between diurnal changes in Goldmann tonometry, corneal geometry, and ocular response analyzer parameters. *Cornea,* 31**,** 639-44.

Lee, R., Chang, R. T., Wong, I. Y., Lai, J. S., Lee, J. W. & Singh, K. 2016. Assessment of corneal biomechanical parameters in myopes and emmetropes using the

Corvis ST. *Clin Exp Optom*.

Lee, Y. W., Choi, C. Y. & Yoon, G. Y. 2015. Comparison of dual rotating Scheimpflug-Placido, swept-source optical coherence tomography, and Placido-scanning-slit systems. *J Cataract Refract Surg,* 41**,** 1018-29.

Leite, M. T., Alencar, L. M., Gore, C., Weinreb, R. N., Sample, P. A., Zangwill, L. M. & Medeiros, F. A. 2010. Comparison of corneal biomechanical properties between healthy blacks and whites using the Ocular Response Analyzer. *Am J Ophthalmol,* 150**,** 163-168 e1.

Leung, C. K., Ye, C. & Weinreb, R. N. 2013. An ultra-high-speed Scheimpflug camera for evaluation of corneal deformation response and its impact on IOP measurement. *Invest Ophthalmol Vis Sci,* 54**,** 2885-92.

Leung, E. W., Medeiros, F. A. & Weinreb, R. N. 2008. Prevalence of ocular surface disease in glaucoma patients. *J Glaucoma,* 17**,** 350-5.

Leung, L. K., Ko, M. W., Ye, C., Lam, D. C. & Leung, C. K. 2014. Noninvasive measurement of scleral stiffness and tangent modulus in porcine eyes. *Invest Ophthalmol Vis Sci,* 55**,** 3721-6.

Lewis, P. N., White, T. L., Young, R. D., Bell, J. S., Winlove, C. P. & Meek, K. M. 2015. Three-dimensional arrangement of elastic fibers in the human corneal stroma. *Exp Eye Res,* 146**,** 43-53.

Li, Y., Meisler, D. M., Tang, M., Lu, A. T., Thakrar, V., Reiser, B. J. & Huang, D. 2008. Keratoconus diagnosis with optical coherence tomography pachymetry mapping. *Ophthalmology,* 115**,** 2159-66.

Lim, L., Gazzard, G., Chan, Y. H., Fong, A., Kotecha, A., Sim, E. L., Tan, D., Tong, L. & Saw, S. M. 2008a. Cornea biomechanical characteristics and their correlates with refractive error in Singaporean children. *Invest Ophthalmol Vis Sci,* 49**,** 3852-7.

Lim, L., Gazzard, G., Chan, Y. H., Fong, A., Kotecha, A., Sim, E. L., Tan, D., Tong, L. & Saw, S. M. 2008b. Corneal biomechanics, thickness and optic disc morphology in children with optic disc tilt. *Br J Ophthalmol,* 92**,** 1461-6.

Liu, J. & Roberts, C. J. 2005. Influence of corneal biomechanical properties on intraocular pressure measurement: quantitative analysis. *J Cataract Refract Surg,*

31**,** 146-55.

Liu, J. H., Kripke, D. F., Twa, M. D., Gokhale, P. A., Jones, E. I., Park, E. H., Meehan, J. E. & Weinreb, R. N. 2002. Twenty-four-hour pattern of intraocular pressure in young adults with moderate to severe myopia. *Invest Ophthalmol Vis Sci,* 43**,** 2351-5.

Liu, R., Chu, R. Y., Wang, L. & Zhou, X. T. 2008. [The measured value of corneal hysteresis and resistance factor with their related factors analysis in normal eyes]. *Zhonghua Yan Ke Za Zhi,* 44**,** 715-9.

Lu, F., Simpson, T., Sorbara, L. & Fonn, D. 2008. Malleability of the ocular surface in response to mechanical stress induced by orthokeratology contact lenses. *Cornea,* 27**,** 133-41.

Lu, F., Xu, S., Qu, J., Shen, M., Wang, X., Fang, H. & Wang, J. 2007. Central corneal thickness and corneal hysteresis during corneal swelling induced by contact lens wear with eye closure. *Am J Ophthalmol,* 143**,** 616-22.

Luce, D. 2006. Methodology for Cornea Compensated IOP and Corneal Resistance Factor for the Reichert Ocular Response Analyzer. *Invest Ophthalmol Vis Sci,* 47**,** ARVO E-Abstract 2266.

Luce, D. A. 2005. Determining in vivo biomechanical properties of the cornea with an ocular response analyzer. *J Cataract Refract Surg,* 31**,** 156-62.

Malik, N. S., Moss, S. J., Ahmed, N., Furth, A. J., Wall, R. S. & Meek, K. M. 1992. Ageing of the human corneal stroma: structural and biochemical changes. *Biochim Biophys Acta,* 1138**,** 222-8.

Mandalos, A., Anastasopoulos, E., Makris, L., Dervenis, N., Kilintzis, V. & Topouzis, F. 2013. Inter-examiner reproducibility of Ocular Response Analyzer using the waveform score quality index in healthy subjects. *J Glaucoma,* 22**,** 152-5.

Mangouritsas, G., Morphis, G., Mourtzoukos, S. & Feretis, E. 2009. Association between corneal hysteresis and central corneal thickness in glaucomatous and non-glaucomatous eyes. *Acta Ophthalmol,* 87**,** 901-5.

Mansouri, K., Leite, M. T., Weinreb, R. N., Tafreshi, A., Zangwill, L. M. & Medeiros, F. A. 2012. Association between corneal biomechanical properties and glaucoma severity. *Am J Ophthalmol,* 153**,** 419-427 e1.

Mao, X. J., Huang, C. C., Chen, L. & Lu, F. 2010. [A study on the effect of the corneal biomechanical properties undergoing overnight orthokeratology]. *Zhonghua Yan Ke Za Zhi,* 46**,** 209-13.

Maresca, N., Zeri, F., Palumbo, P. & Calossi, A. 2014. Agreement and reliability in measuring central corneal thickness with a rotating Scheimpflug-Placido system and ultrasound pachymetry. *Cont Lens Anterior Eye,* 37**,** 442-6.

Mark, H. H. & Mark, T. L. 2003. Corneal astigmatism in applanation tonometry. *Eye (Lond),* 17**,** 617-8.

Marsich, M. W. & Bullimore, M. A. 2000. The repeatability of corneal thickness measures. *Cornea,* 19**,** 792-5.

Matteoli, S., Virga, A., Paladini, I., Mencucci, R. & Corvi, A. 2016. Investigation into the elastic properties of ex vivo porcine corneas subjected to inflation test after cross-linking treatment. *J Appl Biomater Funct Mater***,** 0.

McAlinden, C., Khadka, J. & Pesudovs, K. 2011. Statistical methods for conducting agreement (comparison of clinical tests) and precision (repeatability or reproducibility) studies in optometry and ophthalmology. *Ophthalmic Physiol Opt,* 31**,** 330-8.

McBrien, N. A., Jobling, A. I. & Gentle, A. 2009. Biomechanics of the sclera in myopia: extracellular and cellular factors. *Optom Vis Sci,* 86**,** E23-30.

McMonnies, C. W. 2012. Assessing corneal hysteresis using the Ocular Response Analyzer. *Optom Vis Sci,* 89**,** E343-9.

McMonnies, C. W. 2016. An examination of the relation between intraocular pressure, fundal stretching and myopic pathology. *Clin Exp Optom,* 99**,** 113-9.

Medeiros, F. A., Meira-Freitas, D., Lisboa, R., Kuang, T. M., Zangwill, L. M. & Weinreb, R. N. 2013. Corneal hysteresis as a risk factor for glaucoma progression: a prospective longitudinal study. *Ophthalmology,* 120**,** 1533-40.

Medeiros, F. A., Sample, P. A., Zangwill, L. M., Bowd, C., Aihara, M. & Weinreb, R. N. 2003. Corneal thickness as a risk factor for visual field loss in patients with preperimetric glaucomatous optic neuropathy. *Am J Ophthalmol,* 136**,** 805-13.

Medeiros, F. A. & Weinreb, R. N. 2006. Evaluation of the influence of corneal biomechanical properties on intraocular pressure measurements using the ocular

response analyzer. *J Glaucoma,* 15**,** 364-70.

Medeiros, F. W., Sinha-Roy, A., Alves, M. R. & Dupps, W. J., Jr. 2011. Biomechanical corneal changes induced by different flap thickness created by femtosecond laser. *Clinics (Sao Paulo),* 66**,** 1067-71.

Meek, K. M., Tuft, S. J., Huang, Y., Gill, P. S., Hayes, S., Newton, R. H. & Bron, A. J. 2005. Changes in collagen orientation and distribution in keratoconus corneas. *Invest Ophthalmol Vis Sci,* 46**,** 1948-56.

Metzler, K. M., Mahmoud, A. M., Liu, J. & Roberts, C. J. 2014. Deformation response of paired donor corneas to an air puff: intact whole globe versus mounted corneoscleral rim. *J Cataract Refract Surg,* 40**,** 888-96.

Mikielewicz, M., Kotliar, K., Barraquer, R. I. & Michael, R. 2011. Air-pulse corneal applanation signal curve parameters for the characterisation of keratoconus. *Br J Ophthalmol,* 95**,** 793-8.

Morita, T., Shoji, N., Kamiya, K., Fujimura, F. & Shimizu, K. 2012. Corneal biomechanical properties in normal-tension glaucoma. *Acta Ophthalmol,* 90**,** e48-53.

Mountford, J. 1997. An analysis of the changes in corneal shape and refractive error induced by accelerated orthokeratology. *International Contact Lens Clinic,* 24**,** 128-144.

Nakagawa, T., Maeda, N., Higashiura, R., Hori, Y., Inoue, T. & Nishida, K. 2011. Corneal topographic analysis in patients with keratoconus using 3-dimensional anterior segment optical coherence tomography. *J Cataract Refract Surg,* 37**,** 1871-8.

Narayanaswamy, A., Chung, R. S., Wu, R. Y., Park, J., Wong, W. L., Saw, S. M., Wong, T. Y. & Aung, T. 2011. Determinants of corneal biomechanical properties in an adult Chinese population. *Ophthalmology,* 118**,** 1253-9.

Nash, I. S., Greene, P. R. & Foster, C. S. 1982. Comparison of mechanical properties of keratoconus and normal corneas. *Exp Eye Res,* 35**,** 413-24.

Nemeth, G., Hassan, Z., Csutak, A., Szalai, E., Berta, A. & Modis, L., Jr. 2013. Repeatability of ocular biomechanical data measurements with a Scheimpflug-based noncontact device on normal corneas. *J Refract Surg,* 29**,** 558-63.

Neri, A., Malori, M., Scaroni, P., Leaci, R., Delfini, E. & Macaluso, C. 2012. Corneal thickness mapping by 3D swept-source anterior segment optical coherence tomography. *Acta Ophthalmol,* 90**,** e452-7.

Nichols, J. J., Marsich, M. M., Nguyen, M., Barr, J. T. & Bullimore, M. A. 2000. Overnight orthokeratology. *Optom Vis Sci,* 77**,** 252-9.

Nieto-Bona, A., Gonzalez-Mesa, A., Nieto-Bona, M. P., Villa-Collar, C. & Lorente-Velazquez, A. 2011a. Long-term changes in corneal morphology induced by overnight orthokeratology. *Curr Eye Res,* 36**,** 895-904.

Nieto-Bona, A., Gonzalez-Mesa, A., Nieto-Bona, M. P., Villa-Collar, C. & Lorente-Velazquez, A. 2011b. Short-term effects of overnight orthokeratology on corneal cell morphology and corneal thickness. *Cornea,* 30**,** 646-54.

Nieto-Bona, A., González-Mesa, A., Villa-Collar, C. & Lorente-Velázqueza, A. 2012. Biomechanical properties in corneal refractive therapy during adaptation period and after treatment interruption: A pilot study. *J Optometry,* 5**,** 164-170.

Nomura, H., Ando, F., Niino, N., Shimokata, H. & Miyake, Y. 2004. The relationship between intraocular pressure and refractive error adjusting for age and central corneal thickness. *Ophthalmic Physiol Opt,* 24**,** 41-5.

Nongpiur, M. E., Png, O., Chiew, J. W., Fan, K. R., Girard, M. J., Wong, T., Goh, D., Perera, S. A. & Aung, T. 2015. Lack of Association Between Corneal Hysteresis and Corneal Resistance Factor With Glaucoma Severity in Primary Angle Closure Glaucoma. *Invest Ophthalmol Vis Sci,* 56**,** 6879-85.

Nyquist, G. W. 1968. Rheology of the cornea: experimental techniques and results. *Exp Eye Res,* 7**,** 183-8.

O'Neal, M. R. & Polse, K. A. 1986. Decreased endothelial pump function with aging. *Invest Ophthalmol Vis Sci,* 27**,** 457-63.

Ogbuehi, K. C. 2012. Corneal biomechanical parameters and intraocular pressure: the effect of topical anesthesia. *Clin Ophthalmol,* 6**,** 871-8.

Oncel, B., Dinc, U. A., Gorgun, E. & Yalvac, B. I. 2009. Diurnal variation of corneal biomechanics and intraocular pressure in normal subjects. *Eur J Ophthalmol,* 19**,** 798-803.

Orssengo, G. J. & Pye, D. C. 1999. Determination of the true intraocular pressure and

modulus of elasticity of the human cornea in vivo. *Bull Math Biol,* 61**,** 551-72.

Ortiz, D., Pinero, D., Shabayek, M. H., Arnalich-Montiel, F. & Alio, J. L. 2007. Corneal biomechanical properties in normal, post-laser in situ keratomileusis, and keratoconic eyes. *J Cataract Refract Surg,* 33**,** 1371-5.

Owens, H., Garner, L. F., Craig, J. P. & Gamble, G. 2004. Posterior corneal changes with orthokeratology. *Optom Vis Sci,* 81**,** 421-6.

Oyster, C. W. 1999. The cornea and the sclera. *The human eye : structure and function.* Sunderland, Mass.: Sinauer Associates.

Pakravan, M., Afroozifar, M. & Yazdani, S. 2014. Corneal Biomechanical Changes Following Trabeculectomy, Phaco-trabeculectomy, Ahmed Glaucoma Valve Implantation and Phacoemulsification. *J Ophthalmic Vis Res,* 9**,** 7-13.

Pakravan, M., Parsa, A., Sanagou, M. & Parsa, C. F. 2007. Central corneal thickness and correlation to optic disc size: a potential link for susceptibility to glaucoma. *Br J Ophthalmol,* 91**,** 26-8.

Pallikaris, I. G., Kymionis, G. D., Ginis, H. S., Kounis, G. A. & Tsilimbaris, M. K. 2005. Ocular rigidity in living human eyes. *Invest Ophthalmol Vis Sci,* 46**,** 409-14.

Park, J. H., Jun, R. M. & Choi, K. R. 2015. Significance of corneal biomechanical properties in patients with progressive normal-tension glaucoma. *Br J Ophthalmol,* 99**,** 746-51.

Pensyl, D., Sullivan-Mee, M., Torres-Monte, M., Halverson, K. & Qualls, C. 2012. Combining corneal hysteresis with central corneal thickness and intraocular pressure for glaucoma risk assessment. *Eye (Lond),* 26**,** 1349-56.

Pepose, J. S., Feigenbaum, S. K., Qazi, M. A., Sanderson, J. P. & Roberts, C. J. 2007. Changes in corneal biomechanics and intraocular pressure following LASIK using static, dynamic, and noncontact tonometry. *Am J Ophthalmol,* 143**,** 39-47.

Perkins, E. S. 1981. Ocular volume and ocular rigidity. *Exp Eye Res,* 33**,** 141-5.

Pillunat, K. R., Hermann, C., Spoerl, E. & Pillunat, L. E. 2016. Analyzing biomechanical parameters of the cornea with glaucoma severity in open-angle glaucoma. *Graefes Arch Clin Exp Ophthalmol,* 254**,** 1345-51.

Pinero, D. P., Alio, J. L., Barraquer, R. I., Michael, R. & Jimenez, R. 2010. Corneal

biomechanics, refraction, and corneal aberrometry in keratoconus: an integrated study. *Invest Ophthalmol Vis Sci,* 51**,** 1948-55.

Pinero, D. P., Nieto, J. C. & Lopez-Miguel, A. 2012. Characterization of corneal structure in keratoconus. *J Cataract Refract Surg,* 38**,** 2167-83.

Plakitsi, A., O'Donnell, C., Miranda, M. A., Charman, W. N. & Radhakrishnan, H. 2011. Corneal biomechanical properties measured with the Ocular Response Analyser in a myopic population. *Ophthalmic Physiol Opt,* 31**,** 404-12.

Prata, T. S., Lima, V. C., Guedes, L. M., Biteli, L. G., Teixeira, S. H., de Moraes, C. G., Ritch, R. & Paranhos, A., Jr. 2012. Association between corneal biomechanical properties and optic nerve head morphology in newly diagnosed glaucoma patients. *Clin Experiment Ophthalmol,* 40**,** 682-8.

Pruett, R. C. 1988. Progressive myopia and intraocular pressure: what is the linkage? A literature review. *Acta Ophthalmol Suppl,* 185**,** 117-27.

Qazi, M. A., Sanderson, J. P., Mahmoud, A. M., Yoon, E. Y., Roberts, C. J. & Pepose, J. S. 2009. Postoperative changes in intraocular pressure and corneal biomechanical metrics Laser in situ keratomileusis versus laser-assisted subepithelial keratectomy. *J Cataract Refract Surg,* 35**,** 1774-88.

Quinn, G. E., Berlin, J. A., Young, T. L., Ziylan, S. & Stone, R. A. 1995. Association of intraocular pressure and myopia in children. *Ophthalmology,* 102**,** 180-5.

Rad, A. S., Jabbarvand, M. & Saifi, N. 2004. Progressive keratectasia after laser in situ keratomileusis. *J Refract Surg,* 20**,** S718-22.

Radhakrishnan, H., Miranda, M. A. & O'Donnell, C. 2012. Corneal biomechanical properties and their correlates with refractive error. *Clin Exp Optom,* 95**,** 12-8.

Randleman, J. B., Dawson, D. G., Grossniklaus, H. E., McCarey, B. E. & Edelhauser, H. F. 2008. Depth-dependent cohesive tensile strength in human donor corneas: implications for refractive surgery. *J Refract Surg,* 24**,** S85-9.

Rask, G. & Behndig, A. 2006. Effects of corneal thickness, curvature, astigmatism and direction of gaze on Goldmann applanation tonometry readings. *Ophthalmic Res,* 38**,** 49-55.

Read, S. A. & Collins, M. J. 2009. Diurnal variation of corneal shape and thickness. *Optom Vis Sci,* 86**,** 170-80.

Read, S. A., Collins, M. J. & Iskander, D. R. 2008. Diurnal variation of axial length, intraocular pressure, and anterior eye biometrics. *Invest Ophthalmol Vis Sci,* 49**,** 2911-8.

Reichel, E., Miller, D., Blanco, E. & Mastanduno, R. 1989. The elastic modulus of central and perilimbal bovine cornea. *Ann Ophthalmol,* 21**,** 205-8.

Reinstein, D. Z., Archer, T. J. & Gobbe, M. 2012. Repeatability of intraoperative central corneal and residual stromal thickness measurement using a handheld ultrasound pachymeter. *J Cataract Refract Surg,* 38**,** 278-82.

Reissner E. 1946. Stresses and small displacements of shallow spherical shells II. *J Math Phys,* 25**,** 80-85.

Roberts, C. J. 2014. Concepts and misconceptions in corneal biomechanics. *J Cataract Refract Surg,* 40**,** 862-9.

Roberts, C. J. & Dupps, W. J., Jr. 2014. Biomechanics of corneal ectasia and biomechanical treatments. *J Cataract Refract Surg,* 40**,** 991-8.

Roberts, C. J., Mahmoud, A. M., Ramos, I., Caldas, D., Silva, R. S. d. & Jr, R. A. 2011. Factors Influencing Corneal Deformation and Estimation of Intraocular Pressure. *Invest. Ophthalmol. Vis. Sci.,* 52**,** 4384-4384.

Roberts, C. J., Reinstein, D. Z., Archer, T. J., Mahmoud, A. M., Gobbe, M. & Lee, L. 2014. Comparison of ocular biomechanical response parameters in myopic and hyperopic eyes using dynamic bidirectional applanation analysis. *J Cataract Refract Surg,* 40**,** 929-36.

Rosa, N., Lanza, M., De Bernardo, M., Signoriello, G. & Chiodini, P. 2015. Relationship Between Corneal Hysteresis and Corneal Resistance Factor with Other Ocular Parameters. *Semin Ophthalmol***,** 1-5.

Ruberti, J. W., Roy, A. S. & Roberts, C. J. 2011. Corneal biomechanics and biomaterials. *Annu Rev Biomed Eng,* 13**,** 269-95.

Ruisenor Vazquez, P. R., Delrivo, M., Bonthoux, F. F., Pfortner, T. & Galletti, J. G. 2013. Combining ocular response analyzer metrics for corneal biomechanical diagnosis. *J Refract Surg,* 29**,** 596-602.

Ryan, D. S., Coe, C. D., Howard, R. S., Edwards, J. D. & Bower, K. S. 2011. Corneal biomechanics following epi-LASIK. *J Refract Surg,* 27**,** 458-64.

Saad, A., Lteif, Y., Azan, E. & Gatinel, D. 2010. Biomechanical properties of keratoconus suspect eyes. *Invest Ophthalmol Vis Sci,* 51**,** 2912-6.

Salman, A. G. 2016. Corneal Biomechanical and Anterior Chamber Parameters Variations after 1-year of Transepithelial Corneal Collagen Cross-linking in Eyes of Children with Keratoconus. *Middle East Afr J Ophthalmol,* 23**,** 129-34.

Salvetat, M. L., Zeppieri, M., Tosoni, C., Felletti, M., Grasso, L. & Brusini, P. 2015. Corneal Deformation Parameters Provided by the Corvis-ST Pachy-Tonometer in Healthy Subjects and Glaucoma Patients. *J Glaucoma,* 24**,** 568-74.

Santodomingo-Rubido, J., Villa-Collar, C., Gilmartin, B. & Gutierrez-Ortega, R. 2012. Myopia control with orthokeratology contact lenses in Spain: refractive and biometric changes. *Invest Ophthalmol Vis Sci,* 53**,** 5060-5.

Scarcelli, G., Besner, S., Pineda, R., Kalout, P. & Yun, S. 2015. IN vivo biomechanical mapping of normal and keratoconus corneas. *JAMA Ophthalmology,* 133**,** 480-482.

Scarcelli, G., Pineda, R. & Yun, S. H. 2012. Brillouin optical microscopy for corneal biomechanics. *Invest Ophthalmol Vis Sci,* 53**,** 185-90.

Schiano Lomoriello, D., Lombardo, M., Tranchina, L., Oddone, F., Serrao, S. & Ducoli, P. 2011. Repeatability of intra-ocular pressure and central corneal thickness measurements provided by a non-contact method of tonometry and pachymetry. *Graefes Arch Clin Exp Ophthalmol,* 249**,** 429-34.

Schmid, K. L., Li, R. W., Edwards, M. H. & Lew, J. K. 2003. The expandability of the eye in childhood myopia. *Curr Eye Res,* 26**,** 65-71.

Schweitzer, C., Roberts, C. J., Mahmoud, A. M., Colin, J., Maurice-Tison, S. & Kerautret, J. 2010. Screening of forme fruste keratoconus with the ocular response analyzer. *Invest Ophthalmol Vis Sci,* 51**,** 2403-10.

Sedaghat, M., Bagheri, M., Ghavami, S. & Bamdad, S. 2015. Changes in corneal topography and biomechanical properties after collagen cross linking for keratoconus: 1-year results. *Middle East Afr J Ophthalmol,* 22**,** 212-9.

Sedaghat, M., Naderi, M. & Zarei-Ghanavati, M. 2010. Biomechanical parameters of the cornea after collagen crosslinking measured by waveform analysis. *J Cataract Refract Surg,* 36**,** 1728-31.

Sedaghat, M. R., Sharepoor, M., Hassanzadeh, S. & Abrishami, M. 2012. The corneal volume and biomechanical corneal factors: Is there any orrelation? *J Res Med Sci,* 17**,** 32-9.

Seiler, T., Matallana, M., Sendler, S. & Bende, T. 1992. Does Bowman's layer determine the biomechanical properties of the cornea? *Refract Corneal Surg,* 8**,** 139-42.

Sergienko, N. M. & Shargorogska, I. 2012. The scleral rigidity of eyes with different refractions. *Graefes Arch Clin Exp Ophthalmol,* 250**,** 1009-12.

Seymenoglu, G., Baser, E. F., Zerdeci, N. & Gulhan, C. 2011. Corneal biomechanical properties during the menstrual cycle. *Curr Eye Res,* 36**,** 399-403.

Shah, S. & Laiquzzaman, M. 2009. Comparison of corneal biomechanics in pre and post-refractive surgery and keratoconic eyes by Ocular Response Analyser. *Cont Lens Anterior Eye,* 32**,** 129-32; quiz 151.

Shah, S., Laiquzzaman, M., Bhojwani, R., Mantry, S. & Cunliffe, I. 2007. Assessment of the biomechanical properties of the cornea with the ocular response analyzer in normal and keratoconic eyes. *Invest Ophthalmol Vis Sci,* 48**,** 3026-31.

Shah, S., Laiquzzaman, M., Cunliffe, I. & Mantry, S. 2006. The use of the Reichert ocular response analyser to establish the relationship between ocular hysteresis, corneal resistance factor and central corneal thickness in normal eyes. *Cont Lens Anterior Eye,* 29**,** 257-62.

Shah, S., Laiquzzaman, M., Mantry, S. & Cunliffe, I. 2008. Ocular response analyser to assess hysteresis and corneal resistance factor in low tension, open angle glaucoma and ocular hypertension. *Clin Experiment Ophthalmol,* 36**,** 508-13.

Shen, M., Fan, F., Xue, A., Wang, J., Zhou, X. & Lu, F. 2008a. Biomechanical properties of the cornea in high myopia. *Vision Res,* 48**,** 2167-71.

Shen, M., Wang, J., Qu, J., Xu, S., Wang, X., Fang, H. & Lu, F. 2008b. Diurnal variation of ocular hysteresis, corneal thickness, and intraocular pressure. *Optom Vis Sci,* 85**,** 1185-92.

Shin, J., Kim, T. W., Park, S. J., Yoon, M. & Lee, J. W. 2015a. Changes in biomechanical properties of the cornea and intraocular pressure after myopic laser in situ keratomileusis using a femtosecond laser for flap creation determined using ocular response analyzer and Goldmann applanation

tonometry. *J Glaucoma,* 24**,** 195-201.

Shin, J., Lee, J. W., Kim, E. A. & Caprioli, J. 2015b. The effect of corneal biomechanical properties on rebound tonometer in patients with normal-tension glaucoma. *Am J Ophthalmol,* 159**,** 144-54.

Shin, T. J., Vito, R. P., Johnson, L. W. & McCarey, B. E. 1997. The distribution of strain in the human cornea. *J Biomech,* 30**,** 497-503.

Simon, G. & Ren, Q. 1994. Biomechanical behavior of the cornea and its response to radial keratotomy. *J Refract Corneal Surg,* 10**,** 343-51; discussion 351-6.

Sloan, S. R., Jr., Khalifa, Y. M. & Buckley, M. R. 2014. The location- and depth-dependent mechanical response of the human cornea under shear loading. *Invest Ophthalmol Vis Sci,* 55**,** 7919-24.

Song, Y., Congdon, N., Li, L., Zhou, Z., Choi, K., Lam, D. S., Pang, C. P., Xie, Z., Liu, X., Sharma, A., Chen, W. & Zhang, M. 2008. Corneal hysteresis and axial length among Chinese secondary school children: the Xichang Pediatric Refractive Error Study (X-PRES) report no. 4. *Am J Ophthalmol,* 145**,** 819-26.

Soni, P. S., Nguyen, T. T. & Bonanno, J. A. 2003. Overnight orthokeratology: visual and corneal changes. *Eye Contact Lens,* 29**,** 137-45.

Soni, P. S., Nguyen, T. T. & Bonanno, J. A. 2004. Overnight orthokeratology: refractive and corneal recovery after discontinuation of reverse-geometry lenses. *Eye Contact Lens,* 30**,** 254-62; discussion 263-4.

Spoerl, E., Terai, N., Scholz, F., Raiskup, F. & Pillunat, L. E. 2011. Detection of biomechanical changes after corneal cross-linking using Ocular Response Analyzer software. *J Refract Surg,* 27**,** 452-7.

Sridharan, R. 2001. *Response and regression of the cornea with short-term OK lens wear.* MSc, University of New South Wales.

Sridharan, R. & Swarbrick, H. 2003. Corneal response to short-term orthokeratology lens wear. *Optom Vis Sci,* 80**,** 200-6.

Stamper, R. L. 2011. A history of intraocular pressure and its measurement. *Optom Vis Sci,* 88**,** E16-28.

Streiner DL, N. G. 2003. *Health Measurement Scales: A Practical Guide to their Development and Use.* New York, Oxford University Press

Strobbe, E., Cellini, M., Barbaresi, U. & Campos, E. C. 2014. Influence of age and gender on corneal biomechanical properties in a healthy Italian population. *Cornea,* 33**,** 968-72.

Sullivan-Mee, M., Billingsley, S. C., Patel, A. D., Halverson, K. D., Alldredge, B. R. & Qualls, C. 2008. Ocular Response Analyzer in subjects with and without glaucoma. *Optom Vis Sci,* 85**,** 463-70.

Sullivan-Mee, M., Katiyar, S., Pensyl, D., Halverson, K. D. & Qualls, C. 2012. Relative importance of factors affecting corneal hysteresis measurement. *Optom Vis Sci,* 89**,** E803-11.

Sun, L., Shen, M., Wang, J., Fang, A., Xu, A., Fang, H. & Lu, F. 2009. Recovery of corneal hysteresis after reduction of intraocular pressure in chronic primary angle-closure glaucoma. *Am J Ophthalmol,* 147**,** 1061-6, 1066 e1-2.

Swarbrick, H. A. 2006. Orthokeratology review and update. *Clin Exp Optom,* 89**,** 124-43.

Swarbrick, H. A., Wong, G. & O'Leary, D. J. 1998. Corneal response to orthokeratology. *Optom Vis Sci,* 75**,** 791-9.

Szalai, E., Berta, A., Hassan, Z. & Modis, L., Jr. 2012. Reliability and repeatability of swept-source Fourier-domain optical coherence tomography and Scheimpflug imaging in keratoconus. *J Cataract Refract Surg,* 38**,** 485-94.

Tan, P. & Mehta, J. S. 2011. Collagen crosslinking for keratoconus. *J Ophthalmic Vis Res,* 6**,** 153-4.

Tang, W., Collins, M. J., Carney, L. & Davis, B. 2000. The accuracy and precision performance of four videokeratoscopes in measuring test surfaces. *Optom Vis Sci,* 77**,** 483-91.

Tanter, M., Touboul, D., Gennisson, J. L., Bercoff, J. & Fink, M. 2009. High-resolution quantitative imaging of cornea elasticity using supersonic shear imaging. *IEEE Trans Med Imaging,* 28**,** 1881-93.

Terai, N., Raiskup, F., Haustein, M., Pillunat, L. E. & Spoerl, E. 2012. Identification of biomechanical properties of the cornea: the ocular response analyzer. *Curr Eye Res,* 37**,** 553-62.

Tonnu, P. A., Ho, T., Sharma, K., White, E., Bunce, C. & Garway-Heath, D. 2005. A

comparison of four methods of tonometry: method agreement and interobserver variability. *Br J Ophthalmol,* 89**,** 847-50.

Touboul, D., Benard, A., Mahmoud, A. M., Gallois, A., Colin, J. & Roberts, C. J. 2011. Early biomechanical keratoconus pattern measured with an ocular response analyzer: curve analysis. *J Cataract Refract Surg,* 37**,** 2144-50.

Touboul, D., Roberts, C., Kerautret, J., Garra, C., Maurice-Tison, S., Saubusse, E. & Colin, J. 2008. Correlations between corneal hysteresis, intraocular pressure, and corneal central pachymetry. *J Cataract Refract Surg,* 34**,** 616-22.

Tsikripis, P., Papaconstantinou, D., Koutsandrea, C., Apostolopoulos, M. & Georgalas, I. 2013. The effect of prostaglandin analogs on the biomechanical properties and central thickness of the cornea of patients with open-angle glaucoma: a 3-year study on 108 eyes. *Drug Des Devel Ther,* 7**,** 1149-56.

Uchio, E., Ohno, S., Kudoh, J., Aoki, K. & Kisielewicz, L. T. 1999. Simulation model of an eyeball based on finite element analysis on a supercomputer. *Br J Ophthalmol,* 83**,** 1106-11.

Uzbek, A. K., Kamburoglu, G., Mahmoud, A. M. & Roberts, C. J. 2011. Change in biomechanical parameters after flap creation using the Intralase femtosecond laser and subsequent excimer laser ablation. *Curr Eye Res,* 36**,** 614-9.

Vantomme, M., Pourjavan, S. & Detry-Morel, M. 2013. The range of the waveform score of the ocular response analyzer (ora) in healthy subjects. *Bull Soc Belge Ophtalmol***,** 91-7.

Villa-Collar, C., Gonzalez-Meijome, J. M., Queiros, A. & Jorge, J. 2009. Short-term corneal response to corneal refractive therapy for different refractive targets. *Cornea,* 28**,** 311-6.

Villas-Boas, F. S., Doi, L. M., Sousa, A. K. & Melo, L. A., Jr. 2009. Correlation between diurnal variation of intraocular pressure, ocular pulse amplitude and corneal structural properties. *Arq Bras Oftalmol,* 72**,** 296-301.

Vinciguerra, P., Albe, E., Mahmoud, A. M., Trazza, S., Hafezi, F. & Roberts, C. J. 2010. Intra- and postoperative variation in ocular response analyzer parameters in keratoconic eyes after corneal cross-linking. *J Refract Surg,* 26**,** 669-76.

Vu, D. M., Silva, F. Q., Haseltine, S. J., Ehrlich, J. R. & Radcliffe, N. M. 2013.

Relationship between corneal hysteresis and optic nerve parameters measured with spectral domain optical coherence tomography. *Graefes Arch Clin Exp Ophthalmol,* 251**,** 1777-83.

Wang, D., Liu, M., Chen, Y., Zhang, X., Xu, Y., Wang, J., To, C. H. & Liu, Q. 2014. Differences in the corneal biomechanical changes after SMILE and LASIK. *J Refract Surg,* 30**,** 702-7.

Wang, J., Li, Y., Jin, Y., Yang, X., Zhao, C. & Long, Q. 2015. Corneal Biomechanical Properties in Myopic Eyes Measured by a Dynamic Scheimpflug Analyzer. *J Ophthalmol,* 2015**,** 161869.

Wells, A. P., Garway-Heath, D. F., Poostchi, A., Wong, T., Chan, K. C. & Sachdev, N. 2008. Corneal hysteresis but not corneal thickness correlates with optic nerve surface compliance in glaucoma patients. *Invest Ophthalmol Vis Sci,* 49**,** 3262-8.

Whitacre, M. M., Stein, R. A. & Hassanein, K. 1993. The effect of corneal thickness on applanation tonometry. *Am J Ophthalmol,* 115**,** 592-6.

Wilson, S. E., Lin, D. T. & Klyce, S. D. 1991. Corneal topography of keratoconus. *Cornea,* 10**,** 2-8.

Wolffsohn, J. S., Safeen, S., Shah, S. & Laiquzzaman, M. 2012. Changes of corneal biomechanics with keratoconus. *Cornea,* 31**,** 849-54.

Wollensak, G. & Iomdina, E. 2009. Long-term biomechanical properties of rabbit cornea after photodynamic collagen crosslinking. *Acta Ophthalmol,* 87**,** 48-51.

Wollensak, G., Spoerl, E. & Seiler, T. 2003. Stress-strain measurements of human and porcine corneas after riboflavin-ultraviolet-A-induced cross-linking. *J Cataract Refract Surg,* 29**,** 1780-5.

Wong E., Y. M. K. H. 1991. Factors affecting ocular rigidity in the Chinese. *Clin Exp Optom,* 74**,** 156-159.

Wong, Y. Z. & Lam, A. K. 2011. Influence of corneal astigmatism, corneal curvature and meridional differences on corneal hysteresis and corneal resistance factor. *Clin Exp Optom,* 94**,** 418-24.

Wong, Y. Z. & Lam, A. K. 2015. The roles of cornea and axial length in corneal hysteresis among emmetropes and high myopes: a pilot study. *Curr Eye Res,* 40**,** 282-9.

Woo, S. L., Kobayashi, A. S., Schlegel, W. A. & Lawrence, C. 1972. Nonlinear material properties of intact cornea and sclera. *Exp Eye Res,* 14**,** 29-39.

Xu, S., Xu, A., Tao, A., Wang, J., Fan, F. & Lu, F. 2010. Corneal biomechanical properties and intraocular pressure in high myopic anisometropia. *Eye Contact Lens,* 36**,** 204-9.

Ye, C., Yu, M., Lai, G. & Jhanji, V. 2015. Variability of Corneal Deformation Response in Normal and Keratoconic Eyes. *Optom Vis Sci,* 92**,** e149-53.

Yeh, T. N., Green, H. M., Zhou, Y., Pitts, J., Kitamata-Wong, B., Lee, S., Wang, S. L. & Lin, M. C. 2013. Short-term effects of overnight orthokeratology on corneal epithelial permeability and biomechanical properties. *Invest Ophthalmol Vis Sci,* 54**,** 3902-11.

Yenerel, N. M., Kucumen, R. B. & Gorgun, E. 2010. Changes in corneal biomechanics in patients with keratoconus after penetrating keratoplasty. *Cornea,* 29**,** 1247-51.

Young, W. C. & Budynas, R. G. 2002. Shells of revolution; Pressure vessels; Pipes. *Roark's formulas for stress and strain.* 7th ed. New York: McGraw-Hill Book Co.

Zeng, Y., Yang, J., Huang, K., Lee, Z. & Lee, X. 2001. A comparison of biomechanical properties between human and porcine cornea. *J Biomech,* 34**,** 533-7.

Zhong, X., Chen, X., Xie, R. Z., Yang, J., Li, S., Yang, X. & Gong, X. 2009. Differences between overnight and long-term wear of orthokeratology contact lenses in corneal contour, thickness, and cell density. *Cornea,* 28**,** 271-9.